Role of Rho GTPase networks in Keratinocyte migration

Inaugural-Dissertation

Zur Erlangung des Doktorgrades

Dr. rer. nat.

der Fakultät für Biologie

an der Universität Duisburg-Essen

vorgelegt von

Rutuja Patwardhan
aus Indien

Oktober 2019

Die der vorliegenden Arbeit zugrunde liegenden Experimente wurden am Zentrum für medizinische Biotechnoloy (ZMB) in der Abteilung für Molecululare Zellbiology der Universität Duisburg-Essen durchgeführt.

1. Gutachter: Prof. Dr. Perihan Nalbant

2. Gutachter: Prof. Dr. Stefan Westermann

Vorsitzender des Prüfungsausschusses: Prof. Dr. Hemmo Meyer

Tag der mündlichen Prüfung: 13 January 2020

Table of contents

List of Figures

List of Tables

Abbreviations

A: ampere

Approx.: approximately

Arp2/3: Actin-related-protein 2/3

ADP: adenosine diphosphate

AOTF: acousto optic tunable filter

ATP: adenosine triphosphate

AU: arbitrary unit

Bp: base pairs

BSA: *Bovine* serum albumin

°C: degrees Celsius

C: centi

CCD: charge-coupled device

CMV: *cytomegalovirus*

CytoD: Cytochalasin D

Da: Dalton

DAD: diaphanous autoregulation domain

DAPI: 4',6-diamidino-2- phenylindole

DH: Dbl homology

Dia: diaphanous

DIC: differential interference contrast

DMEM: Dulbecco's modified eagle's medium

DMSO: dimethyl sulfoxide

DPBS: Dulbecco's phosphate- buffered saline

DRF: diaphanous-related formins

DTE: dithioerythritol

E. : Escherichia

e.g. : exempli gratia

EB: elution buffer

ECL: entry-level peroxidase substrate for enhanced chemiluminescence

L: liter

LIMK: LIM Kinases

M: meter

m: milli

M: molar

M: micro

MAPK: Mitogen-activated protein kinase

Min: minute(s)

Myo9b: Myosin9b

MLC: Myosin Light Chain

MLCK: Myosin Light chain Kinase

MRCK: Myotonic dystrophy related Kinase

N: number of cells

NA: numerical aperture

NMHC: non-muscle myosin heavy chain

NTP: nucleoside 5-triphosphates

OD: optical density

Osc: oscillation(s)

Pa: pascal

PAGE: polyacrylamide gel electrophoresis

PAK: p21 activating Kinase

PAR: Protease activator receptor

PBS: phosphate-buffered saline

Pi: inorganic phosphate

PIP2: phosphatidylinositol (4,5)-bisphosphate

PIP3: phosphatidylinositol 1,4,5-triphosphate

PH:Pleckstrin homology

PMT: photo multiplier

PVDF: polyvinylidene difluoride

ECM: Extra cellular matrix

EDTA: ethylene diamine tetraacetic acid

EGF: Epidermal growth factor

EGFP: enhanced green fluorescent protein

EMCCD: electron multiplying charge-coupled device

ERM: Ezrin/radixin/Moesin

FA: Focal ashesion

FAK: focal adhesion kinase

FBP: formin-binding protein

FCS: fetal calf serum

FHOD: formin-homology domain

FML: formin-like proteins

GAP: GTPase-activating protein

GBD: GTPase-binding domain

GDI: GTP-dissociation inhibitor

GDP: guanosine diphosphate

GEF: GTP-exchange factor

GTP: guanosine triphosphate

HRP: horseradish peroxidase

LatA: Latrunculin A

LUT: look up table

H: hour(s)

HBSS: Hank's Balanced Salt

HEPES: 4-(2-hydroxyethyl)-1-piperazineethanesulfonic acid

K: kilo

KO: knockout

L: liter

LB: Luria-Bertani

r: mean crosscorrelation coefficient

rpm: revolutions per minute

RBD: Rho-binding-domain

RFP: red fluorescent protein

RIPA: radioimmunoprecipitation assay buffer

ROCK: Rho-associated protein kinase

RT: room temperature

s: second(s)

SDS: sodium dodecyl sulfate

s.e.: standard error

s.e.m.: standard error of the mean

ss: steady state

TAE: Tris, acetic acid, EDTA

TBS: Tris-buffered saline

TEMED: tetramethylethylenediamine

TIRF: total internal reflection fluorescence

Tris: Tris(hydroxymethyl) aminomethane

TSS: transformation & storage solution

U: enzyme unit

V: volt

VASP: Vasodilator-stimulated phosphoprotein

v/v: volume solution per volume solution

wt: wild-type

w/v: mass solute per volume solution

WASP: Wiskott-aldrich syndrome protein

Summary

Keratinocytes are skin cells, which undergo proliferation, differentiation and migration during normal homeostasis and wound healing. Several groups have shown that the Rho GTPases Cdc42, Rho and Rac play critical role in Keratinocyte maintenance and differentiation. However, little is known about their function in Keratinocyte motility and how their subcellular activity patterns might mediate these effects. Here, a multifaceted approach was used which includes fluorescent live-cell activity sensors, TIRF microscopy, RNAi and overexpression studies to characterize spatio-temporal activity patterns of two major Rho GTPases, Cdc42 and Rho, in Keratinocytes during migration and to understand the underlying mechanisms.

The work here confirmed Cdc42 to be an integral part of Keratinocyte migration machinery. First, a live cell sensor for Cdc42 activity was used revealing two major Cdc42 activity patterns during migration. In addition, Cdc42 activity pulses were observed in the lamellum region in the front of the cells as well as a more persistent Cdc42 activity pool at the trailing edge. Interestingly, the latter strongly correlated with the direction of cell migration and overlapped with the retrograde flow of actin and Myosin-II. Next, the potential regulatory mechanisms controlling Cdc42 activity patterns in migratory Keratinocytes were explored. Prior studies have revealed binding of the Cdc42/Rac1 effector PAK to the guanine nucleotide exchange factor (GEF) βPix suggesting a positive feedback loop. Using pharmaceutical inhibition and RNAi mediated depletion of PAK2 as well as βPix lead to strong decrease of the Cdc42 trailing-edge activity, further strengthening potential existence of such positive feedback loop to control Cdc42 activity patterns in Keratinocytes. Finally, depletion of Cdc42 lead to decrease in cell migration as well as to significant reduction of contraction sites. This confirms that Cdc42 is critical for Keratinocyte migration possibly via controlling actomyosin dynamics.

Growth factor stimulation is a major trigger of Keratinocyte cell motility. Interestingly, EGF stimulation did not affect Cdc42 activity patterns suggesting that it is a part of intrinsic cell migration machinery, which does not rely on growth factor stimulation. In contrast to Cdc42, significantly altered Rho activity patterns were seen upon EGF stimulation. However, the changes in subcellular Rho activity signals were very transient. For example, low amplitude activity pulses in the entire cell increased within the first 12 minutes and decreased after an hour. Also, a very prominent, albeit

transient, Rho activity increase around the entire cell periphery was observed shortly after EGF addition that was followed by strong contraction of these regions. Such transient global cell contraction may be required to stimulate enhanced migratory behavior, for example, by reorganizing topology of signal networks controlling Rho GTPase activity. The steep and transient rise of Rho activity upon EGF addition may be due to excitability in the system and a focused overexpression screen revealed several Rho activating Lbc type GEFs that enhanced Rho activity waves and thus might be potentially involved in Rho excitability in Keratinocytes.

In the last part of the work, a previously established cell system (U2OS) was used to better understand the role of the extracellular matrix and the cellular cortex in the regulation of Rho activity. Rho activity pulses were enhanced by the ECM substrates collagen and fibronectin implicating integrin signaling linked to the pulsatory Rho network dynamics. Furthermore, our findings revealed sub-cellular localization pulses of the ERM proteins ezrin and moesin at the cell cortex that strongly correlated with actin dynamics and Rho activity pulses. Inhibition of Rho-ROCK signaling reduced ezrin pulses suggesting that ERM protein dynamics might be downstream of Rho activity and actomyosin pulses in adherent cells.

Together, the work presented here revealed novel insight into the role of the Rho GTPase Cdc42 in Keratinocyte cell migration and advanced knowledge of the molecular mechanisms controlling its sub-cellular activity patterns in this process. Furthermore, our findings link growth factor induced distinct Rho activity patterns to cellular morpho-dynamics and identified potential regulatory GEFs. We are far from understanding the entire complexity of the underlying mechanisms that give rise to distinct local Rho GTPase activity patterns. Future work building on the novel findings presented in this thesis will greatly advance our understanding of Keratinocyte motility and increase the scope of therapeutics for aberrant processes related to wound healing and reepithelization.

Zusammenfassung

Keratinozyten sind Hautzellen, welche während für die Aufrechterhaltung der Homöostase und die Durchführung der Wundheilung proliferieren, differenzieren und migrieren. Mehrere Gruppen zuvor haben gezeigt, dass Rho-GTPasen wichtig für die Aufrechterhaltung und Differenzierung von Keratinozyten sind. Die Funktion dieser Proteine in der Migration von Keratinozyten sowie die Bedeutung und Regulation ihrer räumlich-zeitlichen Aktivierung sind jedoch weitgehend unbekannt. Zur Untersuchung der Rolle der zwei prominenten Rho-GTPasen, Cdc42 und Rho in migrierenden Keratinozyten wurde in dieser Arbeit ein vielfältiger Ansatz verfolgt. Dieser umfasst eine Kombination aus Fluoreszenz-markierten Aktivitätssensoren für Lebend-Zell-Mikroskopie (TRIF Mikroskopie), siRNA-Depletion sowie die Anwendung von Überexpressionsstudien.

Die vorliegende Arbeit zeigte zunächst, dass Cdc42 eine wichtige Rolle in der Migration von Keratinozyten einnimmt. So konnten mit Hilfe eines Fluoreszenzsensors zwei diskrete Aktivitätsmuster in migrierenden Zellen beobachtet werden. Zum einen wurden Cdc42 Aktivitätspulse im vorderen Bereich der Zellen, dem Lamellum, detektiert. Des Weiteren konnte ein sehr beständiges Cdc42 Aktivitätssignal im hinteren Bereich der Zellen beobachtet werden. Interessanterweise zeigten die letzteren Aktivitätssignale eine starke Korrelation mit der Direktionalität der Migration und eine deutliche Überlagerung mit dem retrograden Fluss von Aktin und Myosin-II in diesem Bereich. Als nächstes wurde der molekulare Mechanismus, welcher die Cdc42 Aktivitätspulse in migrierenden Keratinozyten kontrolliert, untersucht. Frühere Studien konnten die Interaktion des Cdc42 Effektors PAK mit dem Guaninnukleotid-Austauschfaktor ßPix zeigen, welcher wiederum die GTPase aktiviert und somit einen potentiellen positiven Feedback-Mechanismus erlaubt. Mit Hilfe von pharmakologischen Inhibitoren sowie der siRNA vermittelten Depletion von PAK2 und ßPix konnte in dieser Arbeit eine starke Verringerung der Cdc42 Aktivität im hinteren Teil der Zelle ermittelt werden, welche tatsächlich die Existenz eines solchen Mechanismus zur Kontrolle von Cdc42 Aktivitätsmustern in Keratinozyten stützt. Letztendlich äußerte sich die Depletion von Cdc42 in einer Verminderung der Zellmigration sowie in einer signifikanten Reduktion der Kontraktion von peripheren Regionen. Dies bestätigt die Relevanz von Cdc42 für die Migration von Keratinozyten und deutet darauf, dass dabei die Kontrolle der Aktomyosin-Kontraktilität eine wichtige Rolle spielt..

Die Motilität von Keratinozyten wird unter anderem durch die Stimulierung von Wachstumsfaktoren, wie EGF, reguliert. Interessanterweise beeinflusste die EGF-Stimulation nicht die Cdc42 Aktivitätsmuster. Dies deutet darauf, dass die lokalen Aktivierungsmechanismen ein Teil der intrinsischen Zellmigrationsmaschinerie ist, welcher nicht durch Wachstumsfaktoren beeinflusst werden. Im Gegensatz hierzu wurden für die verwandte GTPase Rho signifikante Veränderungen der Aktivitätsmuster nach EGF-Stimulation beobachtet. Die Veränderungen der subzellulären Rho-Aktivitätssignale waren jedoch sehr transient. Beispielsweise wurden in der gesamten Zelle innerhalb der ersten 12 Minuten verstärkt Aktivitätspulse mit niedriger Amplitude beobachtet, welche jedoch nach einer Stunde wieder abnahmen.

Ebenfalls wurde nach EGF-Zugabe ein deutlicher, wenn auch vorübergehender Anstieg der Rho-Aktivität in der Zellperipherie beobachtet, dem eine starke Kontraktion dieser Regionen folgte. Eine

solche globale Zellkontraktion könnte erforderlich sein, um die Zellmigration effizienter zu induzieren, beispielsweise durch die Reorganisation der Topologie von Signalnetzwerken zur Steuerung der Rho-GTPase-Aktivität. Dieser vorübergehende Anstieg der Rho-Aktivität nach EGF-Zugabe kann daher auf ein empfindliches System hindeuten, welches durch Wachstumsfaktoren moduliert werden kann. Mit Hilfe eines fokussierten Überexpressions-Screens, welcher die Mitglieder der Lbc-Rho-GEFs umfasste, wurden im Folgenden tatsächlich mehrere GEFs identifiziert, welche in solch einem System die EGF-stimulierte transiente Erhöhung der Rho-Aktivität vermitteln können und daher potentiell an der Regulation von Rho in Keratinozyten beteiligt sind.

Im letzten Teil dieser Arbeit wurde die bereits in diesem Labor etablierte Zelllinie (U2OS) verwendet, um die früheren Studien zur der Regulation des Rho Aktivitätsnetzwerks weiter auszubauen und die Rolle der extrazellulären Matrix (ECM) besser zu verstehen. Hierbei konnte eine deutliche Verstärkung der Rho Aktivitätspulse durch die Verwendung der ECM-Substrate Fibronektin und Kollagen I gezeigt werden, was auf eine Verknüpfung von Integrin-abhängigen Signalwegen mit dem dynamischen Rho Aktivitätsnetzwerk hinweist. Des Weiteren konnten Lokalisationspulse der ERM Proteine Ezrin and Moesin am Zellkortex beobachtet werden, welche stark mit der Aktindynamik und den Rho Aktivitätspulsen korrelierten. Die Inhibierung des Rho-ROCK Signalweges führte zu einer deutlichen Reduktion der subzellulären Ezrin Pulse. Dieser Befund legt nahe, dass die ERM Protein-Dynamik in adherenten Zellen stromabwärts der Rho Aktivität und der Aktomyosin Pulse stattfindet.

Zusammenfassend ergeben sich, basierend auf den Daten dieser Arbeit, neue Erkenntnisse zur Rolle der Rho-GTPase Cdc42 in der Migration von Keratinozyten, insbesondere im Hinblick auf Dynamik und Regulation der subzellulären Aktivitätsmuster der GTPase. Des Weiteren zeigen unsere Daten eine Korrelation der wachstumsfaktor-induzierten Rho Aktivitätspulse mit der dynamischen Änderung der Zellmorphologie beim Einsetzen der Zellmigration und präsentieren potenziell regulatorische GEF Proteine in diesem Zusammenhang. Bis dato sind wir weit davon entfernt, die zugrundliegenden Mechanismen zu verstehen, welche die lokalen Rho Aktivitätspulse regulieren und wie diese Aktivitätsmuster die Migration von Kerationzyten kontrollieren. Zukünftige Arbeiten, die auf den hier vorgestellten Erkenntnissen aufbauen, werden unser Verständnis diesbezüglich erheblich voranbringen und die therapeutischen Anwendungsbereiche bei krankhaft veränderten Prozessen im Zusammenhang mit Wundheilung und Reepithelisierung erweitern.

3. Introduction

3.1. Cell migration

Throughout adult life and during embryonic development complex cellular processes like cell proliferation, morphogenesis, migration and arrangement takes place. The intrinsic property of a cell to move from one place to another despite its surroundings or signals is known as cell migration (Etienne-Manneville 2013). Cell migration is a fundamental process performed by single to multicellular organisms. Cells migrate not only during embryonic development but also in adult tissues for immunosurveillance, wound healing and tissue homeostasis (Friedl and Mayor 2017; Scarpa and Mayor 2016). Disease conditions like atherosclerosis, rheumatoid arthritis, asthma (Montoya et al. 2002), tumour cell spreading and metastasis also rely on cell migration (Friedl and Gilmour 2009; Bravo-Cordero et al. 2012). Numerous studies on cell migration have shown that cells can adopt different modes of migration such as mesenchymal migration as seen in fibroblasts, amoeboid migration by leukocytes, gliding motion seen in fish Keratocytes as well as bleb-based migration (Chugh and Paluch 2018) and collective sheet migration (Vicente-Manzanares et al. 2005). It is now believed that some cell types can adopt one or more migration modes depending their neighbours and the extra cellular matrix (ECM) composition they encounter (Petrie et al. 2012).

1.1.1 Morphodynamic processes underlying cell migration

Classically, cell migration is based on four basic processes namely, protrusion, adhesion, contraction and retraction or detachment. The spatial and temporal coordination of these cytoskeleton-based processes may alter depending on the mode of migration acquired (Chugh and Paluch 2018). In addition, other tightly controlled regulatory processes like cell polarity, environmental sensing and matrix degradation are also coupled to the basic migratory machinery and need to be tightly co-ordinated in space and time. Aberrant control of these complex mechanisms might thus lead to pathological cell migration, one of the major reasons for metastasis in cancer cells or inflammation in rheumatoid arthritis (Yamaguchi and Condeelis 2007; Montoya et al. 2002). Therefore, understanding the underlying molecular mechanisms of migration related cytoskeletal regulation is key to generate therapeutic actions for such conditions. Rho GTPase family of Ras related small GTPases are well-known to control the dynamics of the actin cytoskeleton and associated adhesion complexes in

space and time and they have been established to be crucial for efficient and directional cell migration. Thus, work in this thesis will focus on Rho GTPase function in cell migration with particular emphasis on molecular mechanisms that control their spatio-temporal activity dynamics in cellular morphodynamics.

1.1.2. Cellular processes underlying migration

1.1.2.1. Protrusions and the cell front

Cell migration is triggered when a cell encounters certain chemical or mechanical signals or both. In response to such stimuli, cells undergo numerous cytoskeletal changes and polarize to form a cell front and rear (fig. 1.1). At the cell front, cells form protrusive structures such as lamellipodia, filopodia and invadopodia as well as in some instances membrane blebs depending on the migration mode a cell pursues (Petrie and Yamada 2012; Svitkina 2018). Lamellipodia are thin sheet-like membrane protrusions driven by a meshwork of short cross-linked actin filaments which undergo constant polymerization and depolymerization pushing the membrane forward (Pollard and Borisy 2003). Actin tread-milling in lamellipodia includes actin nucleation, short elongation, decapping and severing/depolymerisation (Pollard and Borisy 2003). This provides particular plasticity to the leading edge and allows rapid adaptation to altered conditions such as change in cells environment. Microtubules generally do not enter the dense actin filled lamellipodium. However, in certain cases a few pioneer microtubules appear in the lamellipodia and it is thought that these might support protrusion formation and persistency via their mechanical properties, cellular trafficking and signalling capacities (Etienne-Manneville 2013). In cells like astrocytes, microtubules are even essential at the cell front (Osmani et al. 2010). Lamellipodia are commonly observed in cells migrating in 2D, but are also seen in cells migrating in 3D depending on matrix stiffness and available signalling cues (Petrie et al. 2012). Further, crawling carcinoma cells also have lamellipodia like extensions at cell front (Yamaguchi and Condeelis 2007).In contrast to lamellipodia, filopodia are thin membrane projections (fig. 1.1) induced by parallel bundles of long actin filaments emerging at protruding edges which may act to sense local cues (Svitkina 2018). An unconventional Myosin, Myosin-X was found to be functional in filopodia elongation at the tip (Watanabe et al. 2010). Finally there are structures like invadopodia or Podosomes, which are integrin based adhesion dependent small membrane protrusions composed of adhesion molecules, actin, actin regulating proteins and distinguishably ECM degrading proteins (Linder and Kopp 2005). Focal adhesion

associated microtubules regulate podosome turn over by means of vesicular trafficking and transport mechanisms (Destaing et al. 2005). Podosomes are observed in dendritic cells (Burns et al. 2001), macrophages, endothelial cells (Moreau et al. 2003; Linder and Kopp 2005), osteoclasts (Destaing et al. 2005) and in invasive cancer cells (Yamaguchi and Condeelis 2007). Membrane blebs are spherical deformations seen on the cell surface that arise due to detachment of plasma membrane from the cell cortex and that are usually observed in 3D migration (fig. 1.1) (Chugh and Paluch 2018).

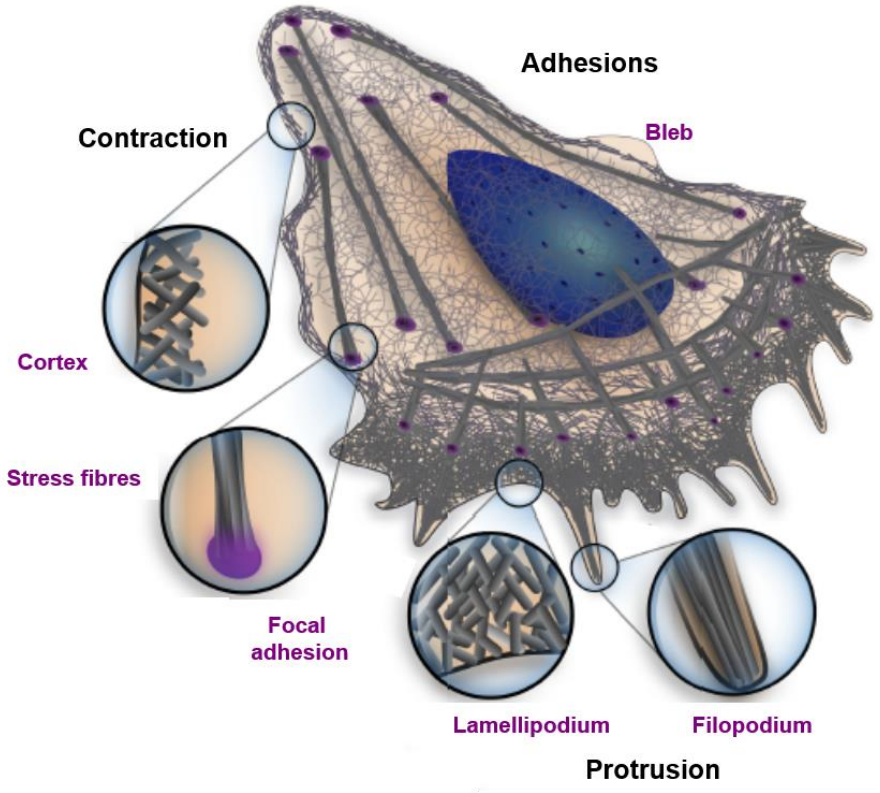

Figure 1.1: Actin structures in a migrating cell. The cell cortex is composed of a thin meshwork of crosslinked actin fibres in which Myosin-II is embedded and that are attached to the plasma membrane. Cell protrusions consist of a thin lamellipodium with branched actin filaments, filopodia which are composed of parallel actin bundles and in some instances membrane blebs which are membrane protrusions without contact with the actin cortex. Cell contraction is mainly enabled by contracting stress fibers of antiparallel, Myosin-II decorated filaments, and the cell cortex and detachment or ripping of trailing adhesion molecules (Figure taken from (Blanchoin et al. 2014)).

1.1.2.2. Cell Adhesion

Cell protrusions are stabilised by formation of nascent cell-substrate adhesions at the leading edge which over time mature into focal adhesions (FAs) within the , the cell region(lamellum), just behind the lamellipodium (fig1.1) (Devreotes and Horwitz 2015;

Svitkina 2018). Focal adhesions are integrin mediated adhesions and have been widely studied since several decades. Mature focal adhesions at the cell front are involved into actin polymerization and Myosin-II activation and they link contractile stress fibres to the substrate (Parsons et al. 2010). Via mechanosensing proteins, in particular vinculin and talin, focal adhesions mediate cellular mechanosensing and transmit variations of extracellular forces such as different matrix stiffness (Yan et al. 2015).

1.1.2.3. Contraction and the cells rear

Interestingly, in addition to protrusive structures, the cell front also encompasses contractile forces by actomyosin bundles. Myosin activity is regulated by phosphorylation of Myosin light chain (MLC) (Vicente-Manzanares et al. 2011). Active Myosin-II forms bipolar structures and binds to antiparallel actin bundles facilitating actin contraction. In lamellum at the base of lamellipodia, such Myosin-II activity leads to retrograde flow of actin away from polymerizing front (Devreotes and Horwitz 2015; Svitkina 2018; Gupton et al. 2005). The rate of protrusions progression depends on the balance between the rate of actin polymerization and Myosin-II mediated retrograde flow (Vicente-Manzanares et al. 2011). As retrograde flow is moved by linking actin filaments to integrins and thus increasing rate of protrusions (Vicente-Manzanares et al. 2005).

At the cell rear, contractile forces mediated by actomyosin are applied to focal adhesions which lead to release of adhesion and cell retraction. This rear-end detachment is a co-ordinated process involving actomyosin contractility, actin effectors, degrading proteases, kinases and phosphatases (Kirfel et al. 2004). Further, cells like Keratinocytes leave behind patches of membrane with integrin molecules that are thought to act as tracks for other cells (Kirfel et al. 2004). Nascent focal adhesions develop in front of the cell. The cell rear mainly has mature focal adhesions which have strong traction forces, enabling rear end ripping or detachment. In slow moving cells, detachment of the cells rear is brought about by the protease calpain which is activated by Epidermal growth factor (EGF) receptor activation (Glading et al. 2000). Among kinases responsible for cell detachment and rear end contraction are Rho Associated protein Kinase (ROCK) and Myotonic dystrophy related Kinase (MRCK) which are downstream effectors of small proteins in cells known as Rho GTPases (Ridley 2001).

3.2. Rho GTPases

Rho GTPases are 21 to 25 KDa small proteins and are members of the Ras super family. Rho proteins have a GTPase domain with a distinguishable Rho insert domain (Ridley 2001). As other GTPase proteins, Rho proteins act as molecular switches cycling between an active GTP bound or the inactive GDP bound confirmation. In their active state, they can interact with downstream effectors and can thus bring about various cellular processes. Rho GTPases are best known for their regulatory role in control of the actin cytoskeleton and therefore are involved in actin dependent processes such cell proliferation, migration, transcriptional regulation and environment sensing (David et al. 2012; Engler et al. 2006; Hodge and Ridley 2016). To date, at least 20 Rho GTPases are found in humans. Of these, Rac, Rho and Cdc42 are the most extensively studied.

Mainly three types of Rac proteins are found in humans (Rac 1, 2 and 3), while Rac 1 is ubiquitously expressed, Rac 2 and Rac 3 are found only in certain tissues. Further, embryonic deletion of Rac 1 leads to embryonic lethality (Sugihara et al. 1998; Malosio et al. 1997; Haataja et al. 1997). Rac activates the Arp2/3 complex, which in turn leads to formation of new actin filaments. Rac also promotes uncapping of actin filaments at the plasma membrane to further enhance polymerization. Thus, Rac activity not only affects actin polymerization but also depolymerization. LIM kinases are activated by p21 activating Kinase (PAK) which are effectors of Rac and Cdc42. LIM kinase inactivates cofilin thereby reducing actin depolymerization. Further, Rac is also responsible for focal complex formation and initiation (Nobes and Hall 1995). Microtubule induced activation of Rac has been shown to promote focal adhesion formation (Etienne-Manneville 2013). Use of various activity sensors have shown Rac activity in membrane ruffles and a gradient of Rac activity at the leading edge or cell front (Kraynov et al. 2000; Beco et al. 2018; Martin et al. 2016). Rac activity is not only essential in 2D but is seen in lamellipodia guided 3D migration as well (Petrie and Yamada 2012). Rac activity is highly dependent on phosphoinositide-3 kinase (Pi3K) activity, the activating Rac GEFs, several adaptor proteins and its interaction with effectors (Ridley 2001).

Similar to Rac1, Cdc42 null mice are embryonic lethal with defects starting at the primitive ectoderm (Duquette and Lamarche-Vane 2014). As Rac, Cdc42 is thought to regulate cell protrusions at the cell front. Furthermore, Cdc42 has been shown to be instructive for cell polarity, actin dynamics, directionality and matrix

sensing in the cell front and is known for filopodia formation (Nobes and Hall 1995; Hall 1998). Cdc42 interacts with Wiskott-aldrich syndrome protein (WASP) and neuronal Wiskott-aldrich syndrome protein (N-WASP) and activates the Arp2/3 complex and further actin polymerization (Ridley 2001). Formation of invadopodium is also dependent on Cdc42 activity, as seen in adenocarcinoma cells (Razidlo et al. 2014). Cdc42 also participates in focal adhesion formation and dynamics (Nobes and Hall 1995). Along with localization to the plasma membrane, there increasing evidence has been providing for Cdc42 to localize at Golgi and other endocytic vesicles and regulate cellular trafficking (Osmani et al. 2010; Farhan and Hsu 2016). In astrocytes and epithelial cells, the molecular signal pathway was shown that involve Cdc42 and its effectors Par3/6 and PKC and that establishes polarity (Etienne-Manneville 2013). Use of different types of Cdc42 activity sensors have shown that the Rho GTPase is highly active at trans Golgi, cell periphery and zones in cell front (Nalbant et al. 2004; Martin et al. 2016). Furthermore, Cdc42 activity has been shown to precede cell polarization and to determine the direction of cell migration (Yang et al. 2016).

The homologous Rho proteins Rho A, B, C share multiple common effectors and activators (Lawson and Ridley 2018). Among these, RhoA has been most extensively studied and it has been shown to mediate contractile actomyosin stress fibers via multiple downstream effectors. Rho associated coiled coil containing protein Kinases (ROCKs) are serine/threonine kinases that regulate multiple processes such as actin dynamics through LIM kinases, Myosin light chain (MLC) phosphorylation both by inactivating Myosin phosphatase and by phosphorylating MLC (Ridley 2001) and Ezrin/Moesin/Radixin (ERM) protein phosphorylation for attachment of cortical actin filaments to the plasma membrane (Ivetic and Ridley 2004). Rho also stimulates stress fibres by promoting actin polymerization via its effector formin effector mDia1 (Watanabe et al. 1999). Classically, Rho proteins have been thought to act at the cells rear due to their role in cellular contractility (Ridley 2001). However, there is increasing evidence for Rho activity being essential also in cell front. Biosensor studies have shown localization of Rho activity at cell rear, centre and in very thin zone and transiently at protrusion retraction cycles at cell front (Nalbant et al. 2009; Martin et al. 2016; Pertz 2010). Furthermore, lack of elevated Rho activity in this region was accompanied by dramatically perturbed protrusion-retraction cycles supporting a critical role of Rho in this process (Nalbant et al., 2009).

1.2.1. Regulators of Rho GTPase activities

Activity of Rho GTPase proteins is mainly regulated by guanine exchange factors (GEFs) which catalyse exchange of GDP to GTP nucleotide to activate the GTPase, GTPase-activating proteins which increase the GTP hydrolysis rate and which therefore deactivate the Rho proteins and guanine nucleotide dissociation inhibitors (GDIs) which sequester the active GTPase to the cytoplasm to prevent its activation. Along with these main regulators, Rho GTPases are also regulated by post translational modifications as prenylation, SUMOylation, phosphorylation and ubiquitination.

Two major families of GEFs have been identified, The Dbl family of GEFs encompass a common shared catalytic domain for nucleotide exchange, called DH (Dbl homology) domain and is mostly followed by the PH (Pleckstrin homology) domain in the majority of the Dbl-family of GEFs. The DOCK family of GEFs share the DOCK homology region 1 (DHR1) as the catalytic domain followed by the DOCK homology region 2 (DHR2) which aids membrane targeting (Meller et al. 2005). In addition to their distinct catalytic domains, GEFs also contain additional domains facilitating distinct functions and localization or allowing the GEFs to act as scaffolding proteins (Lawson and Ridley 2018).

1.2.1.1. GEFs in cell migration

Numerous GEFs identified so far, have been shown to control Rho GTPase activities in cell migration. TIAM1 is a Rac specific Dbl family GEF, with an ambivalent role as it was show to enhance or inhibit cell migration in different cases (Lawson and Ridley 2018). In Keratinocytes TIAM1 associates with Protease activator receptor (PAR) complex and binds and activates talin thereby promoting Rac activity for polarised migration (Wang et al. 2012; Mertens et al. 2005). On the other hand, TIAM1 also can associate with cadherin junctions to promote cell-cell adhesion by Rac activation and thereby inhibiting cell migration (Marei et al. 2016). DOCK1 is a Rac specific GEF, which has been shown to form multiple protein complexes and can stimulate lamellipodia as well as focal adhesions. DOCK1 can form a complex with Engulfment and cell motility protein(ELMO) (Grimsley et al. 2004) that facilitates its GEF activity. Also, interaction of DOCK1 with another GEF, cytohesin 2, was shown to promote cell migration via Rac mediated lamellipodia formation (Koubek and Santy 2018). On the other hand, dynamics of Rac localization at focal complexes is mediated by DOCK1

interaction with p130Cas and paxillin (Kiyokawa et al. 1998). Similar to DOCK1, closely related GEFs DOCK2, DOCK3 and DOCK5 also have been shown to regulate cell migration in various cell systems albeit their interactome is distinctively different from DOCK1 in many cases. (Goicoechea et al. 2014; Lawson and Ridley 2018). P-REX1 is a GEF for Cdc42 and Rac and its interaction with mTORC (Hernández-Negrete et al. 2007) promotes cell migration. The interaction of P-Rex-1 and the actin remodelling protein flightless-1 homologue (FLI1) (Marei et al. 2016) activate Rac for cell migration and crosstalk with Ras GTPases. P-Rex1has been shown to increase cell metastasis in prostrate cancer and melanoma (Lindsay et al. 2011; Qin et al. 2009). The Pix family proteins α and βPix are closely related, Cdc42 and Rac GEFs playing role in cell migration. These proteins are examples of forming several multiprotein complexes to localizes GTPase activity for specific functions as shown in figure 1.2 (Lawson and Ridley 2018). βPix is expressed ubiquitously, while αPix is expressed mainly in heart, skeletal and immune cells (Zhou et al. 2016; Manser et al. 1994). αPIX forms a complex with PAK1 which associates with chemoattractant activator receptor Gβɣ (Rossman et al. 2005). Here αPix activates Cdc42 which in turn activates PAK1, a Cdc42 effector. This complex leads to formation of leading edge and is essential for directional sensing (Li et al. 2003).The extensively studied, GIT-βPix-PAK complex activates Rac and promotes cell migration when GIT interacts with paxillin at focal complexes (Frank and Hansen 2008). . βPix also localises at cell-cell contacts by interacting with P-Cadherin and enhancing collective cell migration through Cdc42 activation (Plutoni et al. 2016). In astrocytes, βPix binds to mammalian scribble protein (SCRIB) (Goicoechea et al. 2014) and activates Cdc42 for leading edge formation and polarity (Osmani et al. 2006; Lawson and Ridley 2018). Further, βPix-GIT complex interacts with the endosomal protein sorting nexin 27 (SNX27) influencing trafficking between early endosome and focal adhesion for optimal cell migration (Goicoechea et al. 2014; Valdes et al. 2011). TUBA is Cdc42 GEF with BAR domain instead of PH domain, which is known for localization to curved membranes. TUBA is responsible for Cdc42 mediated ruffling and invasion in melanoma cells (Kovacs et al. 2006).

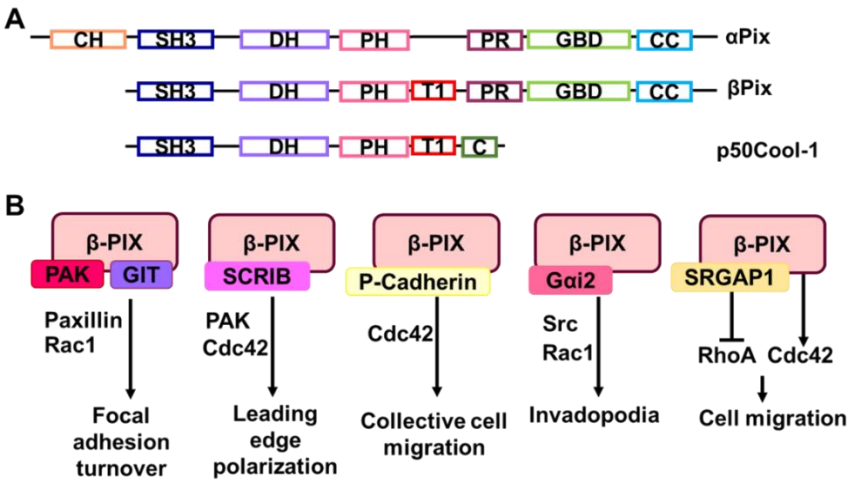

Figure 1.2: Multiprotein complexes formed by Rac and Cdc42 GEF βPix during cell migration. (A) Domains present in the related Pix proteins, α, β Pix and a splice variant p50Cool-1. In addition to the GTPase interacting and activating Dbl homology (DH) domain and regulatory pleckstrin homology (PH) domain, several potential modulatory domains as Calponin homology domain (CH), Src homology 3 domain (SH3), a GEF activity inhibitory T1 insert, proline rich regions (PR) for POPX1 and 2 binding, GIT binding domain (GBD), coiled coil region (CC) for homo and heterodimerization. These may participate in protein-protein interaction to enable formation of multiprotein complexes with varying composition of proteins. (B) Multiprotein complexes shown to be formed by βPix, which participates in various process of cell migration. Figure adapted from (Frank and Hansen 2008; Lawson and Ridley 2018).

Similar to Rac and Cdc42 GEFs, several Rho GEFs have also been shown to be involved in cell migration (figure 1.3) (Goicoechea et al. 2014; Lawson and Ridley 2018). Along with Rho activation these GEFs also have other domains for protein-protein interaction (figure 1.3) and may form multiprotein complexes. For example, ARHGEF28 (p190 RhoGEF) and ARHGEF2 (GEF-H1) have a C1 homology domain, which is typically for binding to diacylglycerol or probole asters. In case of GEF-H1 this domain is used for microtubule binding (Krendel et al. 2002). In inactive form GEF-H1 is bound to microtubules and is released on activation (Krendel et al. 2002). In migrating cells, GEF-H1 activates Rho A at cell front, where the Rho activity correlated with protrusion retraction cycle (Nalbant et al. 2009; Machacek et al. 2009). GEF-H1 was also shown to mediate participate mechanosensory processes integrin mediated complex (Guilluy et al. 2011b). The p190 RhoGEF interacts with Focal adhesion kinase (FAKs) and regulate cell migration (Miller et al. 2014). . Among the Rho selective GEFs, multiple are found (ARHGEF11 (PDZ RhoGEF), ARHGEF12 (LARG), ARHGEF1 (p115 RhoGEF) that contain an regulator of G protein signalling homology

domain (RH) for interaction with GPCRs (Hodge and Ridley 2016). . Depletion of all three, LARG, PDZ RhoGEF and p115 leads to loss of cell migration in response to thrombin (Mikelis et al. 2013). PDZ RhoGEF and LARG can also interact with plexin B and enhance endothelial cell migration via RhoA (Perrot et al. 2002). PDZ RhoGEF and p115 RhoGEF also interact with β-Arrestin and regulate cell migration. Interestingly, all these GEFs have a very similar DH-PH domain structure and belong to a family of GEFs known as Lbc type GEFs (Medina et al. 2013), which includes p115 RhoGEF, GEF-H1, PDZ RhoGEF, LARG, AKAP13, p114 RhoGEF and p190 RhoGEF.

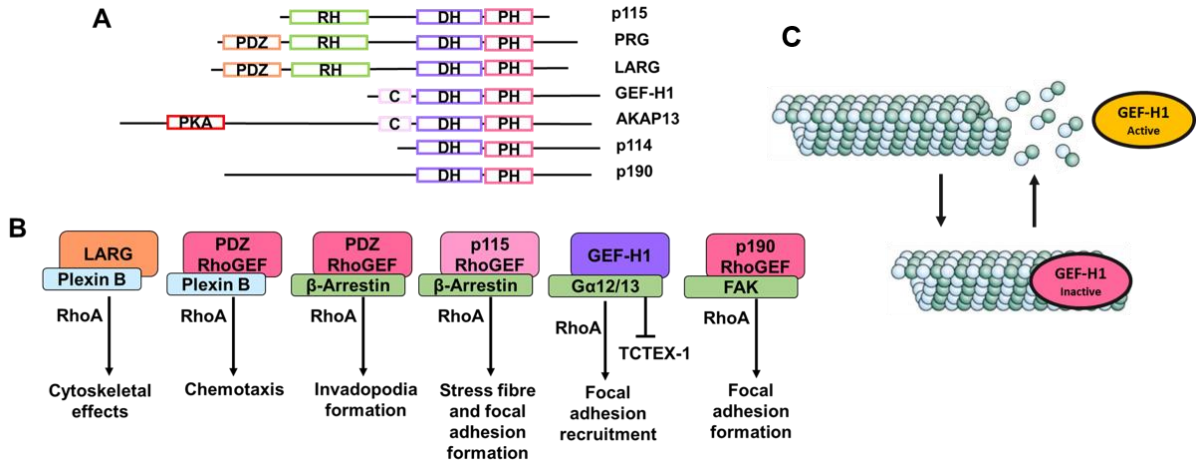

Figure 1.3: Lbc type Rho GEFs family is composed of proteins with highly similar DH-PH domains that activate RhoA in multiple processes like cell migration. (A) Lbc GEFS have a very similar GTPase interacting and activating DH domain and regulatory PH domain. Along with these, several other protein domains like common structural domain of post synaptic density protein, Drosophila disc large tumor suppressor and zonula occludens 1 protein (PDZ); the G protein signalling homology domain (RH); protein kinase A binding domain (PKA) and the probol ester or diacylglycerol binding C1 domain (C) are found, which may participate in protein-protein interactions and provide distinct functionalities and localization patterns. (B) Examples of known or suggested Lbc GEF interactions with different proteins that are thought to mediate activation of Rho at specific locations in cell migration. (C) Schematic representation of Lbc GEF, GEF-H1 attaching to microtubules when inactive and active when not bound to microtubules. Figure adapted from (Medina et al. 2013; Lawson and Ridley 2018; Birkenfeld et al. 2008).

3.3. Excitability in cells

Recently it has been appreciated that physiologically, cell movement is unsteady and so is the actin dynamics propelling it (Weiner et al. 2007). Actin dynamics shows a

range of unsteady behaviour from small actin polymerization bursts, spatiotemporal patterning to travelling actin waves (Allard and Mogilner 2013; Weiner et al. 2007). Early observations of protrusion-retraction cycle dynamics at the leading edge of the cell provided a basis for further investigation (Ryan et al. 2012). Such patterns arise due to presence of excitability in the system. Excitability is a resultant of an activator inhibitor network, where usually the excitable component has a positive self-amplifying module and a negative time delayed factor (fig. 1.4) (Allard and Mogilner 2013).

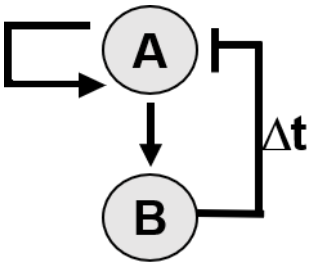

Figure 1.4: Schematic representation of a biochemical activator-inhibitor network. The activator A activates itself via positive feedback and the inhibitor B. The inhibitor B in turn inhibits A, with a time delay closing a negative feedback. The combination of the positive and time-delayed negative results in oscillatory signal dynamics of A and can be integral part of excitability. Figure adapted from (Allard and Mogilner 2013; Graessl et al. 2017))

Excitability can be an intrinsic property of cellular components in biological systems. An excitable system is usually in a steady state and small perturbations are decayed (Tyson et al. 2003). However, when the system undergoes a major perturbation above a certain threshold, it results in an elevated response which eventually goes back to steady state into a refractory phase (Allard and Mogilner 2013). Oscillatory systems, on the other hand do not require any trigger, but can generate the activiator-inhibitor based spontaneous time dependent propagating waves (Tyson et al. 2003). Bistability is observed when there are two steady states and perturbations major than a threshold send the system to another state (Novák and Tyson 2008). Excitability allows for local travelling signal pulses and when local dynamics are spatially coupled to neighbouring areas (Allard and Mogilner 2013). Stimulation of a local excitable signal is rapidly amplified by a positive feedback and eventually inhibited by a slow negative feedback taking the system in refractory phase (Novák and Tyson 2008). After this, the system equilibrates itself in a steady state. Coupling such reactions to diffusion, a propagating wave is generated (Allard and Mogilner 2013; Nalbant and Dehmelt 2018).

There have been several studies showing presence of travelling actin waves in several cell systems (Allard and Mogilner 2013; Gerhardt et al. 2014; Khamviwath et al. 2013) which mainly rely on actin polymerization (Weiner et al. 2007). Weiner and colleagues showed that actin nucleator Hem1 participated in actin polymerization waves as the driving force for chemotactic cell migration in neutrophils (Weiner et al. 2007). Myosin has also been shown to be elementary component of travelling waves in fibroblasts and U2OS cells(Allard and Mogilner 2013; Giannone et al. 2007; Graessl et al. 2017). It was also observed in in vitro studies where Myosin interaction with actin filaments was dependent on the fibre orientation and resulted in actin fibre deformation, reorientation or disassembly (Reymann et al. 2012). Such actomyosin flow participates in cell motility (Ryan et al. 2012). Along with excitability and waves of actin localization, excitability was also observed for PI3K activity (Gerhardt et al. 2014), actin coupled calcium oscillations (Wu et al. 2013) and recently for Rho GTPase activities (Bement et al. 2015; Graessl et al. 2017; Yang et al. 2016).

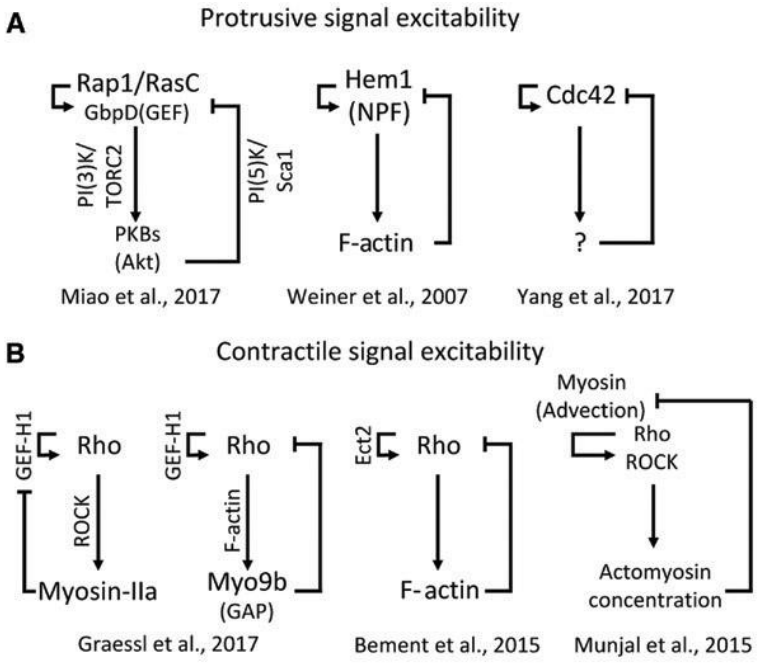

Figure 1.5: Signal networks participating in cell protrusion and contraction. (A) Activator inhibitor signal networks proposed and observed in cell protrusion dynamics (B) Activator inhibitor signal networks proposed to generate excitable cell contraction. (figure taken from a review by (Nalbant and Dehmelt 2018))

Although these studies have shown the existence of excitability and travelling waves in cellular systems, in the majority of the systems network components and topology have just started to be characterised. Furthermore, the overall biological functions of

such patterns are largely unknown with a few studies addressing them. For example, during single cell wound closure of oocytes, cortical contractions, neutrophil migration, morphogenesis (Bement et al. 2015; Graessl et al. 2017; Weiner et al. 2007; Allard and Mogilner 2013; Lecuit and Lenne 2007)

3.4. Human Keratinocytes as a model system to understand mechanisms and role of signal excitability in cell migration

The skin is the largest organ in an organism and acts as a barrier from the outside world and protects animals from external traumas such as infections, water loss, radiation, temperature change and pollutants (Evans et al. 2013). It is also the organ, which can for perceive temperatures and textures via the intervening sensory neurons. The adult skin is composed of almost 20 different cell types that belong to neuroectodermal, mesodermal and the neural crest cells in origin (Blanpain and Fuchs 2006). The epidermis, dermis and basement membrane are most prominent components of skin (Evans et al. 2013). The mature epidermis is a stratified squamous epithelium whose outermost layer is the skin. Cells in the basal layer are mitotically active and secrete extracellular matrix (ECM) components of the basement membrane. The basement membrane separates the dermis from the epidermis (Fuchs 2007). Fibroblast, vascular cells, arrector pilli muscles, subcutaneous fat cells and the infiltrating immune cells are all mesodermal in origin. The melanocytes, sensory nerve endings and dermis head all arise from neural crest cells (Blanpain and Fuchs 2006; Evans et al. 2013). The stratified epidermis, hair follicles, sebaceous glands, apocrine glands arise from the epidermal layer originating from neuroectoderm. Major structural proteins of the epidermal cells are the intermediate filament Keratins, which provide a framework for the cells. Hence the cells are also called as Keratinocytes (Omary et al. 2004). Removal of the dead outer layer and proliferation and differentiation of the basal layer occurs continuously in adults and is brought about by the respective stem cells. Some stem cells such as those for immune cells reside outside the skin while the melanocytes and epidermal skin stem cells reside within the skin itself (Fuchs 2007). The basal epidermis undergoes continuous renewal during homeostasis and undergoes a major proliferative and migration phase during traumatic events as wound healing.

All adults experience skin wounding during their everyday life. Delayed and incomplete wound healing leads to increase in risk of infection, scar formation or in worst cases patient morbidity (Evans et al. 2013). In addition, there are numerous other skin diseases are known and it is likely that several more remain undiagnosed and may cause detrimental psychological effects. The Global Burden Disease Project show skin diseases to be the fourth leading cause of non-fatal disease burden worldwide (Seth et al. 2017).

The process of wound healing mainly involves three phases, which partially overlap. The first phase involves mostly activity of platelets and immune cells (Seeger and Paller 2015). Shortly after wounding of skin tissue a blood clot and a platelet plug seals the wound temporarily. Infiltration by inflammatory cells allows protection from invading bacteria and secretion of cytokines, proteinases and growth factors (Martin and Nunan 2015). Skin fibroblasts are also seen at the wound bed and secrete similarly growth factors and ECM components. Overall, the secretion of soluble factors in the wound be is required for the beginning of the second wound healing phase (Schneider et al. 2008). This phase involves extensive proliferation and migration of Keratinocytes towards the wound bed in response to chemical and mechanical signals and leads to covering of wound with new epidermis (Martin and Nunan 2015). The last phase which is also called as re-epithelization involves tissue repair and renewal (Schäfer and Werner 2008; Safferling et al. 2013). Hence, Keratinocytes respond to signals of homeostasis as well as wounding to proliferate and directionally migrate distinct directions.

Many approaches have been implied to understand the complex process of wound coverage by Keratinocytes including study of growth factors effects (Seeger and Paller 2015), use of allogenic skin grafts or use of external ECM like substrates (Evans et al. 2013). Several growth factors have been implicated in Keratinocyte proliferation and migration (Seeger and Paller 2015). Epidermal growth factor (EGF) has been extensively studied and is shown to enhance migration and proliferation in Keratinocytes (Ando and Jensen 1993). Bioavailability of EGF is crucial for optimal EGF response by Keratinocytes (Gorouhi et al. 2014).

For timely response to growth factor signaling combined with extracellular matrix sensing Keratinocytes need molecular mechanisms that control their response to directional migration and proliferative cues. In particular very less is known about the role of Rho GTPases in Keratinocyte migration mechanism and response to cues.

Previous studies showed that EGF stimulation of Keratinocytes induces front rear polarity through Engulfment and cell motility (ELMO)-Rac1 integrin activation (Ho and Dagnino 2012). Further, Tiam1-Rac activation was shown to be necessary for Tight junction formation in Keratinocytes for maintenance of polarity (Mertens et al. 2005). These studies indicate Rac 1 to be necessary for Keratinocyte polarity. Cdc42 is shown to be necessary for basement membrane maintenance (Wu et al. 2006a) and progenitor cell differentiation in mouse Keratinocytes (Wu et al. 2006b). While, RhoA was shown to be dispensable for skin development (Jackson et al. 2011), loss of RhoA cell migration in a contraction independent manner. None of the studies had addressed the role of Rho GTPases in and the migration machinery involved in Keratinocyte motility. In this work, the gaps in our knowledge will be addressed by studying the role of spatio-temporal activity patterns of the majorly known Rho GTPases Cdc42 and Rho in EGF-stimulated migrating Keratinocytes. Based on previously available literature and recently developed methodology, the dynamics of Rho activity patterns and their control by regulatory mechanisms such as excitable signal networks that have been previously shown to control dynamic pattern formation in other cell types will be dissected. Spatio-temporal activities with cellular morphodynamics during Keratinocyte migration will be correlated to better understand the relevance of activity patterns for efficiency of the migratory process.

4. Materials and Methods

4.1. Materials

2.1.1. Cell lines used

Table 2.1. List of cell lines used in the study.

Cell line	Species	Type	Organ/ Tissue	Morphology	Company
NHEK	*Homo sapiens*	Primary Cell line	Skin	Epithelial	Promocell
U2-OS	*Homo sapiens*	Osteosarcoma	Bone	Epithelial	ATCC HTB-96

4.1.2. Media used for cell culture

Table 2.2. Media and its components used for cell culture.

Medium	Components
Growth medium for NHEK cells (light sensitive) (Derma Life complete medium)	Derma life Basal Medium 500 ml rh insulin Life factor 5 µg/ml L-Glutamine Life factor 6 mM Epinephrine Life factor 1 µM Apo-Transferrin Life factor 5µg/ml Extract P Life factor 0.4 % Hydrocortisone Life factor 100 ng/ml
Imaging medium for NHEK cells	Derma Life complete medium 20 mM HEPES
Growth medium for U2OS cells	DMEM GlutaMAX™ 10 % (v/v) FCS 50 µg/ml Penicillin 50 µg/ml Streptomycin
Imaging medium for U2OS cells	1 mM Calcium chloride 10 % (v/v) FCS 10 mM L-Glutamine 10 mM HEPES

	HBSS (Hank's balanced salt solution) 1 mM Magnesium chloride

4.1.3. Bacterial strains for cloning

Table 2.3. List of Bacterial strains used in the study.

Cell line	Species	Type	Company
DH5α	*E. coli*	F-, supE44, ΔlacU169, [Φ80lacZΔM15], hsdR17, recA1, endA1, gyrA96, thi-1, (res-, mod+), deoR	Invitrogen

4.1.4. Media used for bacterial culture

Table 2.4. List of bacterial growth media and components used.

Medium	Components
Luria-Bertani (LB)-Medium	1 % (w/v) Sodium chloride 1 % (w/v) Tryptone 0.5 % (w/v) Sodium hydroxide 0.25 % (w/v) Yeast Extract pH 7.4
LB Agar	1 % (w/v) Sodium chloride 1 % (w/v) Tryptone 0.5 % (w/v) Sodium hydroxide 0.25 % (w/v) Yeast Extract 1.5 % (w/v) Agar pH 7.4
Antibiotics	Ampicillin 100 µg/ mL Kanamycin 30 µg/mL

Media sterilised before use. For selections and growth of strains with antibiotic resistance, antibiotics with concentration as indicated above added to sterilised media.

4.1.5. Reagents and buffers

4.1.5.1. Reagents used for human cell culture

Table 2.5. List of reagents and buffers used in cell culture.

Description	Company
Dulbecco's Modified Eagle Medium (DMEM) GlutaMAX™	Life Technologies
Dulbecco´s phosphate buffered saline (DPBS)	Life Technologies
Fetal calf serum (FCS) Lot Nr. 41Q1142K, 42G8271K	Life Technologies
HBSS (Hank´s balanced salt solution)	Life Technologies, Gibco
HEPES (4-(2-hydroxyethyl)-1-piperazineethanesulfonic acid)	Life Technologies, Gibco
Collagen (Type I)	Sigma-Aldrich, C-8919
Fibronectin	Invitrogen
Poly-L-Lysine	Sigma
L-Glutamine 200 mM	Life Technologies, Gibco 40725
Derma life® Basal medium and life factors	Lifeline
TransIT transfection reagent	Mirus
siRNA transfection reagent Lipofecatamine 2000; RNAiMax	Life Technologies 11668-019; 13778150
Isopropanol	Roth
Lipofectamine 2000	Life Technologies
OptiMEM without phenol red	Life Technologies
Penicillin/Streptomycin	Life Technologies
Puromycin	Sigma-Aldrich
Trypsin-EDTA	Life Technologies
Trypsin Kit	Life line

4.1.5.2. Inhibitors used for cell culture and biochemical experiments

Table 2.6. List of pharmacological inhibitors used in cell culture and biochemistry.

Drug	Sepcification	Final concentration used	Company, ordering number

Protease-Inhibitor Cocktail complete Mini-EDTA-free	Protease inhibitor	1x	Roche 11836170001
Phosphatase-Inhibitor Cocktail Phospho STOP	Phosphatase inhibitor	1x	Roche 04906837001
Nocodazole	Microtubule depolymerizing drug	30 µM	Sigma Aldrich M1404
rhEGF	Recombinant human EGF	100 ng/ml	R&D Systems, 236-EG
Y27632 (Y compound)	Specific ROCK inhibitor	30 µM	Selleckchem, S1049
FRAX597	PAK 1/2/3 inhibitor	1 µM	Selleckchem, S7271

4.1.5.3. Reagents used for cloning

Table 2.7. List of reagents used in cloning or plasmid preparation.

Description	**Company**
Agar	Roth
Agarose	Bio-enzyme
Antibiotics, Ampicillin	Roth
Antibiotics, Kanamycin	Roth
Bromophenol blue	Serva
CutSmart	New England Biolabs
T4 DNA Ligase Buffer	New England Biolabs
1kb DNA ladder	Bio Budget
dNTP Mix (10 mM each)	Roth
Phusion HF DNA polymerase	New England Biolabs
Taq DNA Ligase	New England Biolabs
Q5 HF DNA Polymerase	New England Biolabs
T5 exonuclease	New England Biolabs
T4 DNA Ligase	New England Biolabs
Glycerol	AppliChem

Plasmid Purification Kit, Endofree	Qiagen
Plasmid Purification Kit	Qiagen
Gel Extraction Kit	Qiagen
Potassium chloride	Roth
Potassium hydrogen phosphate	Roth
Sodium chloride	Roth
Sodium hydroxide	Roth
Sodium hydrogen phosphate	Roth
Tryptone	BD Biosciences
Yeast extract	Serva

4.1.6. Buffers and reagents

4.1.6.1. Buffers for western blots and electrophoresis

Table 2.8. List of buffers for western blot

Name	Components
Anode buffer I	300 mM Tris, pH 10.4 10 % (v/v) Methanol
Anode buffer II	25 mM Tris, pH 10.4 10 % (v/v) Methanol
DNA loading buffer 6x	0.25 % (w/v) Bromo phenol blue 0.325 % (w/v) Xylen cyanol 30 % (v/v) Glycerol
Cathode buffer	25 mM Tris, pH 9.4 40 mM 6-Amino-hexanoic acid 10 % (v/v) Methanol
PBE	PBS without Mg/Ca (Pan P04-36500) 2 mM EDTA (Ethylenediaminetetraacetic acid) 0.5 % Bovine serum Albumin
PBS	2.7 mM Potassium Chloride 1.5 mM Potassium hydrogen phosphate 137 mM Sodium Chloride

	10 mM Di-sodium hydrogen phosphate pH 7.4
RIPA lysis buffer	50 mM Tris, pH 7.4 150 mM Sodium Chloride 1 % NP-40 0.5 % sodium deoxycholate 1 mM EDTA (Ethylenediaminetetraacetic acid)
SDS running buffer	12.5 mM Tris 0.05 % (w/v) Sodium dodecyl sulphate 125 mM Glycine
SDS loading buffer	0.5 M Tris-HCl pH 6.8 50 % (w/v) Glycerol 10 % (w/v) Sodium dodecyl sulphate 0.025 % Bromophenol blue 300 mM DTE
SDS stacking buffer	1.0 M Tris-HCl pH 6.8
SDS resolving buffer	1.0 M Tris-HCl pH 8.8
TAE buffer	40 mM Tris pH 8.0 5 mM EDTA (Ethylenediaminetetraacetic acid)
TBS buffer	20 mM Tris pH 7.6 137 mM Sodium Chloride
TBS-T buffer	20 mM Tris pH 7.6 137 mM Sodium Chloride 0.1 % (v/v) Tween-20
TSS	85 % (v/v) LB Medium 50 nM Magnesium Chloride 10 % (w/v) PEG6000 5 % (v/v) DMSO pH 6.5

4.1.6.2. Chemicals and pharmacological agents

Table 2.9. List of chemicals used in the study

Name	Hersteller
5-Sulfosalicylic acid	Fluka
5-Bromo-2′-deoxyuridine	Sigma Aldrich
6-Amino-hexanoic acid	Roth
Acrylamide-Mix (Rotiphorese Gel 30)	Roth
Agar	Roth
Agarose	Biozym
Ammoniumchloride	Roth
Ammoniumperoxodisulfate	Roth
Ampicillin	Roth
BSA, Powder pH 6.5-7.5	Sigma Aldrich
Bromphenolblue	Serva
Bradford *protein assay* dye	BioRad
Calcium chloride ($CaCl_2$)	Roth
DMSO	Roth
DTE	Roth
DTT	Roth
EDTA	AppliChem
EGTA	Sigma Aldrich
Acetic acid	Roth
Formaldehyde, 37 %	Roth
Glycerine	AppliChem
Glycine	AppliChem
HD Green	Intas
Yeast extract	Serva
Immersion oil Type F, n_e^{23}=1,5180, v_e=46,	Leica Microsystem CMS GmbH
Isopropanol	Roth
Potassium chloride (KaCl)	Roth
Potassium hydrogen phosphate (KH_2PO_4)	Roth
Kanamycin sulphate	Roth
Magnesium chloride ($MgCl_2$)	Roth
Methanol	VWR

Mes	Sigma Aldrich
Sodium chloride (NaCl)	Roth
Sodium deoxycholate	Sigma Aldrich
Sodium fluoride	Sigma Aldrich
Sodium hydrogen phosphate (Na_2HPO_4)	Roth
Sodium hydroxide (NaOH)	Roth
Sodium ortho vanadate	Sigma Aldrich
Nocodazole	Sigma Aldrich
NP-40	Life Technologies
Nukleotide-Mix (Roti Mix PCR3)	Roth
Odyssey Blocking buffer (TBS)	LiCor
PEG 8000	Merck
PEG 6000	Merck
Penicillin / Streptomycin	Life Technologies
Phenylmethylsulfonylfluoride	Applichem
Ponceau S	Roth
SDS	Roth
Saponin	Sigma
TEMED	Roth
Tris	AppliChem
Triton X-100	Sigma Aldrich
Trypton	Serva
Tween 20	Roth
UltraPure™ DNase/RNase-Free Distilled Water	Gibco Invitrogen

4.1.7. Antibody and dyes

4.1.7.1. Primary antibodies

Table 2.10. List of primary antibodies used for western blotting

Antibody	**Type**	**Dilution**	**Company**
Cdc42 (B-8)	Mouse, monoclonal	1:100	SantaCruz, sc-8401
α/β/ɣ PAK (D-8)	Mouse,	1:500	SantaCruz,

	monoclonal		sc-166174
Phospho-PAK1 (Ser199/204)/PAK2 (Ser192/197)	Rabbit, polyclonal	1:200	Cell Signaling, 2605
βPix/ Cool1	Rabbit, polyclonal	1:200	Cell Signaling, 4515
GAPDH	Mouse, monoclonal	1:1000	Sigma, 8795
Myosin light chain 2, (D18E2)	Rabbit, monoclonal	1:100	Cell Signaling, 8505
Phospho-Myosin light chain 2, (S19)	Mouse, monoclonal	1:100	Cell Signaling, 3675
p115RhoGEF (ARHGEF1) D25D2-XP	Rabbit, monoclonal	1:500	Cell Signaling, 3669
GEF-H1 (ARHGEF2)	Rabbit, polyclonal	1:500	GeneTex, GTX125893
Anti-FAK	Mouse, monoclonal	1:1000	Millipore 05-537
Anti-phospho-FAK (Y397)	Rabbit, polyclonal	1:1000	Invitrogen 44624G
Anti-Ki67	Rabbit, polyclonal	1:500	Novus NB500-170
Anti-YAP	Maus, monoclonal	1:500	SantaCruz sc-101199
Anti-AKT (40D4)	Mouse, monoclonal	1:1000, 0.1 % Tween	Cell Signaling 2920
Anti-phospho-AKT (Ser473) D9E/XP	Rabbit, monoclonal	1:1000, 0.1 % Tween	Cell Signaling 4060
Anti-ERK 1/2 (p44/42 MAPK)	Rabbit, monoclonal	1:500	Cell Signaling 137F5
Anti-phospho ERK 1/2 (T202/Y204)	Mouse, monoclonal	1:500	SantaCruz sc-136521

4.1.7.2. Secondary antibodies

Table 2.11. List of secondary antibodies used for western blotting and immunostaining

Specificity	Conjugation	Dilution	Company
Goat-anti-MouseIgG	Alexa-488	1:500	Invitrogen A11029
Goat-anti-Rabbit IgG	Alexa-488	1:500	Invitrogen A11034
Donkey-anti-Rabbit IgG	IRDye680RD	1:20,000	LiCor Bioscience 925-68073
Goat-anti-Mouse IgG	IRDye680RD	1:20,000	LiCor Bioscience 925-68070
Goat-anti-Rabbit IgG	IRDye800RD	1:20,000	LiCor Bioscience 926-32211
Goat-anti-Mouse IgG	IRDye800RD	1:20,000	LiCor Bioscience 926-32280

4.1.8. siRNA Dharmacon

Table 2.12. Oligos used for siRNA mediated protein depletion

Name	Sequence (5´→ 3´)	Company
ON-TARGET plus non-Targeting #2	UGGUUUACAUGUUGUGUGA	Dharmacon
ON-TARGET plus siRNA Cdc42 #5	CGGAAUAUGUACCGACUGU	Dharmacon
ON-TARGET plus siRNA Cdc42 #6	GCAGUCACAGUUAUGAUUG	Dharmacon
ON-TARGET plus siRNA GEF-H1 #8	GAAGGUAGCAGCCGUCUGU	Dharmacon

ON-TARGET plus siRNA GEF-H1 #9	CCACGGAACUGGCAUUACU	Dharmacon
ON-TARGET plus siRNA (ARHGEF1) p115RhoGEF#5	UGACGUGGCGGGUGACUAA	Dharmacon
ON-TARGET plus siRNA (ARHGEF1) p115RhoGEF#6	AAACUGGUGUGCUCUCAUC	Dharmacon
ON-TARGET plus siRNA (ARHGEF1) p115RhoGEF#7	CCACGGCCCUUCGGAAAGU	Dharmacon
ON-TARGET plus siRNA (ARHGEF1) p115RhoGEF#8	UAUACGAGCUGGUGGCACA	Dharmacon
ON-TARGET plus siRNA (ARHGEF7) βPix	GAGCAUGAUUGAGCGGAUA UGAAUGUCCUCACGGAACA GGACGAGCUUUCCUUCUCA GGAGGAUUAUCAUACAGAU	Dharmacon
ON-TARGET plus siRNA PAK1 (αPAK)	ACCCAAACAUUGUGAAUUA GGAGAAAUUACGAAGCAUA UCAAAUAACGGCCUAGACA CAUCAAAUAUCACUAAGUC	Dharmacon
ON-TARGET plus siRNA PAK2 (ɣPAK)	GAAACUGGCCAAACCGUUA GAGCAGAGCAAACGCAGUA ACAGUGGGCUCGAUUACUA GAACUGAUCAUUAACGAGA	Dharmacon

4.1.9. Plasmids used

Table 2.13. Plasmids used in the study

Name	Description	Source
del-CMV-mCherry-WASP	WASP-GBD at C terminus of mCherry with truncated CMV promoter for low expression.	(Graessl et al. 2017)

del-CMV-mCherry	Empty vector mCherry with truncated CMV promoter for low expression.	Leif Dehmelt, (TU Dortmund)
del-CMV-EGFP	Empty vector, EGFP with truncated CMV promoter for low expression.	By Melanie Grassel, Nalbant Group
del-CMV-mCitrine-WASP	WASP-GBD at C terminus of mCitrine with truncated CMV promoter for low expression.	Leif Dehmelt, (TU Dortmund)
del-CMV-mCherry-RBD	Rhotekin-GBD at C terminus of mCherry with truncated CMV promoter for low expression.	(Graessl et al. 2017)
del-CMV-mCitrine-RBD	Rhotekin-GBD at C terminus of mCitrine with truncated CMV promoter for low expression.	Leif Dehmelt, (TU Dortmund)
EGFP-C1	Empty Vector backbone for EGFP	Clontech
EGFP-N1	Empty Vector backbone for EGFP	Clontech
mCherry-C1	Empty Vector backbone for EGFP	Clontech
del-CMV-EGFP-Actin	Low expressing EGFP Actin	Naokao Watanabe, (Japan) (Watanabe and Mitchison 2002)
pCMV-GFP-NMHCIIA	Myosin-IIa	Addgene 11347, (Wei and Adelstein 2000)
pCMV-mCherry-NMHCIIA	Myosin-IIa	Addgene 35687, (Dulyaninova et al. 2007)
mCherry-p114-RhoGEF	p114RhoGEF at C terminus of mCherry	Oliver Rocks (Canada), (Müller et al. 2018)

mCherry-p115-RhoGEF	p115RhoGEFat C terminus of mCherry	Oliver Rocks (Canada), (Müller et al. 2018)
mCherry-LARG	LARG-RhoGEF at C terminus of mCherry	Wedegaertner Group; (Grabocka and Wedegaertner 2007)
mCherry-p190-RhoGEF	p190RhoGEF at C terminus of mCherry	Oliver Rocks (Canada), (Müller et al. 2018)
mCherry-AKAP13	AKAP13-RhoGEF at C terminus of mCherry	Oliver Rocks (Canada), (Müller et al. 2018)
mCherry-PDZ-RhoGEF	PDZ-RhoGEF at C terminus of mCherry	Oliver Rocks (Canada), (Müller et al. 2018)
mCherry-GEF-H1 wt		Jörg Birkenfeld (Birkenfeld et al. 2007)
pCMV5- EGFP-GEF-H1 Wt		Jörg Birkenfeld (Birkenfeld et al. 2007)
Ezrin-EGFP	Ezrin at N term of EGFP	Addgene 20680, (Hao et al. 2009)
Moesin-EGFP	Moesin at N term of EGFP	Addgene 20671, (Hao et al. 2009)

4.1.10. Microscopes used

4.1.10.1. Andor/Nikon Spinning Disc confocal and TIRF

The inverted Nikon Ti/E microscope can be used for Confocal imaging (spinning disc), TIRF, FRAP, multiposition acquisition, fast live cell experiments.

It is equipped with Perfect Focus System PFS, EMBLEM microscope incubator box with control device (temperature & CO2 control for live-cell imaging). For the experiments here, Apo TIRF 100×1.49 NA oil immersion objective, a Clara Interline CCD camera (Andor Technology) and an iXon3 897 single photon EMCCD camera (Andor) were used. For the excitation of GFP and RFP, laser light with wavelengths of 488 or 561 nm was emitted by an AOTF Laser Combiner (Andor Technology) and filtered by a dual bandpass dichroic mirror (zt488/561rpc, AHF) for TIRF imaging, and a CSU Quad Dichroic mirror/emission filter set (405/488/568/647 nm; Semrock) for widefield imaging. Multiple positions were imaged at the same time (up to 40 frames with a frame rate of 3/min) or single cell measurements were performed (up to

300 frames with a frame rate of 20/min) under the control of Andor IQ Software (Andor Technology). For fixed cell managing, CFI PI Apo 40X/0.95 dry objective was used.

4.1.10.2. Nikon Ti-E inverse

The inverted Nikon Ti-E inverse microscope can be used for epifluorescence and transmitted light applications (DIC, phase contrast, bright field). For the phase contrast applications, CFI Plan Flour 10X/0.13 dry objective was used. The setup has halogen lamp for transmitted light and an external mercury burner (100W) fluorescent lamp. It is also equipped with okolab microscope cage incubator box with control device (temperature & CO2 control for live-cell imaging). For acquisition a Roper Scientific CoolSNAP HQ2 interline-transfer CCD camera, 1392 x 1040 imaging array, 6.45 x 6.45 µm pixels, 14-bit digitization is available. For fluorescence, EGFP/mCherry Dualband sbxm ET Filterset (AHF F89-002), BFP/GFP/HcRed Tripleband sbx HC Filterset (AHF F66-422), CFP/YFP Dualband sbxm ET Filterset (AHF F89-002) is available. The system is controlled by Nikon NIS Elements AR software.

4.2. Methods

2.2.1. Molecular biological methods

2.2.1.1. Media preparation for bacterial culture

The media composition was as followed in (BERTANI 1951). Components for media were added in half the required volume and dissolved. The pH was adjusted to 7.4 as required. Volume made to the given amount and the contents sterilised at 121°C, 15 psi, for 60 to 90 mins. For preparation of solid media, 1.5 % agar was added to given liquid media before sterilization. When the temperature of the agar contents was reduced but the components were still liquid, media was poured in petri dishes and allowed to solidify.

2.2.1.2. Preparation of heat-shock competent *E.coli*

Heat-shock competent *E. coli* cells were prepared according to Chung et al. (Chung et al. 1989). Cultured 10 µl bacterial suspension (DH5α, Invitrogen) was added to 4 ml of antibiotic-free LB-medium and incubated for 14-16 h (37°C; 180 rpm). This overnight culture was then used to inoculate 400 ml warm LB-medium, which were incubated shaking (180 rpm) until an OD_{600} of 0.4 to 0.5 was reached. The bacterial suspension with OD_{600} of 0.5 was incubated for at least 20 min on ice and sedimented by centrifugation (10 min, 4000 rpm, 4°C). The obtained bacterial pellet was

suspended in 15 ml ice cold TSS buffer. TSS buffer was freshly prepared. Finally, the suspension of competent bacterial cells was portioned in 200 µl aliquots, shock frozen in liquid nitrogen and stored at -80°C.

2.2.1.2. Bacterial transformation using heat-shock

To obtain and amplify the available plasmids, these were first amplified by culturing in bacterial strains. The frozen aliquot of heat competent *E.coli* cells was thawed on ice and about 25 to 50 ng of plasmid DNA was added for plasmid transformations. The mix was incubated on ice for 30 mins with intermittent mixing. A heat sock was given to the cells for 90 sec at 42°C and immediate snap cooled on ice. It was further incubated on ice for 10 min. To this 200 µl mixture, 800 µl of antibiotic-free LB-medium was added to each tube, which was then incubated (180 rpm) at 37°C for 60 min. Bacterial cells were sedimented by centrifugation (3 min, 13000 rpm) and 800 µl of the supernatant was discarded, while the remaining media was used to suspend the pelleted *E.coli* cells. This suspension was plated on LB Agar plates containing the corresponding antibiotic and incubated overnight at 37°C. The petri plates with transformed bacterial colonies were stored at 4°C for approximately three weeks.

2.2.1.4. Preparation of bacterial glycerol stocks

Cloned DNA plasmids and obtained DNA plasmids were also stored as bacterial glycerol stocks as a backup. A single colony obtained after transformation was inoculated in LB media and grown overnight (37°C; 180 rpm). 500 µl of the overnight culture was then mixed with glycerol (50 % (v/v)) and stored at -80°C.

2.2.1.5. Isolation of plasmid DNA from *E.coli*

Small amounts of plasmids were purified from bacterial overnight cultures using the GenElute plasmid Miniprep Kit (Sigma-Aldrich), procedure as indicated by manufacturer. For large scale preparations and for tricky plasmids Endo free, maxi preparation was performed using the QIAprep Spin Maxiprep Endofree Kit (Qiagen). Plasmids were stored at -20°C for use and an aliquot stored at -80°C as a backup.

2.2.1.6. Determination of DNA concentrations

The DNA concentrations of isolated plasmids was determined spectrophotometrically. The absorption maxima of DNA were seen at 260 nm while that of proteins was observed at 280 nm, thus OD260/OD280 indicates the ratio between nucleic acids and proteins and therefore the purity of the DNA solution. All spectrophotometrically measurements were performed with a Nanodrop spectrophotometer (ND-100, PeqLab) using pure solvent (water or EB) as reference.

4.2.2. Biochemical methods

4.2.2.1. Protein isolation from cultured cells

Total protein isolation from adherent cells is the first step for protein based biochemical assays like immune blotting, immuno-precipitation, protein pull down assays and so on. Here RIPA buffer originally developed for radioimmunoprecipitation assays) was utilized in combination with a protease-inhibitor cocktail to prepare cell lysis and protein isolation buffer. Stocks of all solutions were prepared and stored at 4°C or -20°C as directed by manufacturers. Lysis buffer prepared fresh for ever isolation procedure.

Table 2.14. Lysis buffer components:

Components	Final concentration
RIPA	
Protease inhibitor (7X)	1X
Phosphatase inhibitor (10X)	1X
Sodium fluoride (200mM)	1mM
Sodium orthovanadate (200mM)	1mM

Cells cultured in one or two 35 mm dishes (one or two wells of a 6 well dish) were washed with ice cold PBS buffer and 65 µl of Lysis buffer was added to each dish and incubated for 5 min. Cells were scraped and incubated on dish for another 5 min post scaping. The scrapped cell and solution were then collected and centrifuged for 30 min at 4°C (14000 rpm). The supernatant obtained post sedimentation was placed in a fresh tube and pellet discarded. The concentration of total protein was determined

for each sample and the lysates were then prepared for followed by SDS-PAGE, western blot and immunodetection.

4.2.2.2. Determination of protein concentration

Bradford methods (Bradford 1976) is one of the simpler colorimetric methods commonly used to determine total protein concentration in biology. When sulfonic acid groups of the dye bind to basic amino acids (mainly arginine, lysine and histidine) of proteins, its maximal absorbance is shifted from 470 nm to 595 nm. This color change of the dye from red to blue is measurable via the level of absorbance at 595 nm. The more the amount of protein more is the binding and hence deeper the colour change. By comparing the absorbance to a freshly prepared standard curve, protein concentration can be determined. Here Bradford solution from Bio-Rad was used. Bradford-solution (BioRad) was diluted 1:5 in water and 1 ml of this assay buffer was mixed with 5 µl of five BSA solutions of varying concentrations (0.4; 0.8; 1.2; 1.6; 2.0 µg/µl in Tris-HCl Buffer) each, as well as 5 µl of fresh cell lysate. All samples were prepared as duplicates and incubated for 5 min at RT, before the absorbance at 595 nm was documented with a spectrophotometer (Thermo Scientific).

4.2.2.3. SDS-PAGE

Separation of proteins according to their molecular weight after reduction is a technique described by Laemmili, (Laemmli 1970). SDS (sodium dodecyl sulfate) plays a key role in this method, since it denaturizes the proteins and masks their electrical charges, generating micelles with a constant negative charge / mass ratio. The polyacrylamide gel hinders those micelles to move towards the anode if an electric field is applied, resulting in drift velocities inversely proportional to the molecular weight of the proteins. Here, polyacrylamide gels containing 5 % acrylamide-bisacrylamide mix (30 %) were used for stacking and 10 or 15 % gels for separating the proteins, see Table,

Table 2.15. Components of stacking and separating gels for SDS-PAGE

Reagent	**15 % Resolving Gel (10 ml)**	**10 % Resolving Gel (10 ml)**	**5 % Stacking Gel (4 ml)**
Water	2,3 ml	4 ml	2,7 ml
Acryl-Bisacrylamid-Mix (30 %)	5 ml	3,3 ml	670 µl
SDS (10 %)	100 µl	100 µl	40 µl
Stacking gel buffer Tris pH 6,8	--	--	500 µl
Resolving gel buffer Tris pH 8,8	2,5 ml	2,5 ml	--
APS (10 %)	100 µl	100 µl	40 µl
TEMED	4 µl	4 µl	4 µl

Six Whatman filter papers were stacked from anode to cathode of the blotting chamber, in the following order: - Two filter papers soaked in anode buffer I
- One filter paper soaked in anode buffer II
- PVDF membrane incubated in anode buffer I
- Gel incubated in cathode buffer
- Three filter papers soaked in cathode buffer

The proteins were transferred at 20 V for 15 to 60 min, depending on molecular weight of protein of interest. This was then verified by staining the membrane with total protein stain (LiCor). In order to precisely identify the immobilized proteins, primary antibodies were used that bind specifically to the target proteins. The secondary antibodies bind to the Fc region of immunoglobulins, specific for the organisms from which the primary antibody originated. Additionally, the secondary antibodies are fused to fluorescent dyes detectable using Odyssey scanner or horseradish peroxidase (HRP), enabling an enzyme-based quantification of the target proteins. To prevent unspecific binding of the antibodies, the PVDF membrane was incubated with blocking solution (LiCor blocking bufferr or 5 % BSA in TBS-T buffer) at RT for 1 h. Afterwards the membrane was immunostained (overnight, 4°C) with the primary antibody diluted in blocking solution (see Table 2.17 for dilution factors). The next day, unbound antibody was washed off by three incubation steps with TBS-T for 10 min, before the membrane

was placed in blocking solution, containing the secondary antibody. After 1 h incubation at RT the unbound secondary antibody was washed off with TBS-T again, whereat the last of the three washing steps (10 min, RT) was performed with TBS, to prevent an impairment of the detection reagent by the Tween enclosed in the TBS-T buffer. Fluorescent detection was documented in Odyssey scanner and with Image Studio software LiCor. For enzymatic detection, reagent entry-level peroxidase substrate for enhanced chemiluminescence (ECL, SuperSignal West Pico, Thermo Scientific) was used for 5 min at RT. This substrate enables a quantitative detection of HRP activity, which was documented on a Fusion FX7 system and analysed using densitometrical properties in Bio1D software (PeqLab).

Table 2.16. Blotting time and method for given proteins

Protein	**Method**	**Resolving Gel**	**Blotting**
Cdc42	Flourescence, IRDye Antibody	15 %	15 min
pPAK/PAK	Flourescence, IRDye Antibody	10%	25 min
βPix	Flourescence, IRDye Antibody	10%	25 min
GAPDH	Enzymatic, HRP	10 or 15 %	All times suitable
GEF-H1	Flourescence, IRDye Antibody	10%	45 min
p115 RhoGEF	Flourescence, IRDye Antibody	10%	45 min
pFAK/FAK	Flourescence, IRDye Antibody	10%	40 min

4.2.3. Cell biological methods and microscopy

Human primary, Neonatal human Keratinocytes (NHEK) and human osteosarcoma cell line (U2OS) was used in this study. All cell cultural methods involving direct handling of living cells were performed under sterile conditions in a biosafety cabinet (Thermo Scientific). Cells were cultured at constant temperature (37°C), carbon dioxide concentration (5 %) and high humidity (90-95 %) in a CO2-incubator (Thermo Scientific). At regular intervals, the cells were examined microscopically for bacterial contaminations, an infection with *mycoplasma* was excluded by periodic testing (VenorGeM, Minerva Biolabs; GATC mycoplasma tests).

4.2.3.1. Subculture of adherent cells

Socks of NHEK cells were cultured in T_{25} polystyrene flasks, suitable for adherent cells with filtered caps for air exchange (Corning). Stocks of U2OS cells were cultured in polystyrene dishes, suitable for sensitive adherent cells (35 x 10 mm, Cell+, Sarstedt). Every three to four days, when a confluency of 80-90 % was reached, the cells were seeded into fresh growth medium. For cell splitting, aliquots of growth media, PBS and trypsin were warmed up in a water bath (37°C). NHEL cells were incubated with 5 ml ward DBPS for 5 mins followed by 400 µl of Trypsin for 7 min at 37°C. Cells were also dislodged by tapping the flask gently and trypsin neutralised by adding trypsin neutralising solution. 4.2 ml DPBS was added to make a volume of 5 ml and cells were pelleted at 200g for 5 min. The trypsin containing DPBS was discarded and cells were suspended in 2 ml of complete derma life media. Cells were counted and seeded for maintenance. Since NHEKs are primary cells, these were used for 5 passages after thawing. For U2OS cells, the adherent cells were washed with 10 ml PBS and incubated with 2 ml of trypsin at 37°C for 5 mins. Cells were examined with a light microscope and incubated for another 2-5 min, if some cells still remained attached to the surface. When all cells were brought into suspension, trypsin was inactivated by addition of 8 ml warm growth medium and clustered cells were split up by pipetting up and down several times. The number of cells in the suspension was determined using a counting chamber (Improved Neubauer, depth 0.1 mm, Hartenstein) and 3-4 x105 cells were added to a new dish, filled with 10 ml fresh growth medium. This procedure was repeated up to passage twenty, before a new, low-passage cell stock of U2OS cells was thawed and cultivated (see next section).

4.2.3.2. Cryopreservation of cells

To conserve cells during long-term storage, they are frozen at -150°C, inhibiting enzymatic or chemical activity that could damage the cells. The major problem in cryopreservation is reaching low temperatures without the formation of intercellular ice crystals, which is solved by DMSO addition and the usage of a cryo freezing container that cools down the cells very slowly, with a rate of 1°C / h. NHEK cells were cultured and every early passage was frozen. Typically, 500 µl cell suspension containing 1 to 5 *10^6 cells were mixed with equal volume of the cryo preservative CryoSFM and mixed dropwise in a cryo tube (Roth). For U2OS cells, dishes with 70 % confluency were washed and trypsinized, and cells sedimented (5 min, 1000 rpm). The supernatant was discarded and the cell pellet was resuspended in 8 ml freezing

medium (growth medium, containing 5 % DMSO). The resulting cell suspension was aliquoted in cryogenic tubes (Roth), This was then transferred to an isopropanol-filled cryo freezing container (Sigma-Aldrich) and frozen overnight at -80°C. The next day the tubes were transferred into a -150°C freezer for long-term storage.

To bring back frozen cells to culture, aliquots were transported on ice and incubated in a water bath (37°) just until the cell suspension was thawed. At this point, the cells were transferred into 14 ml of warm growth medium and centrifuged for 5 min at 1000 rpm. The DMSO or cryo-preservative containing supernatant was discarded, while the pelleted cells were resuspended in 5 ml warm growth medium and placed into appropriate dishes or flasks for culturing.

4.2.3.3. Transient transfection with siRNAs and plasmid DNAs

Transient siRNA transfection was performed using the Fast-Forward transfection reagent Lipofectamine® RNAiMax (Invitrogen). This method is constituted by simultaneous cell seeding and transfection. Here NHEK cells were prepared according to usual procedure and counted. Simultaneously, transfection mix was prepared by adding 100 µl OptiMEM (Life Technologies) per well, mixed with 20 nM of siRNA of interest (Cdc42 siRNA oligo #5, Cdc42 siRNA oligo #6, Smart Pool siRNA oligo mix for PAK1, Smart Pool siRNA oligo mix for PAK2, Smart Pool siRNA oligo mix for βPix or non-targeting siRNA) and incubated for 5 min at room temperature. Simultaneously, 2.4 µl of Lipofecatamine RNAiMAX was added to 100 µl OptiMEM and incubated for 5 min. The siRNA aliquot and RNAiMAX aliquot was mixed and then incubated for 5 min together. In a 6 well dish, each well was labelled according to the required siRNA mix and cell suspension was added and RNAi solution was added dropwise. The volume was made to 2 ml whole and this was incubated overnight at 37°C incubator. The siRNA cells were split after 24h and seeded for required experiments like western blot and imaging in required dishes coated with 10µg/ml of Fibronectin. Cells were used for experiments 72h post siRNA transfection.

4.2.3.4. Transient transfection plasmid DNAs

Cells were transfected with required plasmids one day prior to live cell imaging. For NHEK cells, TRANSiT transfection reagent (MiRUS) was used. In 200µl of OptiMEM, 4 µl of TRANSiT and 1µg of the required plasmid were added. This mix was incubated for 20 mins at room temperature and added on cells without changing medium. In

Keratinocytes, the factors secreted by cells are essential for optimal transfection and hence media change prior to addition of transfection mix is avoided. Adherent U2OS cells were transfected using Lipofectamine 2000 reagent (Invitrogen). Micelles with plasmid DNA were prepared by mixing 100µl of OptiMEM and 3 µl of Lipofectamine 2000 and in a separate tube 100µl of OptiMEM and 200 to 500 ng of required plasmid DNA. Both mixes were incubated for 5 min and mixed together. This was then incubated for 20 min at room temperature. The mix was then added drop wise on cells after

4.2.3.5. Sample preparation for live-cell imaging and drug treatments

For live cell experiments with NHEK cells, glass bottom dishes were coated with 10µg /ml of Fibronectin for 15 mins and washed with DPBS once before seeding cells. For imaging motility induced cells, culture media was replaced to imaging media and 100ng/ml of EGF was added and incubated for 1h before imaging. For on stage growth factor addition, growth media was replaced by imaging media and during imaging interval media with EGF was added, to make complete concentration of 100ng/ml of EGF.

For pharmacological inhibition of PAK 1/2/3 the PAK inhibitor FRAX597 (1µM) was used. Cells were treated with the PAK inhibitor or DMSO control for 1h and then used for Western blot analysis or stimulated with 100ng/ml EGF and imaged for Cdc42 activity or cell migration.

U2OS cells were seeded on either glass bottom dishes or elastomeric substrates coated with collagen type I, to create an ideal environment for U2OS cell that is suitable for high resolution microscopy. For obtaining this, a solution of 1% (v/v) collagen (from rat tail, type I, BD Bioscience) in PBS was added on top of the glass or elastomeric surfaces within the dishes, which where incubated for 1-2 h at 37°C or overnight at 4°C. The abundant collagen was washed off with 3x 1 ml PBS and 1.5 x 10^5 U2OS cells were plated in 2 ml growth medium on each dish. After an incubation at 37°C for 24-30 h, the cells were transfected with Lipofectamine 2000 or were fixed for staining.

For inhibiting the Rho effector ROCK, Y-compound treatment was used. Typically, cells were treated with 30µM of inhibitor or water as a solvent control for 1h. Cells were imaged before addition of inhibitor and 1h post ROCK inhibition.

Cells respond to the environment they are in contact with. For understanding the effect of different extracellular matrix components on Rho activity pulses in U2OS cells glass bottom dishes were coated with a solution of a solution of 1% (v/v) collagen (from rat tail, type I, BD Bioscience) in PBS or 10µg/ml of Fibronectin in PBS or 0.001% Poly-L-Lysine (Sigma) in PBS, independently for overnight at 4°C. Prior to use the coating was removed and dishes washed thrice with DPBS. U2OS cells were split according to above mentioned protocol and sedimented by centrifugation at 1000 rpm, for 5min. Media was discarded and cells were suspended in media without FBS and seeded on respective dishes and incubated for 2h at 37°C. Cells were then transferred to microscope chamber and imaged for Rho activity pulses.

Table 2.17. Conditions used for drug treatments

Drug	*Final concentration*	*Incubation period*
FRX597	1 µM	60 min
Y-27632	30 µM	60 min

4.2.4. Live-cell TIRF and spinning disc microscopy

Total internal reflection fluorescence (TIRF) microscopy enables excitation of fluorophores in an extremely thin optical section. When light is totally internally reflected in a transparent solid, an electromagnetic field is generated at the interface with liquid called as evanescent wave (Fish 2009). It is of the same frequency as the excitation light. The generation of such an evanescent wave is exploited in TIRF microscopy. It has a defined depth, of approximately 100nm and hence is completely suitable observation of cell contacts with the surface (AMBROSE 1956; Axelrod et al. 1984). Such a method provides high spatial resolution, less toxicity and reduces the background signal. Now, TIRF microscopy is widely used for visualizing fluorescent molecules close to the membrane, membrane dynamics and the interaction of membrane bound proteins.

For the TIRF experiments shown in this thesis, the Andor/Nikon Spinning disc TIRF microscope was used. For imaging, cells were plated on glass bottom dishes coated with an extracellular matrix component (fibronectin/ collagen/ Poly-L-Lysine) as per the experimental requirement. Images were acquired with a 2X2 binning and a frame rate of one per min, three per min, fifteen per min or twenty per min. Usually for lower frame rates multi-position images were acquired. For on stage growth factor

stimulations, a frame rate of three per minute was used and the entire image acquired for approximately 12 min. media with growth factor was added at half time during the 20s imaging interval. Spinning disc mode of the same microscope was used for fixed cell imaging of U2OS cells. The Lasers Diode 640, 561, 488 and 405 were used sequentially as required with the corresponding filter settings.

4.2.4.1. Phase contrast microscopy

Migration of Keratinocytes was studies using the Nikon-Ti inverted epifluorescence microscope. The Plan Flour 1=X/0.13 objective was mainly used for this purpose. Typically, cells were seeded on 10µg/ml Fibronectin coated dishes. 1 h prior to imaging the cells were simulated with 100ng/ml of EGF for 1h. For tracking transfected cells, a single fluorescence image was acquired to register the cells with fluorescent proteins followed by a time lapse series phase contrast series with a frame rate of 1 per min for one hour.

4.2.4.2. Immunostaining of cells

U2OS cells plated on glass bottom or with substrates of different elasticity were fixed using 4% formaldehyde for 20 min followed by three PBS washes. Cells were then permeabilised by 0.1% Triton-X 100 for 10 min followed by three PBS washes. Blocking was performed by 10% BSA in PBS solution. Primary antibody for YAP/Ki67 was prepared in blocking solution (1:1000) and incubated for 1h in wet chambers followed by three PBS washes. A mixture of Rhodamine phalloidin for actin labelling and secondary antibody along with DAPI (1:10000) for nuclear staining was prepared in blocking solution. The cells were then incubated with this mixture for 1h followed by three PBS washes. The coverslips were then mounted on glass bottom slides with mounting medium (Prolong, Invitrogen) allowed to stabilise for 1 day at room temperature and then stored at 4°C until microscopy was performed.

4.2.5. Data analysis

Imaging data was analysed using Matlab R2017b and ImageJ 1.52p (http://imagej.nih.gov/ij/) running on Java 1.8 (64-bit). Statistical analysis and generation of software graphs were performed using GraphPad Prism. All Figures were prepared with Adobe Photoshop CC2014. The analyses of oscillatory behaviour were developed in collaboration with Dr. Leif Dehmelt (MPI Dortmund / CCB, TU

Dortmund) and Dr. Tomáš Mazel (Charles University, Prag). The analysis of Myosin flow was performed according to STICS velocimetric flow plugin developed by Jay Unruh ref.

4.2.5.1. Temporal cross correlation analyses

Temporal cross correlation functions were derived from image sequences obtained with a frame rate of 20/min and a 2x2 binning. Further, noise was eliminated by scaling the x-y resolution by a factor of 15-20 with the averaging command in ImageJ. After this processing, the Pearson product-moment correlation coefficient of time shifted corresponding images was calculated using custom Matlab scripts. The spatio-temporal cross-correlation function was determined by using the original 2 x 2 binned image sequence in which time shifting was combined with spatial shifting of corresponding image sequence by steps of 4 pixels. Mono-exponential decay functions were used for fitting the half time and decay length of cross-correlation analysis.

4.2.5.2. Analyses of oscillation amplitude, peak frequency and peak width

Image sequences were recorded with a frame rate of 3/min or 20/min and 2x2 binning. Using ImageJ, individual cells were isolated from these images, thresholded, masked and corrected for background intensity. Afterwards, image x-y resolution was scaled down by a factor of 15-20, to reduce noise. To avoid false measurements originating from fluctuations of cell protrusions, peripheral pixels were removed via a binary erode filter with a neighbourhood count of 1. Global intensity fluctuation was excluded from the analyses by dividing each frame by the average background-corrected intensity. The remaining pixels were evaluated regarding their temporal intensity changes, to assess the local fluctuations associated with irregular oscillations. For this purpose, image series with a frame rate of 20/min were analysed with a walking average of 7 frames and thus, the standard deviation of the intensity in each pixel over time was calculated. If the intensity at the given time-point differed by at least 1 % of the average intensity from the following and preceding intensity, a time-point was measured as a peak. To determine oscillation frequency, only peaks that were above 10% of the average intensity were included. As peak height, the difference between the intensity of a peak and the average intensity of the following and preceding minima was

measured. The peak width, or duration, was determined as the time difference between two intensity minima.

4.2.5.3. STICS velocimetric flow

Myosin flow velocities were calculated using STICS analysis using an Image J plugin (http: //research.stowers .org /imagejplugins /ics plugins .html). The script was originally written by Jay Unruh (Yi et al. 2011). Vector maps of flow velocity and flow velocities for Myosin signal were generated using the STICS plugin on acquired sequences (15 frames/min). A custom ImageJ macro was used to calculate a series of vector maps, each of which was based on sub-sequences containing two frames before and after the respective time point. Resultant vectors were calculated from the obtained individual vectors and averaged for each time point and each cell.

4.2.5.4. Statistical analyses

For statistical analysis of more than two individual conditions One-way anova with Dunnettes Post-test was performed to compare the conditions with control condition (in siRNA experiments). In some cases, when comparison between all columns was experimentally essential, One-way anova with Tukey Post-test was performed. In experiments with only two conditions, two-tailed paired t-tests were performed for data sets derived from the same cells (e.g. pre and post drug treatment), while two tailed-t-tests were used to analyse data sets from different cells. To verify that the temporal delays derived from crosscorrelation analyses are indeed unequal zero, one-sample t-tests were applied. P-values of t-tests are indicated by stars (*: $P<0.05$; **: $P<0.01$; ***: $P<0.001$; ****: $P<0.0001$). Mean values are denoted ± s.e.m. if the corresponding data sets comprised more than ten values, otherwise mean values are given ± s.e.m. In all scatter dot plots mean values are illustrated by red lines

3. Results

3.1. Role of Cdc42 in Keratinocyte migration

Cdc42 is a ubiquitously expressed Rho GTPase essential in various cellular processes such as establishment of cell polarity, cell migration and morphogenesis (Goicoechea et al. 2014; Duquette and Lamarche-Vane 2014). As mentioned earlier, migration, proliferation and differentiation are important cellular functions of Keratinocytes during homeostasis and wound healing. Although, Cdc42 was shown to regulate progenitor cell differentiation in mouse Keratinocytes by controlling β-catenin turnover through Protein Kinase C (PKC) its role in Keratinocyte migration is largely unknown (Wu et al. 2006b). Here, live cell imaging with the Rho GTPase activity sensors available in our lab along with biochemical methods were used to study the role of Cdc42 in Keratinocyte migration.

3.1.1. Cdc42 is a component of Keratinocyte migration machinery

Cdc42 has been reported to be a major component for migration of neutrophils (Kumar et al. 2012), dendritic cells (Lämmermann et al. 2009), astrocytes (Osmani et al. 2010), cancer cells (Reymond et al. 2012) and fibroblasts. To understand its role in Keratinocyte migration, phase contrast microscopy after depletion of Cdc42 was used. For this, cells migrating individually were tracked using Image J, manual tracking plugin and plotted using the IBIDI, Chemotaxis and migration Tool (fig. 3.1A). Depletion of Cdc42 significantly reduced average migration velocity of cells with two different Cdc42 targeting siRNA oligomers (Non-targeting siRNA = 1.77±0.11 S.E.M. µm/min, Cdc42 oligo#5=1.14±0.08 S.E.M. µm/min, Cdc42 oligo#6=1.31±0.10 S.E.M. µm/min) (fig. 3.1A, B). To better understand the underlying reasons for decreased migration velocity in cells lacking Cdc42, analysis of protrusion and cell body retraction was manually performed for individually migrating cells. Cells were polarized from the first frame of imaging and from time point zero, a protruding front and a retracting back was defined. Change in number of protruding edge or contracting edge was recorded as a new protrusion or a retraction for a total duration of 1 h. The control, non targeting cells on an average displayed 1.92±0.2 protrusions per hour. The Cdc42 depleted cells by oligomer 5 had 2.5±1.4 and by oligomer 6 had 2.06±0.2 protrusions per hour (fig. 3.1E) although not significantly more than the non targeting control. A similar measurement of the contracting edges displayed a significant decrease in contractions for Cdc42 depleted cells by oligomer 6 (2.97±0.24 contraction per hour, 2.64±0.19 per

hour for Cdc42 depletion by oligomer 5, and 2.09±0.18 per hour for Cdc42 depletion by oligomer 6, fig. 3.1 D to F). Thus, in agreement with several other cell types, data here suggests that Cdc42 is a regulatory component of the migration machinery in Keratinocytes.

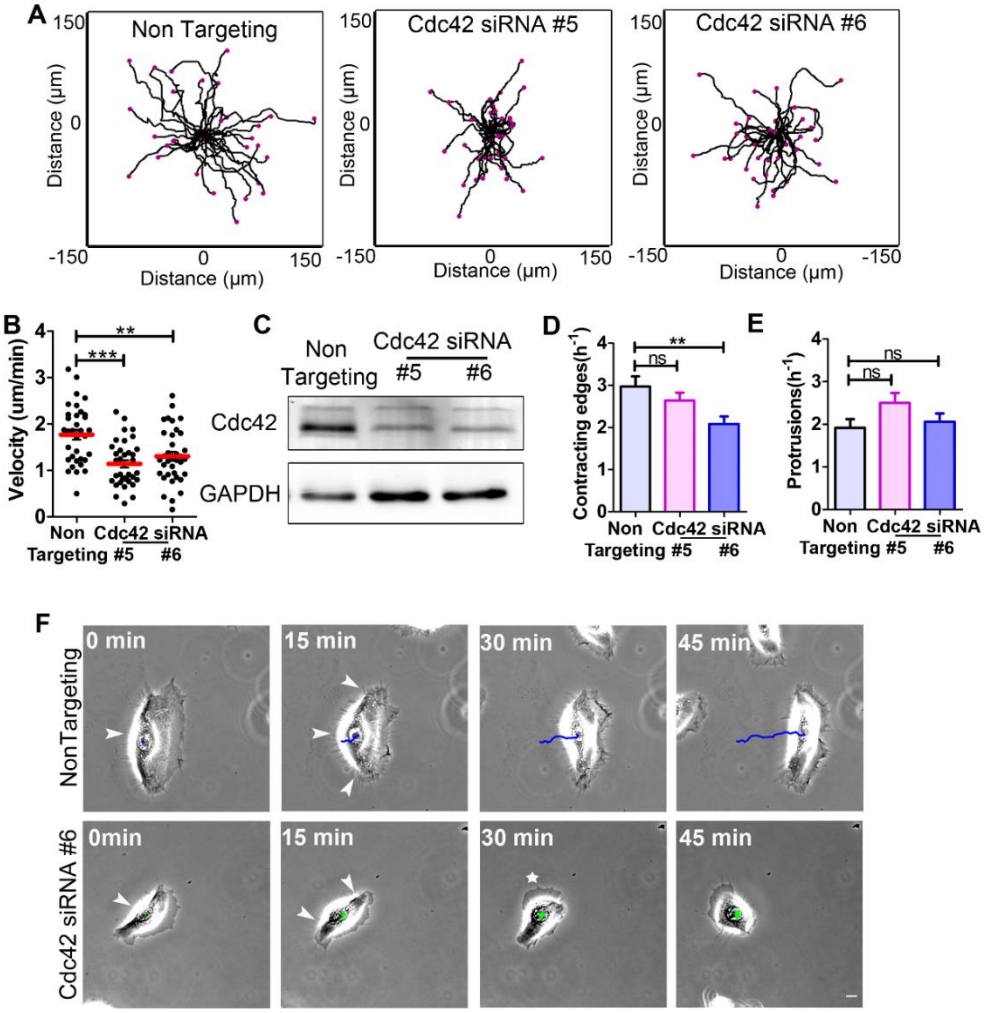

Figure 3.1: Cdc42 depletion leads to impaired migration. (A) Migration plots of individual cells with non-targeting (20nM) and Cdc42 siRNA oligo#5 and oligo#6 (20nM for each). Images were acquired at 1 frame per min. for 1h. (B) Plots of cell migration velocity for control and Cdc42 siRNA treated cells. (C) Representative western blot showing Cdc42 protein and GAPDH as housekeeper control. (D) Plots showing contracting edges per cell during the time of time-lapse experiment (1 h) (A, B) Contracting edges in individual siRNA treated cells were counted manually. (E) Plots showing number of protrusions per cell during the time of time-lapse experiment (1h) (A, B). Protruding edges in individual siRNA treated cells were counted manually. (A to E: ≥ 34 cells from 3 independent experiments, *: P=0.05, **: P=0.01, ***: P=0.001. One-way Anova, Dunnett's post Test) (F) Representative phase contrast images of cells treated with non targeting siRNA and Cdc42 oligo#5, respectively. Blue line indicates migration path for non targeting siRNA treated cell while green line indicates migration path of a Cdc42 siRNA oligo#6 treated cell.

3.1.2 Cdc42 activity is localized at the trailing edge of a migrating Keratinocyte

To further comprehend the role of Cdc42 in Keratinocyte migration, spatio-temporal Cdc42 activity patterns in migrating cells were studied using a fluorescently tagged effector domain based activity sensor (Graessl et al. 2017). Briefly, Cdc42 binding domain of the WASP effector (WASP-GBD) was N-terminally tagged with the fluorescent proteins mCitrine or mCherry, respectively. As this domain only interacts with the activated conformation of Cdc42, its accumulation can be used as a measure for Cdc42 activity. Upon activation, Rho GTPases translocate to the plasma membrane by their post-translational lipid modifications such as prenylation or palmitoylation at the CAAX motif (Hodge and Ridley 2016). Hence, TIRF microscopy was used to monitor Cdc42 activity at the membrane and near membrane regions. In addition, a truncated CMV promoter was used to allow for low expression levels and to avoid high over expression toxic effects resulting in a sensitive approach (Watanabe and Mitchison 2002) .

TIRF time-lapse measurements revealed two distinct subcellular Cdc42 activity patterns in migratory Keratinocytes. First, local activity pulses were observed in the lamellum region, reminiscent of previously detected Cdc42 activity patterns in U2OS cells (fig. 3.2A and B) (Graessl et al. 2017). Secondly, a more prominent activity zone was found in 89.9±5.2% (S.E.M.) of cells that was more persistently localized at the cell periphery (fig. 3.2A and C). To understand the potential link of this persistent activity zone to dynamic cell behavior, normalized intensity plots of Cdc42 activity along the migration axis were generated. Zone of elevated Cdc42 activity significantly coincided with the trailing edge in migrating Keratinocytes.

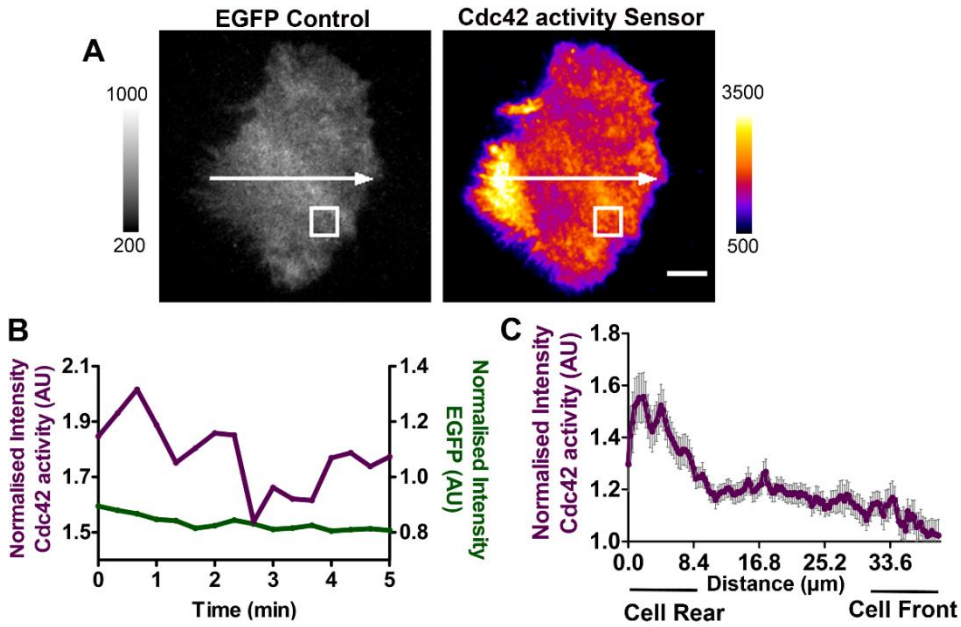

Figure 3.2: Two distinct Cdc42 activity patterns are observed in migrating Keratinocytes. (A) Representative TIRF images showing control sensor (delCMV-EGFP) in gray scale and Cdc42 activity sensor (delCMV-mCherry-WASP-GBD) in fire Look up table (LUT), within the same cell. White arrow indicates direction of migration as well as the line for measuring cell intensity from cell rear to cell front. Here migrating Keratinocytes were studied after treatment with EGF (100 ng/ml, 1h). Scale bar= 10µm. LUT's depict arbitrary units. (B) Cdc42 activity pulses in cell lamellum. Intensity plots are shown for the duration of 5 mins corresponding to the boxed region of interest shown in A, of control sensor or Cdc42 activity sensor, normalised with mean signal intensity of the entire cell at the first frame of imaging. (C) More persistent local activity in the rear end. Intensity plot of Cdc42 activity measured along the white arrow shown in A from cell rear to cell front normalised with mean signal intensity of the entire cell for at the same frame. (n≥28 cells from 3 independent experiments).

To confirm that the signal patterns observed with the delCMV-mCherry-WASP-GBD sensor in migrating Keratinocytes indeed report Cdc42 activity, the GTPase was depleted using siRNA and TIRF measurements with the aforementioned sensor were performed. Depletion of Cdc42 resulted in loss of intense activity localization as seen in figure 3.3. Statistical analysis showed significant loss of sensor signal at the trailing edge (fig. 3.3C) confirming that patterns observed using the delCMV-mCherry-WASP-GBD biosensor (fig.3.2 and 3.3) were indeed due to endogenous Cdc42 activity.

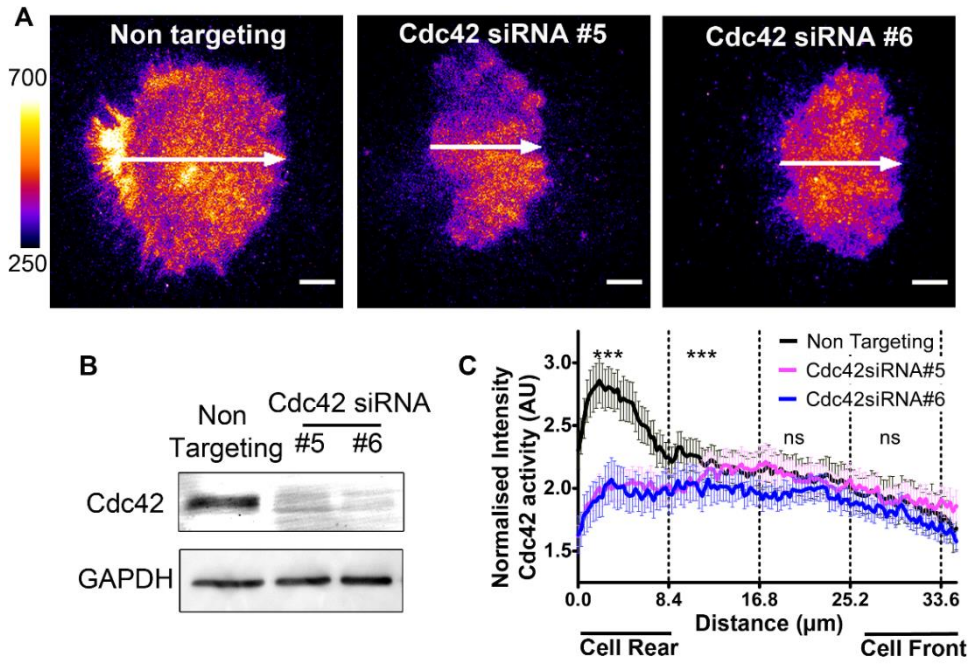

Figure 3.3: Cdc42 Depletion eliminates localized activity signal observed in the trailing edge. (A) Representative TIRF images showing lack of elevated Cdc42 activity sensor signal upon depletion of Cdc42. White arrow indicates direction of migration as well as the line for measuring signal intensities from cell rear to cell front. Scale bar= 10µm. LUT's depict arbitrary units. (B) Representative western blot depicting protein amounts of Cdc42 and GAPDH as housekeeping from cells treated with control siRNA (non targeting, 20nM) and two individual siRNA oligos (#5 and #6, 20nM each) for Cdc42 depletion. N=3 independent experiments. (C) Intensity plot of Cdc42 activity measured along the line from cell rear to cell front (n A) (n≥30 cells from 3 independent experiments). Statistical analyses performed for binned distances indicated by dotted lines (30 pixels). ***: P=0.0001. Unpaired *t* test)

3.1.3. Cdc42 modulates actomyosin retrograde flow at the trailing edge of migrating Keratinocytes

Cdc42 is an actin regulator with its direct effectors controlling actin nucleation and polymerization processes (Hall 1998). Along with actin polymerization, Cdc42 also regulates activity of myotonic dystrophy related kinases (MRCKs) which, similar to ROCK, activate Myosin regulatory light chain by phosphorylation (Unbekandt and Olson 2014). With the aim to understand the relevance of spatio-temporal activity patterns of Cdc42 in Keratinocytes, we performed TIRF time-lapse experiments of Cdc42 activity sensor together with actin (Actin-EGFP) and Myosin-IIa (NMHCIIa-EGFP) localization, respectively. When actin dynamics and Cdc42 sensor signals were measured within the same cell, Cdc42 activity was again strongly localized at the

rear edge of migrating Keratinocytes (fig. 3.4A). This region of high Cdc42 activity coincided with prominent accumulation and flow of actin. To better understand of Cdc42 activity dynamics at the trailing edge and its relation to dynamics of actin a time-distance scan or plot (kymograph) was generated along a line drawn in direction of cell migration (fig. 3.4A, B). A markup of high Cdc42 activity overlaid on an actin dynamics kymograph displayed high actin flow corresponding to regions of robust Cdc42 activity at the trailing edge (fig. 3.4C).

To study the correlation of activity patterns on whole-cell level, pixel based spatio-temporal cross correlation analysis was performed (Cross-correlation analysis in Methods section 2.2.5.1), revealing strong correlation between actin localization dynamics and Cdc42 activity (Cdc42 activity versus actin localization: Correlation co-efficient = 0.45±0.02 S.E.M; Cdc42 activity versus EGFP-control: Correlation co-efficient = 0.15±0.04 S.E.M.) (fig. 3.4D). In addition to the significant positive correlation, local maximal actin enrichment was slightly delayed with respect to Cdc42 activity (time shift of Actin with respect to Cdc42 activity: 2.06±0.38s S.E.M.) suggesting that actin polymerization might be downstream of Cdc42 activity in the trailing edge (fig. 3.4E).

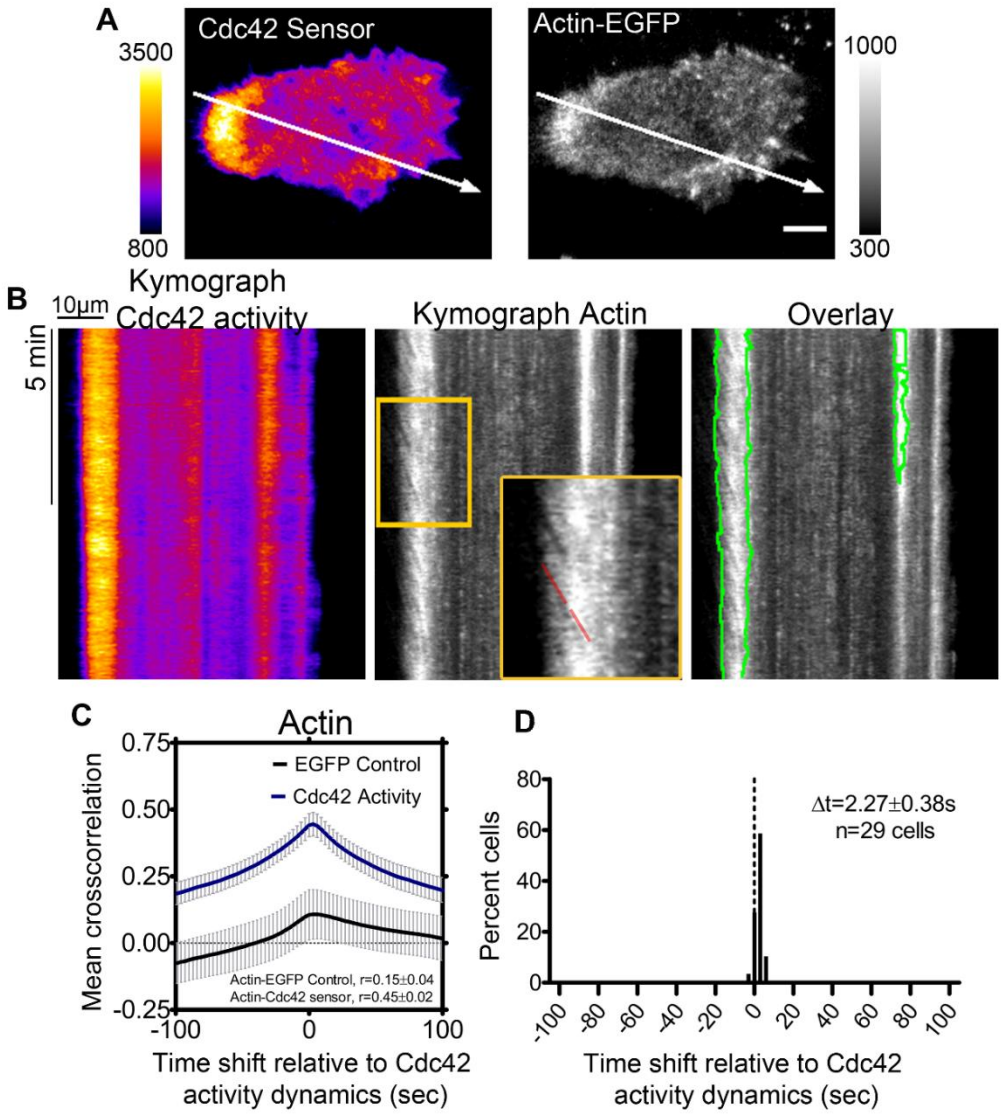

Figure 3.4: Localization of elevated Cdc42 activity in the trailing edge correlates with actin retrograde flow. (A) Representative TIRF images showing Cdc42 activity sensor (delCMV-mCherry-WASP-GBD) and actin (EGFP-Actin) within the same cell. White arrows indicate line for Kymograph analysis. LUT's depict arbitrary units. (B) Kymographs analysis of fluorescence signals along the arrows in A. Left panel: Cdc42 activity sensor signal. White arrow pointing to persistently elevated activity at the trailing edge. Middle panel: EGFP-Actin dynamics. Right panel: Superimposed actin Kymograph with outline of high Cdc42 activity, showing high actin flow at the highlighted area. (D) Plot of cross-correlation of Cdc42 activity (delCMV-WASP-GBDmCherry) with Actin (Actin-EGFP) and control (pEGFP-N1), respectively. (E) Histogram of cells showing a time delay of maxima between actin localization and Cdc42 activity. Images were acquired with a frame rate of 20 per min. Number of cells is indicated in the graph. N = 3 independent experiments

Dynamic localization patterns of Myosin-IIa were more diverse. First strong accumulation of Myosin-IIa in the cell front was found, reflecting well-known contractility within the lamella region (fig. 3.5A, orange arrowhead) (Gupton et al.

2005). In addition, small cortical pulses in central regions were found reminiscent of dynamic Myosin-IIa pulses shown before in U2OS cells (Graessl et al. 2017). Lastly, distinct Myosin-IIa dots were detected at the trailing edge region of cells that appeared to be very dynamic (fig. 3.5A, white arrowhead).

The intense Myosin-IIa localization at the cell front did not coincide with elevated Cdc42 activity (fig. 3.5A, orange arrowhead). However, a substantial Myosin-IIa retrograde flow was observed at the trailing edge partially overlapped with high Cdc42 activity (fig. 3.5C). To quantify subcellular Myosin-IIa flow dynamics within the entire cell, velocimetric flow mapping tools (ImageJ) were used (See methods, section 2.2.5.3). Briefly, based on Myosin pixel intensities, dynamics were tracked using time lapse images to obtain the Myosin flow vectors and velocities. The velocimetric analysis showed high Myosin-IIa retrograde flow at the cell rear during Keratinocyte migration (fig. 3.5C and D). Also, whole cell quantification of flow dynamics revealed that overall Myosin-IIa flow was significantly decreased upon Cdc42 depletion with both Cdc42 siRNA oligomers (non-targeting siRNA: 0.020±0.005 S.E.M. µm/min, Cdc42 oligo#5 = 0.007±0.002 S.E.M. µm/min and Cdc42 oligo#6 = 0.006±0.001 S.E.M. µm/min) suggesting that Myosin-IIa incorporation into actin filaments and contractility in Keratinocytes does depend on Cdc42.

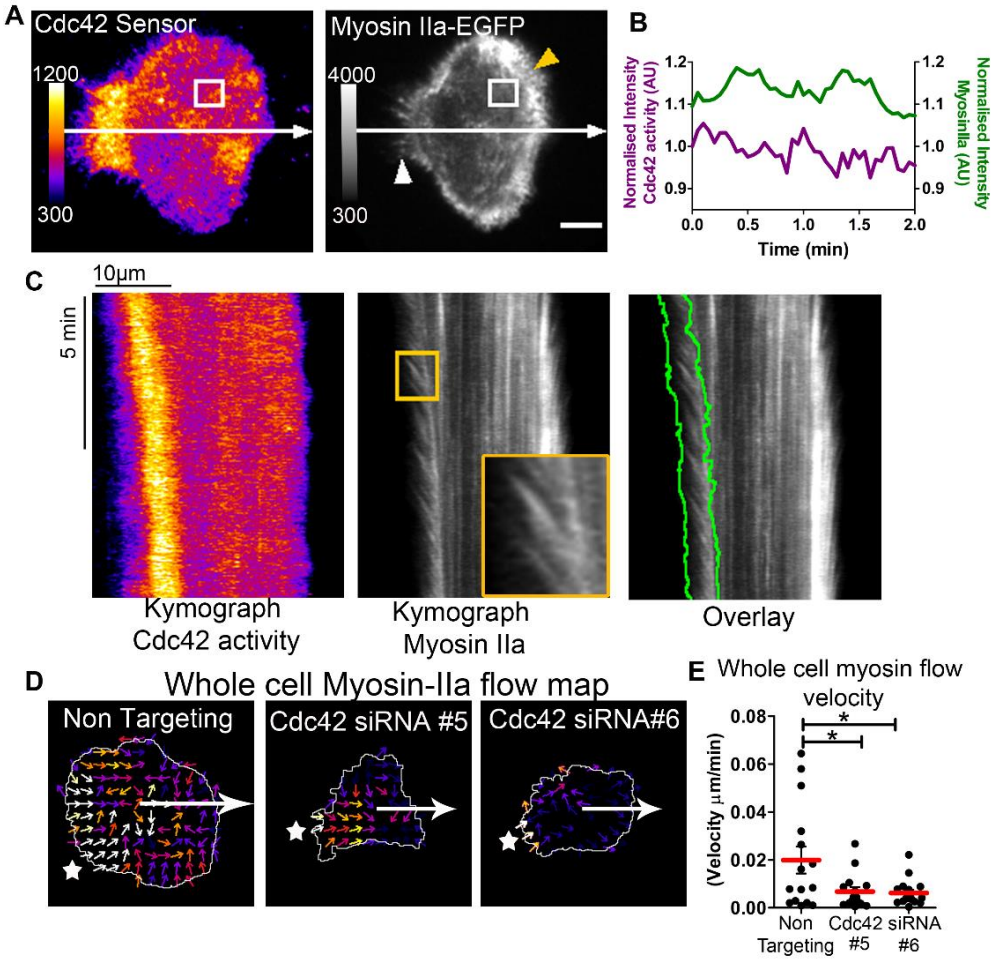

Figure 3.5: Region of elevated Cdc42 activity in the trailing edge overlaps with high retrograde flow Myosin-IIa. (A) Representative TIRF images of Cdc42 activity sensor (delCMV-WASP-GBD) in fire LUT and Myosin-IIa (NMHC-IIA-EGFP) in gray. White arrow indicates line for Kymograph and direction of cell migration. Orange arrow head indicates Myosin-IIa dynamics at cell front, white arrow head indicates Myosin-IIa flow at the trailing edge of the cell. White rectangle shows region of interest to display Myosin-IIa and Cdc42 activity intensities. Scale bar=10µm. (B) Myosin-IIa and Cdc42 activity localization dynamics in central cell regions do not correlate with each other. Mean intensity profiles corresponding to the region of interest in A. Absolute mean intensity values were normalised with average whole cell intensity from first frame for each time point. (C) Kymographs analysis of fluorescence signals along the arrows in A. Left panel: Cdc42 activity sensor. Middle: Dynamics of Myosin-IIa localization. The orange region of interest showing high Myosin-IIa flow is zoomed and inserted for the Kymograph. Right panel: Superimposed kymographs of Cdc42 activity and myosin-IIa. showing overlapping high Cdc42 activity and evident Myosin-IIa flow at the trailing edge of a migrating cell (D-E) Myosin-IIa retrograde flow is lowered on Cdc42 knockdown. Cells treated with control siRNA (non targeting, 20nM) and two individual siRNA oligos (#5 and #6, 20nM each) for Cdc42 depletion. (D) Representative normalised flow vectors of Myosin-IIA-EGFP signal (from STICS velocimetric flow, Image J plugin, see methods) overlaid on cell boundary. White star indicates high flow velocity at the trailing edge of a cell. (D) Plot of average Myosin-IIa retrograde flow in the entire cell obtained from

STICS velocimetric flow analysis. Red line on the graph indicates the mean of the sample. Error bars are S.E.M. N ≥ 15 cells from three independent experiments. *:P≤0.05, One-way Anova.

3.1.4. PAK inhibition in migratory Keratinocytes abolishes rear-end activity of Cdc42

During migration, actin dynamics can be affected at the level of actin nucleators, stabilizers or depolymerizers (Pollard and Borisy 2003). PAK is among the several effectors shared by the Rho GTPases Rac and Cdc42 regulating actin dynamics by phosphorylating and deactivating cofilin (Cotteret and Chernoff 2002) through LIM kinases or by affecting the levels of Myosin phosphorylation (Goeckeler et al. 2000). To understand the activation status of PAK downstream of Cdc42 in Keratinocytes, western blot analysis was performed in control samples and cells lacking Cdc42. Western Blot analysis upon Cdc42 depletion by RNAi showed significant decrease in PAK phosphorylation with both Cdc42 siRNA oligomers as compared to non-targeting siRNA (fig. 3.6) (Ratio of pPAK/PAK for non targeting = 1.46±0.09, Cdc42 depletion Oligo#5 = 0.94±0.14 and Oligo#6 = 0.78±0.16). While the antibody for PAK used here detects the entire group I PAKs (PAK1/2/3), the phospho-PAK antibody detects phosphorylation of PAK1 at Ser 199/204 and of PAK2 at Ser192/197. Thus, significant decrease in phospho-PAK signal in cells lacking Cdc42 indicates that phosphorylation of at least one of these effectors is controlled by this GTPase in Keratinocytes (fig. 3.6).

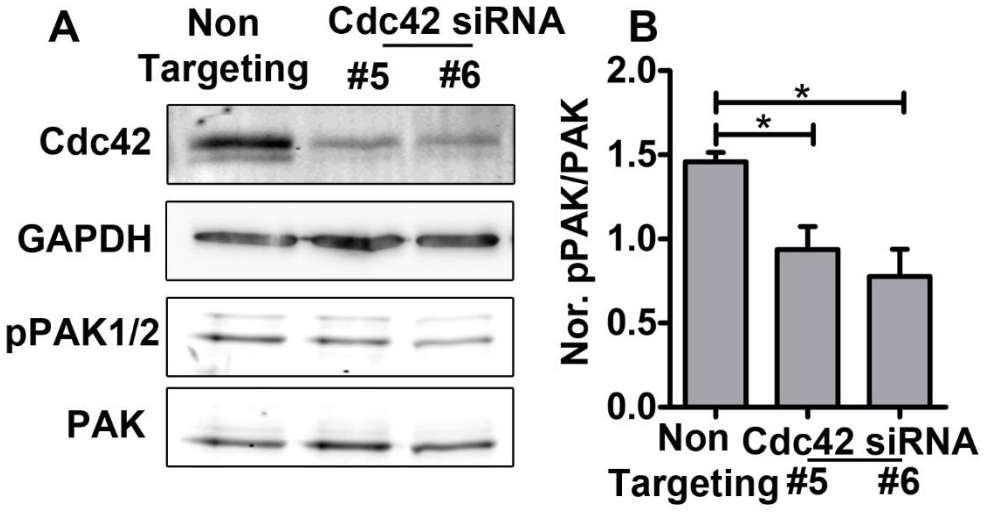

Figure 3.6: Phosphorylation of PAK is decreased in Keratinocytes upon Cdc42 depletion. (A) Representative western blot showing protein levels of Cdc42, PAK (PAK 1/2/3), phosphorylation of PAK1/2 (PAK1 at Ser 199/201 and PAK2 at Ser192/197) and GAPDH upon treatment with control

siRNA (non targeting, 20nM) and two individual siRNA oligos (#5 and #6, 20nM each) for Cdc42 depletion. B: Plots showing ratio of normalized pPAK to normalized PAK (normalized to total protein amount, not shown). N = 3 independent experiments. Error bars are S.E.M. *:P≤0.05, One-way Anova.

PAKs are direct downstream effectors of Cdc42 and are also shown to form a multi-protein complex with the adapter protein GIT and the Cdc42/Rac GEF βPix (Lawson and Ridley 2018) implicating the presence of a positive feedback mechanism. Thus, in the following experiments, the role of PAK effectors was tested in the generation of local Cdc42 activity patterns in Keratinocytes.

First, a pan-PAK inhibitor (FRAX597) for PAK1/2/3 was used and effect on the Cdc42 trailing edge activity and on cell migration were studied. Treatment of cells with this PAK inhibitor reduced migration velocity (fig. 3.7C and D) suggesting that as in other cells types PAK effector proteins are involved in efficient migration of Keratinocytes (Itakura et al. 2013). Furthermore, treatment of migrating Keratinocytes with the inhibitor significantly diminished Cdc42 activity at the trailing edge while significantly increasing activity sensor signal intensity in central regions of cells (fig. 3.7). This finding suggests that PAKs may be involved in processes upstream of Cdc42 that control localized activity of the GTPase.

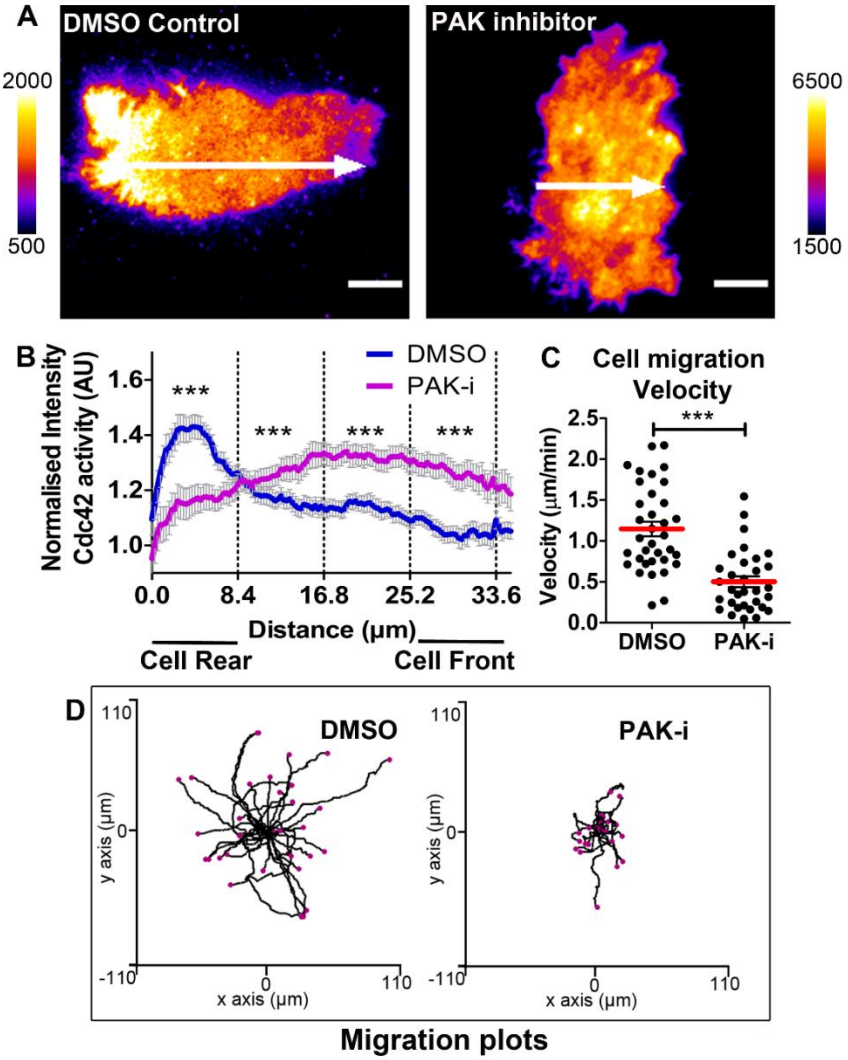

Figure 3.7: PAK inhibition using a pharmacological inhibitor reduces the trailing edge Cdc42 activity. (A): Representative TIRF images of cells expressing Cdc42 sensor (del-CMV-WASP-GBD-mCherry) after treatment with control as DMSO (1:10000, 1h) and PAK1/2/3 inhibitor (FRAX597, 1µM, 1h). White arrow indicates line drawn for measurement of Cdc42 activity signal from cell rear to cell front, as well as to mark direction of motion. Scale Bars=10µm. LUT's depict arbitrary units. (B) Graph showing normalized activity signal along the lines drawn as in A for (normalized with average intensity of whole cell) for DMSO and PAK inhibitor treated cells. (min. 39 cells per condition from 3 independent experiments). Statistical analysis was performed for binned distances indicated by dotted lines (30 pixels) using unpaired t-test. *** indicates P≤0.0001. (C) Graph depicting migration paths of individual cells during time-lapse imaging (not shown). Prior imaging, cells were treated for 1 h with 1µM of PAK inhibitor in combination with 100ng/ml EGF and DMSO as control. Red line indicates average of all cells while bars are S.E.M. Unpaired t-test. ***: P≤ 0.0001. (D) Migration plots for DMSO control and 1µM PAK inhibitor (C and D: n ≥ 32 cells per condition from 2 independent experiments)

For a thorough study of the role of PAK1 and PAK2 in Cdc42 activity pattern formation, siRNA mediated RNAi depletion was performed. Western Blot analyses

revealed insufficient PAK1 depletion with the siRNA oligomer mixture used in the assay (29.43 ± 15.4 S.E.M % knock down), while substantial depletion of PAK2 protein was detected (75.17 ± 4.22 S.E.M % knock down) (fig. 3.8A). Thus, measurements of Cdc42 spatio-temporal activity using the delCMV-WASP-GBD-mCherry activity sensor were only performed in PAK2 depleted cells. Activity sensor signals suggested that PAK2 depletion lead to two distinct changes in the activity pattern of Cdc42. While activity of the GTPase at the trailing edge seemed to be substantially decreased, signals appeared to be increased in the more central regions and at the front (fig. 3.8A and B). A more detailed analysis of subcellular patterns was performed to quantify the changes in Cdc42 activity localization. Similar to Cdc42 depletion experiments a line was drawn in direction of migration from cell rear to cell front. The intensity values through the line were normalized with average whole cell intensity and were plotted on a graph. Different regions were binned along the line plotted and were compared (fig. 3.8C) statistically to detect the difference in signals on PAK inhibition. This revealed a significant loss of Cdc42 activity at the trailing edge of a cell and an increase in activity in center regions (fig. 3.8C). To quantify potential global effects of PAK2 depletion, pixel-based analysis of sensor fluorescence signal was performed to measure average local pulses of Cdc42 activity in the entire cell. However, the average number of activity pulses per cell was not significantly altered upon PAK2 depletion (non targeting = 0.94 ± 0.10 pulses/min, PAK1 siRNA = 0.79±0.10 pulses/min, PAK2 siRNA = 0.81 ± 0.16 pulses/min) (fig. 3.8D).

Overall, this finding implicates that the PAK2 isoform might be involved in control of subcellular Cdc42 patterns, possibly via a GEF-involving positive feedback at the trailing edge, indicating the presence of a positive feedback loop.

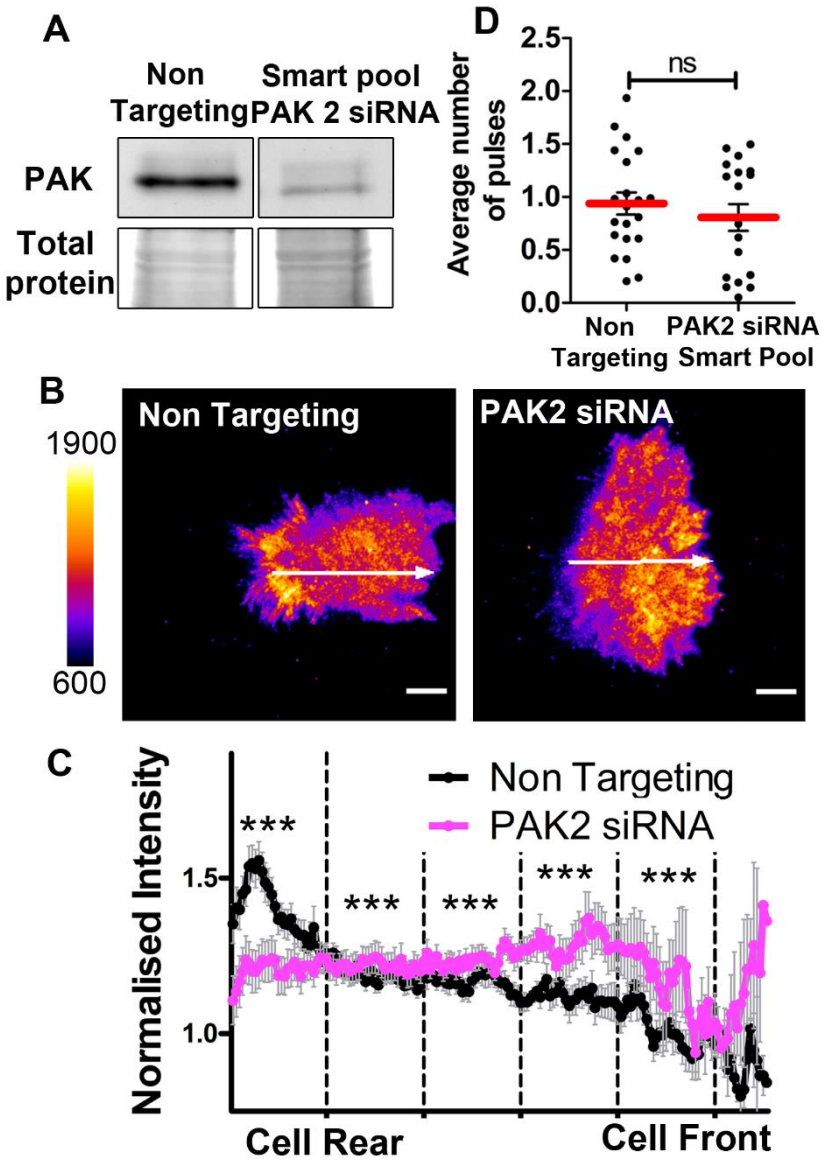

Figure 3.8: Depletion of PAK 2 reduces Cdc42 activity at the trailing edge. (A) Representative western blot showing PAK 1 and PAK 2 knockdowns using smart pool oligomer mixtures (Dharmacon). Non targeting siRNA was used as control. For loading control, a part of total protein staining image is shown. (B) Representative TIRF images of cells expressing the Cdc42 activity sensor (del-CMV-WASP-GBD-mCherry). White arrow indicates direction of motion. Scale Bars=10µm. LUT's indicate arbitrary units. (C) Graph showing normalized activity signals in non targeting siRNA and PAK 2 siRNA treated cells along the arrow in A. Signals were normalized with average whole cell intensity. for N ≥22 cells for each condition from 3 independent experiments. Statistical analysis performed for binned regions (dotted lines; 30 pixel) using unpaired t-test. ***: P≤ 0.0001. (D) Average Cdc42 activity pulses in non targeting control and PAK2 siRNA treated cells. N ≥18 cells from 3 independent experiments. Red line indicates mean of the sample. One way Anova, with ns indicating no significant difference.

3.1.5. Loss of the guanine nucleotide exchange factor βPix leads to altered localization patterns of Cdc42 activity in migrating Keratinocytes

βPix has the ability to form several multiprotein complexes one of which includes PAK, a Cdc42 effector implicated in a positive feedback mechanism to control localized activity of Cdc42. To test the relevance of βPix in Cdc42 activity pattern formation in migrating Keratinocytes the GEF was depleted and Cdc42 activity was measured using delCMV-WASP-GBD-mCherry sensor. Depletion of βPix lead to substantially altered Cdc42 activity patterns in cells (fig. 3.9 A and B). First, similar to PAK2 depletion, lack of βPix lead to significantly reduced trailing edge Cdc42 activity signal (fig. 3.9B and C), albeit this effect was not as radical as upon depletion of PAK2 (fig. 3.8B and C). Furthermore, loss of βPix also significantly increased Cdc42 activity signals at cell center and in the cell front (fig. 3.9B). Based on line analyses shown in fig. 9C, the effect was significant within a broader range of cell regions as compared to PAK2 inhibition (fig. 3.8C). In addition, global, pixel-based analysis of Cdc42 activity revealed significant increase of average Cdc42 activity pulses upon knockdown of βPix (non targeting=1.00±0.10 S.E.M, βPix=1.54±0.12 S.E.M) (fig. 3.9D).Together with the altered spatial activity patterns (fig. 3.8B and C) this indicates elevated levels of Cdc42 activity shifted to activity pulses in the central cell regions thereby substantially decreasing the activity at the cell rear.

To further understand if delocalized Cdc42 activity upon βPix depletion might affect Keratinocyte migration, single cell migration analysis was performed in cells lacking βPix. Again, individual cells were tracked using ImageJ manual tracking plugin and migration velocity and plots were prepared using IBIDI cell migration software. Depletion of βPix did not alter cell migration velocity of Keratinocytes as compared to non-targeting cells (non targeting=1.00±0.10 S.E.M, βPix=1.54±0.12 S.E.M (fig 3.9E and F). More detailed analysis of additional migration parameters such as cell directionality might reveal more subtle but relevant defects in further studies.

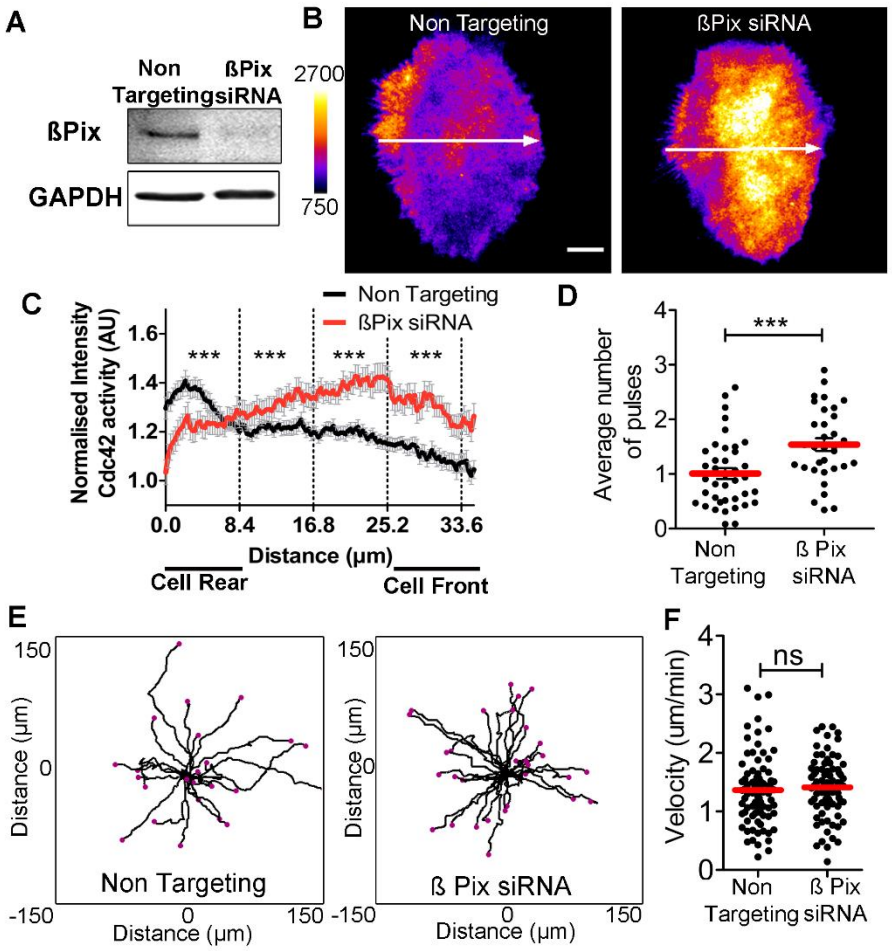

Figure 3.9: βPix depletion leads to altered pattern of Cdc42 activity localization. (A) Representative western blot depicting efficient βPix depletion. The housekeeping protein GAPDH was used as control. (B) Representative TIRF images showing Cdc42 activity sensor signal (delCMV-WASP-GBD-mCherry) in non targeting and βPix siRNA treated cells, respectively. White arrow indicates direction migration and line for polarized intensity measurement. Scale bar=10µm. (C) Plots of normalized Cdc42 activity from cell rear to cell front along the white arrow in B. ***:P≤ 0.0001). (D) Increase of Cdc42 activity pulses upon βPix Knockdown. Average number of Cdc42 activity pulses was determined using the macro for peak analysis (see methods). Red line represents the average of the sample. N≥ 44 cells per condition from 3 independent experiments, ***:P=0.001, Unpaired *t* test (E) Representative migration plots of control and βPix knockdown cells. Frame rate=1/min for 1h. (F) Migration velocity of individual cells were derived from migration plots. N ≥ 80 cells from 3 different experiments, Unpaired *t* test. ns: no significant difference. Red line indicates mean value of all cells per condition.

Overall, results presented in this part of the thesis confirmed the presence of local Cdc42 activity pulses in central regions and in the front of migrating Keratinocytes that are similar to previously observed activity pulses in Graessl et al., 2017 (Graessl et al. 2017). In addition to this pattern, strongly elevated Cdc42 activity was shown at the trailing edge of migrating Keratinocytes which was so far unknown. Depletion of

both the Cdc42 effector PAK2 and the Cdc42 activating GEF βPix, respectively, led to significant decrease of this activity pool implicating potential positive feedback involving tripartite protein complex with Cdc42, PAK2, βPix.

3.1.6. Spatio-temporal Rho GTPase activity dynamics in Keratinocytes upon growth factor stimulation

EGF stimulation influences Keratinocyte behavior probing cells for migration, proliferation and differentiation (Blumenberg 2013). EGF also has been shown to increase expression and activity of Rho GTPase proteins such as (Pothula et al. 2013; Ho and Dagnino 2012; Haase et al. 2003; Pastore et al. 2014). Thus, we studied how acute EGF stimulation of Keratinocytes affects activity of Cdc42 and the related GTPase RhoA in space and time.

3.1.6.1. Acute EGF stimulation does not alter local Cdc42 activity patterns in Keratinocytes

The results presented in the previous sections of this work, establish Cdc42 as a component of cell motility in Keratinocytes. To understand if growth factor stimulation had any immediate effects on Cdc42 activity patterns Keratinocytes were acutely stimulated with EGF.

First, trailing edge Cdc42 activity was not altered by EGF stimulation as is seen by comparison of sensor images and in a time distance plot (Kymograph) analysis (fig. 3.10A and B). In addition to the local activity patterns global Cdc42 activity also did not change on acute EGF stimulation (Mean Intensity 11.66 min before EGF = 2022 ± 393.2 S.E.M. A.U. and 0 to11.66 min EGF stimulation = 1968 ± 385.3 S.E.M. A.U.). This data suggests that Cdc42 is a component of essential basic cell migration machinery that is not necessarily regulated by acutely altered growth factor signaling.

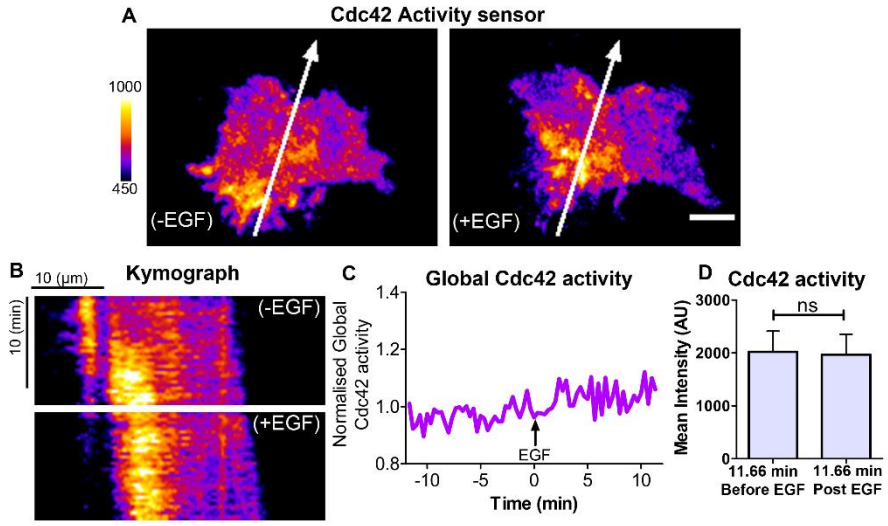

Figure 3.10: Acute EGF stimulation does not alter Cdc42 activity patterns in Keratinocytes. (A) Representative TIRF images of Cdc42 activity sensor (delCMV-WASP-GBD-mCherry) before (-9.3 min) and after (0.6 min) EGF stimulation. Scale bar=10µm. (B) Kymograph analyses of Cdc42 activity signal along white arrows in A before and after EGF stimulation. (C) Normalized mean cell intensity plot of Cdc42 activity signal. For this, mean signal intensity of the whole cell was determined at each time point in background subtracted images and normalized to mean intensities of whole cell at the first frame. (D) Average mean intensity plots of whole cell 11.66 min before and 11.66 min after EGF stimulation. N ≥ 26 cells from 3 independent experiments, Paired *t* test with ns = not significant.

3.1.6.2. Acute EGF stimulation gives rise to a transient single peripheral Rho activity peak

Another Rho GTPase, RhoA, is classically known to mediate cell contraction and adhesion processes via activation of actin regulating proteins like formins and Myosin. Prior studies have suggested cross talk between RhoA and Cdc42 in multiple cellular processes (Guilluy et al. 2011a; Sailem et al. 2014). In agreement with a stimulatory crosstalk between the two Rho proteins, previous work from our lab revealed strong temporal cross-correlation of Cdc42 activity pulses with local Rho activity dynamics (Graessl et al. 2017).

In migrating Keratinocytes, subcellular Rho activity dynamics were studied, using a fluorescently tagged Rho activity sensor (del-CMV-Rhotekin-RBD-mCherry) that was similar to the Cdc42 activity sensor (section 3.1.2.), except with the effector domain that specifically interacts with active Rho instead of Cdc42 (Graessl et al. 2017).

First, Rho activity patterns were studied in migratory cells that were treated long-term (1 hour) with EGF as performed for the migration assays shown in the previous

sections (section 3.1.2). In contrast to evident Cdc42 activity pulses in cells, no prominent Rho activity pulses were detected. Instead, only low amplitude pulses were measured throughout the entire cell area (fig. 3.11).

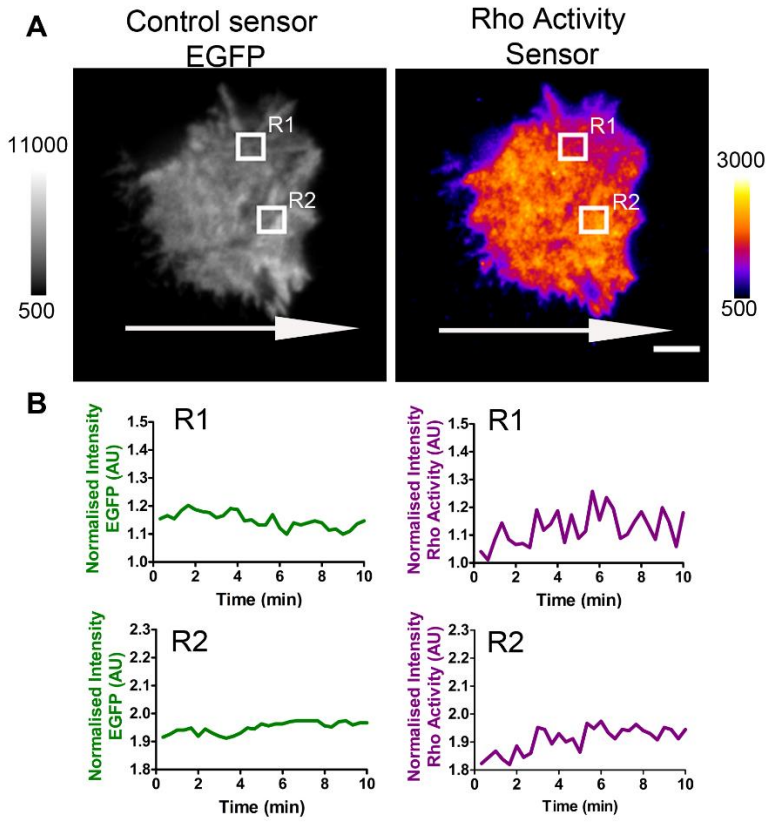

Figure 3.11: Low amplitude Rho activity pulses were detected in Keratinocytes during EGF stimulated migration. (A) Representative TIRF images of control sensor (delCMV-EGFP) and Rho activity sensor (delCMV-Rhotekin-RBD-mCherry). Imaging started at 1 h after EGF stimulation (c = 100ng/ml). White arrow indicates direction of migration. Scale bar=10µm. (B) Normalized intensity plots of average control sensor and Rho activity sensor signal regions indicated in A with average whole cell intensity of the respective channel. Upper panel: white box; R1. Lower panel: white box; R2 in A. N ≥ 24 cells from 3 independent experiments

Next, we aimed to study if Rho activity pulses were altered by acute EGF stimulation. First, phase contrast time-lapse experiments were performed with cells acutely treated with 100ng/ml of EGF on the stage to directly assess cell behavior at early time-points upon growth factor stimulation. Phase contrast movies allowed measurement of time-point and duration of protrusions after treatment. Kymograph analyses of the cell edge revealed that EGF stimulation lead to almost immediate start of cell protrusions (0.78±0.06 S.E.M. min post EGF with maximum around 5.52±2.22 min post EGF).

Protrusion growth lasted for approximately 4.73±0.25 min followed by retraction of this peripheral region (fig. 3.12A and B).

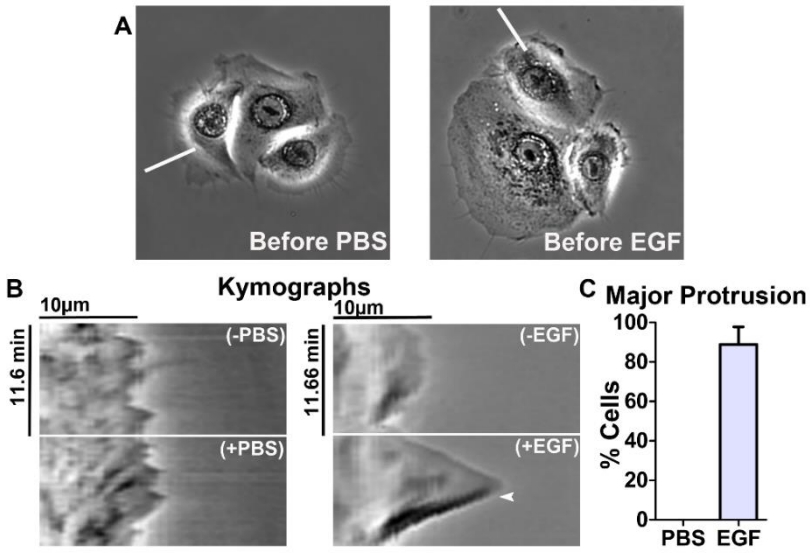

Figure 3.12: Acute EGF stimulation gives rise to major protrusion followed by retraction in Keratinocytes. (A) Representative phase contrast images of Keratinocytes at acutely stimulated with PBS control or 100ng/ml EGF. White line in the images correspond to the lines for Kymographs. (B) Representative kymograph analyses of regions marked with the white line in the corresponding cell images in A. White arrow head indicates cell edge retraction after protrusion. (C) Quantification of number of cells showing major protrusion upon PBS and EGF treatment, respectively. N≥65 cells per condition from 2 independent experiments.

Combination of such acute EGF stimulation and simultaneous Rho activity imaging revealed that at early time points post protrusion (0.78±0.06min post EGF from phase contrast data) initiated by EGF stimulation, a distinct peripheral Rho activity peak was seen, which was followed by cell contraction (fig. 3.13C and D). The Rho activity peak duration was for 2.48±0.45 (S.E.M.) sec and was typically followed by contraction of this region (89.14±7.79 (S.E.M.) % of cells). Further the global Rho activity measurements were analyzed using pixel based peak analysis (see methods). Here along with a distinct Rho activity peak, there was also rise in global Rho activity pulses (fig. 3.13A).

Overall, this data shows that EGF stimulation Keratinocytes stimulates immediate protrusion formation along the cell periphery which is followed by retraction of these

regions. At the temporal peak of protrusion formation strong transient Rho activity pulse is observed likely inducing the subsequent contraction of the edge (fig. 3.12).

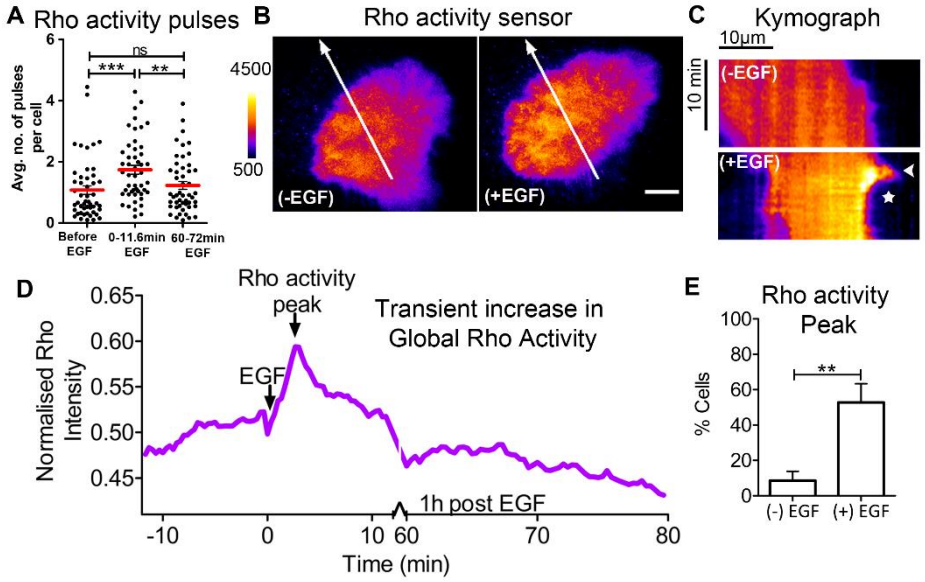

Figure 3.13: EGF induces transient increase of local Rho activity dynamics in Keratinocytes at early time points. (A) EGF treatment (c = 100ng/ml) leads to significant transient increase of average number of Rho activity pulses in the whole cell. Global quantification of local pulses was performed using automated pixel wise analysis of signal change as described in the methods (section 2.2.5.2). Average number of Rho activity pulses per cell significantly increased during the first 11.66 minutes upon EGF stimulation, while at 1 h post EGF no significant change was detected. N ≥ 49 cells from 5 independent experiments. One-way Repetitive measure Anova test. ***=P≤0.001) (B-E) Distinct prominent Rho activity peak in the cell periphery at early time point after EGF treatment. (B) Representative TIRF images of Rho activity sensor signal (delCMV-Rhotekin-RBD-mCherry) before (0.33min) and after (3 min) EGF stimulation. White arrow indicates line for Kymograph in C. Scale bar=10µm. (C) Representative kymograph of Rho activity signal along line depicted in A. Arrow head: Maximum of protrusion initiated immediately generated upon EGF treatment. This time-point also marks the appearance of the strong transient Rho activity pulse followed by peripheral cell contraction (white star). (D) Normalized intensity plot of whole cell in A showing transient global Rho activity signal. (E) Number of cells showing peripheral Rho activity peak upon EGF stimulation N≥40 cells form 5 independent experiments. **:P=0.01, Unpaired *t-test*).

3.1.6.3. GEF-H1 depletion does not abolish transient Rho activity burst upon EGF stimulation but leads to premature signal maximum

Signal pulses as observed with Rho activity upon EGF treatment can arise due to excitable nature of the underlying signal network. In excitable systems a signal pulse

can be the result of a fast positive feedback coupled to a slow negative feedback (Iglesias and Devreotes 2012). Earlier work in our lab revealed an excitable Rho GTPase network controlling local Rho activity pulses in migratory cells in which the positive feedback is mediated by the microtubule bound Lbc GEF, GEF-H1 (fig,ref. Thus, we tested here if GEF-H1 also mediates Rho activity pulse upon acute EGF stimulation. To test the role of this GEF in the generation of the strong transient Rho activity pulse upon growth factor stimulation, GEF-H1 was depleted using two individual siRNA oligomers. Depletion of GEF-H1 did not significantly reduce the occurrence of the peripheral Rho activity pulse after EGF (fig. 3.14) as compared to non-targeting siRNA (non-targeting: 46.65 ± 13.35 (S.E.M) % cells, GEF-H1 oligo#8: 36.50 ± 13.50 (S.E.M) % cells and GEF-H1 oligo#9: 57.40 ± 14.60 (S.E.M) % cells). However, a tendency for premature occurrence of EGF induced Rho activity pulse (albeit not significant) was detected with both GEF-H1 oligomers as the time of pulse maximum was decreased (non-targeting siRNA:6.18 ± 0.16 min (S.E.M), GEF-H1 oligo#8: 4.54 ± 0.71 min (S.E.M) cells and GEF-H1 oligo#9: 4.04 ± 0.65 min (S.E.M)).

No remarkable change in the duration of activity peaks was detected (non-targeting siRNA:1.733 ± 0.27 min (S.E.M), GEF-H1 oligo#8: 1.67 ± 0.24 min (S.E.M) cells and GEF-H1 oligo#9: 1.61 ± 0.22 min (S.E.M), data not shown). Overall, these findings suggest that GEF-H1 might not be integral in generating the EGF induced peripheral Rho activity pulse per se but rather might play a modulatory role.

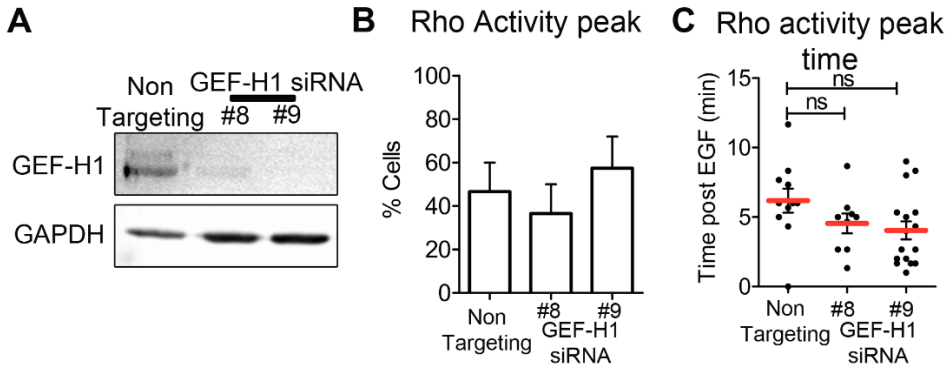

Figure 3.14: GEF-H1 depletion does not abolish Rho activity peak occurrence on EGF stimulation. (A) Representative western blot depicting protein amounts of GEF-H1 and GAPDH as housekeeping from cells treated with control siRNA (non targeting, 20nM) and two individual siRNA oligos (#8 and #9, 20nM each) for GEF-H1 depletion. N=3 independent experiments. (B) Percent siRNA treated cells with prominent Rho activity peak upon EGF stimulation. (C) Time of Rho activity peak detection after EGF stimulation. (B) and (C) N ≥14 cells per condition from 3 independent experiments. One way Anova, Dunnett's post-test.

3.2. Screen for additional Lbc type GEFs with potential modulatory roles in Rho activity dynamics in Keratinocytes

3.2.1. LBC GEFs induce prominent Rho activity pulses and propagating Rho activity waves in Keratinocytes

To screen for additional GEFs with potential modulatory roles in Rho activity dynamics wild type versions of all seven LBC GEFs including GEF-H1 were individually overexpressed in Keratinocytes and Rho activity patterns were detected using the aforementioned activity sensor, Rhotekin-GBD-mCitrine and further analyzed.

Overexpression of all wild type LBC GEFs gave rise to prominently elevated subcellular Rho activity pulses (fig. 3.15). Automated pulse analysis (fig. 3.15I, see also methods section 2.2.5.2.) revealed significant elevation in Rho activity pulses upon overexpression of GEF-H1 (fig. 3.15C), LARG (fig. 3.15E), PDZ Rho GEF (fig. 3.15D) and p190 Rho GEF (fig. 3.15H) (Average Rho activity pulses (± S.E.M.): Control mCherry=1.0 ± 0.13, p115 Rho GEF=1.14 ± 0.14, GEF-H1=1.99 ± 0.24, PDZ Rho GEF=1.96 ± 0.25, LARG=2.53 ± 0.33, AKAP13 =1.35 ± 0.16, p114 Rho GEF=1.53 ± 0.23, p190 Rho GEF=1.89 ± 0.23). Interestingly, localization maxima of GEF-H1, p190 RhoGEF, AKAP13 and LARG were found to have a tendency of preceding Rho activity with p114 Rho GEF and PDZ Rho GEF showing more pronounced effect (data not shown).

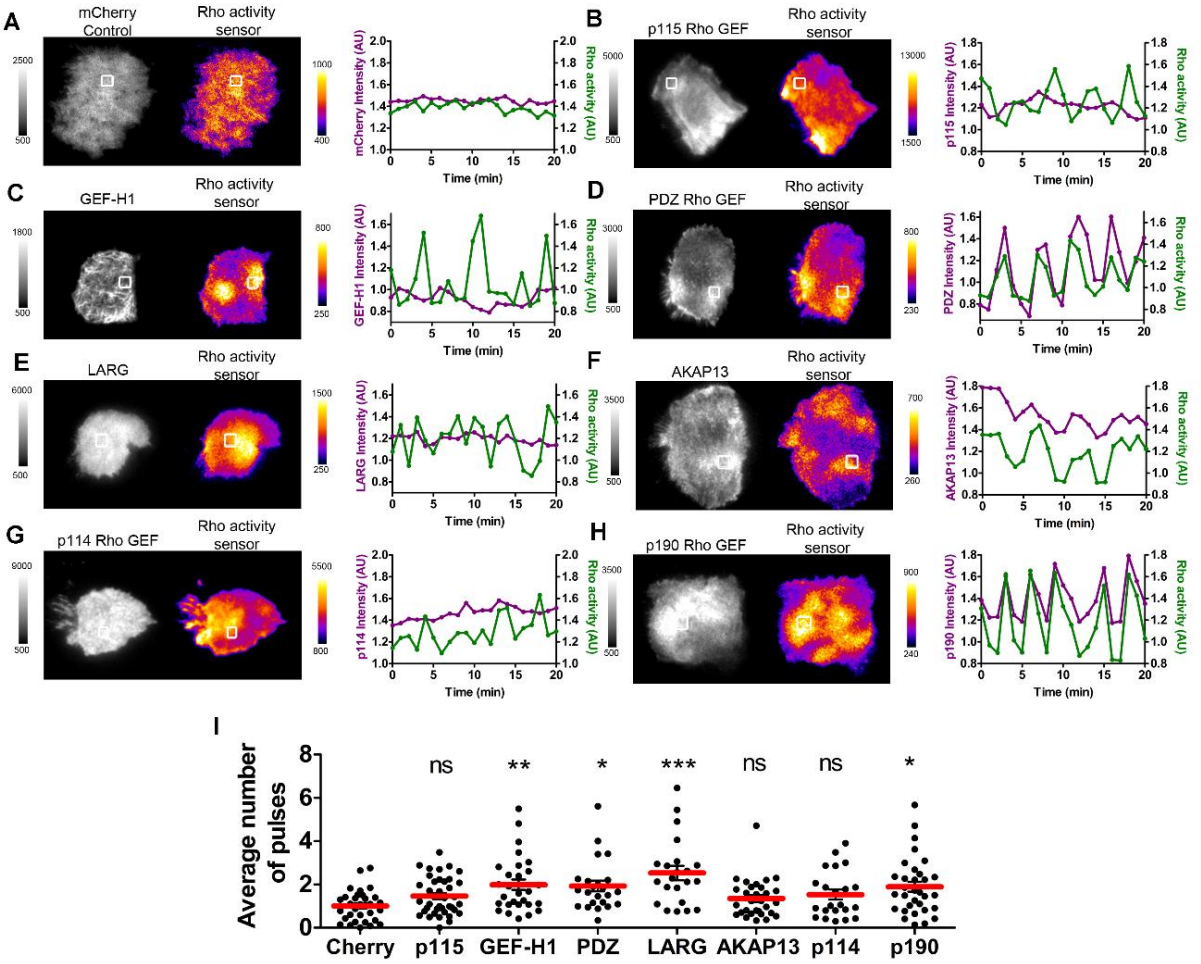

Figure 3.15: Overexpression of LBC type GEFs enhances subcellular Rho activity pulses. Keratinocytes were co-transfected with mCherry tagged LBC Rho GEFs together with the Rho activity sensor (delCMV-Rhotekin-RBD-mCitrine) for TIRF imaging. (A)-(H) Left panels: Representative TIRF images of mCherrry-C1 and mCherry-tagged GEF constructs, respectively and Rho activity sensor (delCMV-Rhotekin-RBD-mCitrine). Scale bar=10µm in all images. Right panels: Normalized activity plots of average activity signal in white box in corresponding images in left panels. (I) Graph showing average Rho activity pulse per cell during time of imaging, **:P=0.01, ***P=0.0001, One-way anova, Dunnett's test. Error bars in red represent mean values of all samples per condition, S.E.M as error bars. N≥22 cells per condition from 3 independent experiments.

Next, as a hallmark of signal excitability, the generation of propagating Rho activity waves upon Lbc GEF overexpression was assessed. As shown previously in U2OS cells (Graessl et al. 2017) significantly elevated number of cells showed propagating Rho activity waves upon overexpression of GEF-H1 and LARG (mCherry control: 1.7±1.7%; GEF-H1: 53.33±7.99%; LARG: 46.30±6.69%) (fig. 3.16). Further analysis showed that overexpression of all seven LBC type GEFs lead to this phenomenon, albeit with different efficiencies (p115 Rho GEF:28.37±8.47%, PDZ:

40.53±9.07%, AKAP13: 27.63±7.80%, p190: 42.82±7.15%). Along with GEF-H1 and LARG, p114 Rho GEF gave rise to significant high number of Rho activity waves (50.83±22.87%) (fig. 3.16). Overall, data acquired here shows that all Lbc type GEFs can modulate subcellular Rho activity dynamics. Such mechanism could involve shared structural elements such as the Rho interacting PH-domain in Lbc GEFs shown to be required for the positive feedback loop during Rho activity pulses (Medina et al. 2013).

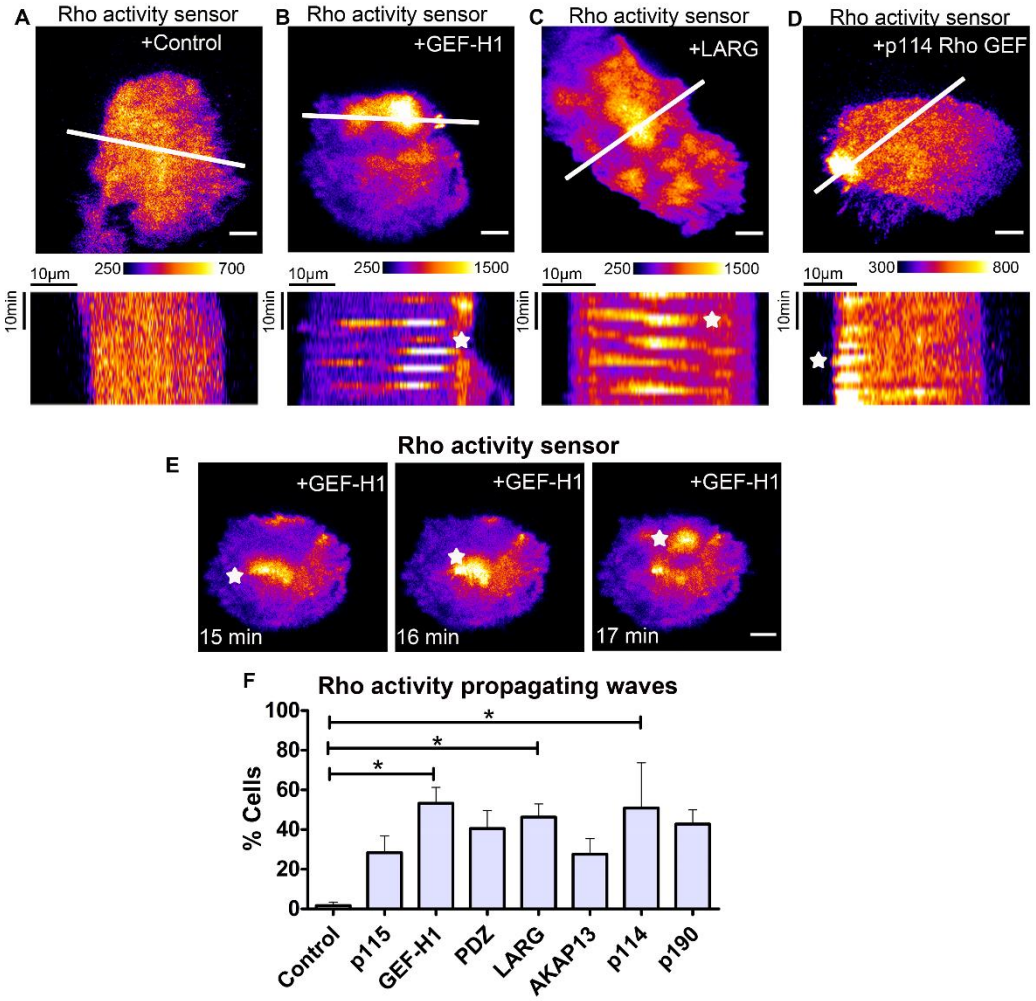

Figure 3.16: Overexpression of Lbc GEFs gives rise to Rho activity waves. (A-D) Upper panels: Representative TIRF images of cells expressing Rho activity sensor (delCMV-Rhotekin-GBD-mCitrine and corresponding GEF constructs (mCherry-C1 as control, mCherry-GEF-H1, mCherry-LARG, mCherry-p114 Rho GEF). Scale bars:10µm, Lower panels: Kymographs of Rho activity signals along the white line in the corresponding cell images. (E) Example Wave propagation in a cell expressing the Lbc GEF, GEF-H1 and Rho activity sensor. White star indicating the position of wave activity. (F) Manual quantification of cells showing Rho activity waves in cells expressing GEFs. N ≥29 cells for each condition from 3 independent experiments. Statistical significance determined from One way ANOVA. **:P=0.01, ***P=0.0001, Dunnett's test. Error bars are S.E.M.

3.2.2. GEF induced Rho activity pulses correspond to repeated local retractions at cell edges in Keratinocytes

To better appreciate the effects of GEF induced Rho activity pulses on cell behavior, dynamics of cell morphology with respect to timing of wave occurrence was assessed. As depicted in fig 3.17 with GEF-H1 as one prominent example with which Rho activity pulses coincided with contractions of associated peripheral regions (fig. 3.17B).

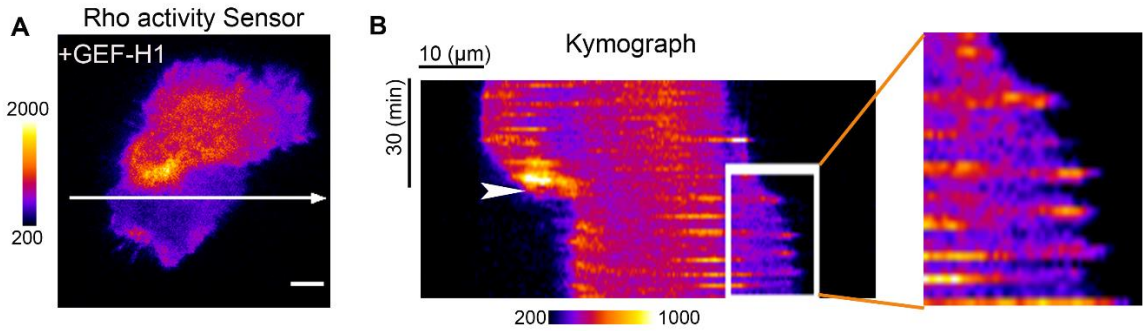

Figure 3.17: GEF-H1 induced Rho activity waves correspond to sites of contraction at the cell periphery. (A) Representative TIRF image of a cells expressing Rho activity sensor (delCMV-Rhotekin-RBD-mCitrine). Scale bar=10µm. (B) Kymograph analysis along arrow depicted in A. White arrow head indicates major contraction site coinciding with intense Rho activity peak. Right panel: Zoomed region in Kymograph depicting additional smaller peripheral regions that are periodically contracting (white box)

3.2.3. Lbc type GEFs that induce Rho activity waves have distinct localization patterns on their own in cells

Along with effects on Rho activity on GEF overexpression, knowledge of actual GEF localization dynamics can also prove to be beneficial for understanding the underlying molecular mechanisms. The localization of overexpressed GEF was therefore examined on overexpression. Since GEFs activate Rho by direct interaction, a relation between the overexpressed GEF localization and Rho activity dynamics was expected. However, this was not observed for all the GEFs after overexpression. Although most Lbc GEFs tested here induced strong Rho activity wave propagation, their own localization dynamics with respect to Rho activity signal was diverse. For example, p115 Rho GEF expression lead to increase of propagating Rho activity waves 28.37 ± 8.46 (S.E.M.) % cells, however the GEF itself was rarely found to be localized to propagating waves (4.7 ± 4.7% S.E.M.). PDZ Rho GEF and LARG even each displayed two different localization patterns in cells. First, a subpopulation of cells

displayed propagating GEF localization waves (PDZ Rho GEF: 36.20 ± 15.61 S.E.M.% cells; LARG: 16.66 ± 9.62 S.E.M. % cells).

In these cells where GEF localization waves were observed also Rho activity waves (fig. 3.16) as well as intense Rho activity pulses (data not shown) were observed. Apart from these cells with dynamic GEF localization, another subpopulation of cells was found with both GEFs that showed high accumulation of GEF localization at the cell periphery that was not dynamic (PDZ Rho GEF: 29.5 ± 8.6 S.E.M. % cells; LARG: 49.07 ± 17.58 S.E.M. % cells. (fig. 3.18 and 3.19). Interestingly, in these zones with accumulated GEF signal, no elevated Rho activity signal was observed (fig. 3.18). Further, cells displaying such high GEF signal intensity at the periphery did not show propagating waves of Rho activity. Thus, we could identify three distinct populations of cells with PDZ Rho GEF and LARG overexpression. One subset of cells displayed GEF activity propagating waves, one subset displayed distinct peripheral GEF accumulation but no Rho activation and one set did not show any localization waves or accumulation (34.43 ± 14.71 % for PDZ Rho GEF, 34.27 ± 21.89 % for LARG).

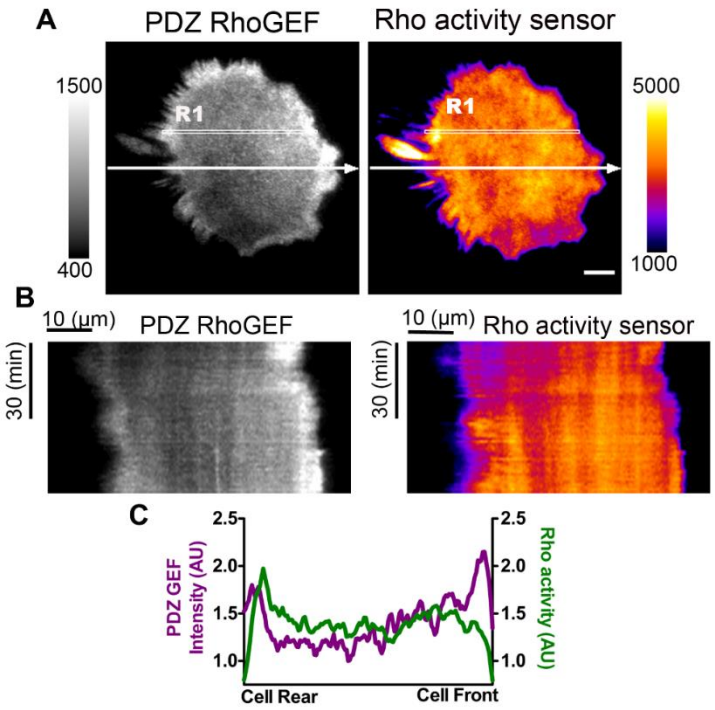

Figure 3.18: Anti-correlation of distinct PDZ Rho GEF localization at the cell periphery with Rho activity signal. (A) Representative TIRF images of mCherry-PDZ RhoGEF and Rho activity sensor (delCMV-Rhotekin-RBD-mCitrine). Scale=10µm. (B) Kymograph analysis of signal intensities along white line in the corresponding image (in A). (C) Average signal intensity in the corresponding region (R1) from left (cell Rear) to right (Cell Front) in A normalised with whole cell intensity..

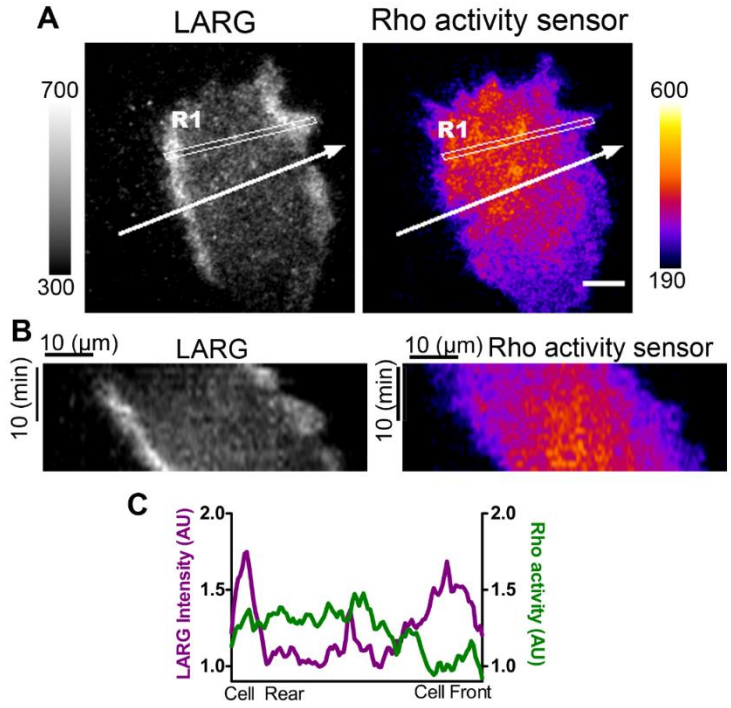

Figure 3.19: Anti-correlation of distinct LARG localization at the cell periphery with Rho activity signal. (A) Representative TIRF images of mCherry-LARG and Rho activity sensor (delCMV-Rhotekin-RBD-mCitrine). Scale=10µm. (B) Kymograph analysis of signal intensities along white line in the corresponding image (in A). (C) Average signal intensity in the corresponding region (R1) from left (cell Rear) to right (Cell Front) in A normalised with whole cell intensity.

3.2.4. Overexpression of p115 Rho GEF, LARG, p114 Rho GEF and p190 Rho GEF leads to decreased Keratinocyte migration

To better understand potential modulatory effects of Lbc type GEFs in Keratinocyte migration each GEF was overexpressed in cells individually and migration measured using phase contrast microscopy and cell tracking with ImageJ (See methods) manual tracking plugin and plotted using IBIDI cell migration software.

Migration studies were performed individually for each GEF with control plasmid used in each round of experiment to account for experimental variations. Cell migration velocity and distance covered on overexpression of the Lbc GEF and control sensor. Overexpression of p115 Rho GEF (Control=1.19 ± 0.05 S.E.M. µm/min and p115 Rho GEF=0.77 ± 0.04 S.E.M. µm/min), p190 Rho GEF (Control=1.15 ± 0.10 S.E.M. µm/min and p190 Rho GEF=0.77 ± 0.08 S.E.M. µm/min), LARG (Control=0.96

± 0.054 S.E.M. µm/min and LARG=0.74 ± 0.04 S.E.M. µm/min) and p114 Rho GEF (Control=0.89 ± 0.05 S.E.M. µm/min and p114 Rho GEF=0.67 ± 0.04 S.E.M. µm/min) reduced migration speed and distance covered by cells (fig. 3.20), while GEF-H1, PDZ Rho GEF and AKAP13 overexpression did not have a significant effect (fig. 3.20J).

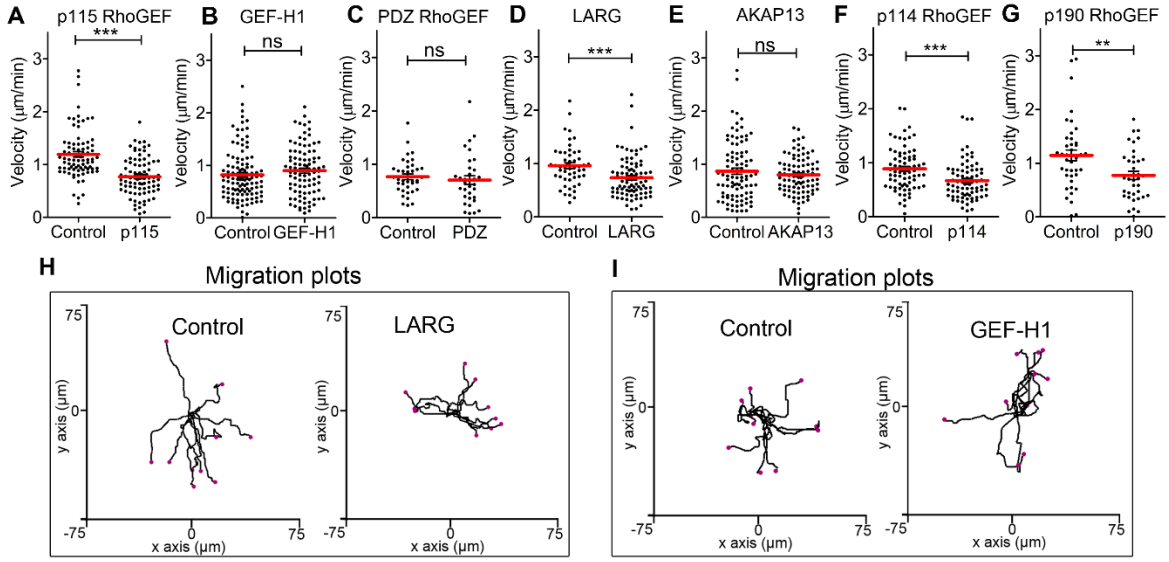

Figure 3.20: Overexpression of several Lbc Type GEFs affects Keratinocyte migration. (A-G) Plots showing migration velocity of individual cells overexpressing GEFs and corresponding control (A) Overexpression of mCherry-p115 RhoGEF and control mCherry-C1. N ≥ 82 cells per condition from 3 independent experiments. (B) Overexpression of GEF-H1 -EGFP and control EGFP-N1. N≥94 cells per condition from 3 independent experiments (C) Overexpression of mCherry-PDZ RhoGEF and control mCherry-C1. N ≥ 33 cells per condition from 3 independent experiments. (D) Overexpression of mCherry-LARG and control mCherry-C1. N ≥ 51 cells per condition from 3 independent experiments. (E) Overexpression of mCherry-AKAP13 and control mCherry-C1. N ≥ 88 cells per condition from 3 independent experiments. (F) Overexpression of mCherry-p114 RhoGEF and control mCherry-C1. N ≥ 75 cells per condition from 3 independent experiments (G) Overexpression of mCherry-p190 RhoGEF and control mCherry-C1. N ≥ 37 cells per condition from 3 independent experiments. (H) Representative subset of migration plots of LARG and control transfected cells. (I) Representative migration plots of GEF-H1 and control. Unpaired *t-test*. Ns = not significant. **, P=0.001; ***, P=0.0001

Table 3.1: Summary of effects on Rho activity waves and migration of Keratinocytes upon Lbc GEF overexpression.

Rho GEF	Migration velocity relative to control	Rho activity propagating waves upon GEF overexpression (% cells ± S.E.M)
Control vector	No effect	1.73±1.73
p115 Rho GEF	Significant decrease	28.37±8.46
GEF-H1	No effect	53.33±7.95
PDZ Rho GEF	No effect	40.53±9.07
LARG	Significant decrease	46.30±6.60
AKAP13	No effect	27.63±7.80
p114 Rho GEF	Significant decrease	50.83±22.87
p190 Rho GEF	Significant decrease	42.82±7.15

Overall, this data confirms the ability of all Lbc GEFs to induce Rho activity pulses and propagating waves in Keratinocytes while some of these GEFs have a stronger propensity for induction of Rho activity pulses as compared to others. Further, overexpression of several Lbc type GEFs leads to decreased Keratinocyte migration.

Although no strong correlation was found between the potency of individual GEFs to induce Rho activity waves and effect on migration (Table 3.1), it was noticeable that GEFs with greater tendency of Rho activity pulse generation and wave propagation (p190 Rho GEF, p114 Rho GEF, LARG) also reduced the migration velocity of cells. Hence, this may point towards an inverse relation between Rho activity wave and cell migration efficiency.

3.3. Control of subcellular Rho activity patterns by the extracellular matrix and ERM proteins

3.3.1. Effect of the extracellular matrix components collagen and fibronectin on Rho excitability

Rho GTPase signaling plays major role sensing the properties of the ECM by cells such as extracellular components or stiffness (Amano et al. 2010; Provenzano et al. 2009). Different ECM components transmit different signals via integrins for cellular functions and for example Collagen and Fibronectin have been previously shown to affect activity of Rho GTPase signaling in several systems (Nardone et al. 2017).

Thus, effect of these prominent matrix proteins on subcellular Rho activity pulses was tested. Since most of the earlier work on Rho activity pulses and its response to environmental changes was performed with U2OS cells (Graessl et al. 2017), these were used as a model system here as well. In order to avoid mixing of Rho activity response brought about by individual ECM components and serum factors, cells were plated on Fibronectin, Collagen or Poly-L-lysine coated glass surfaces, in media without serum. Calculation of Rho activity dynamics on Collagen and Fibronectin revealed high Rho activity dynamics for as compared to Poly-L-Lysine (Average Rho activity pulses per min. S.E.M. on Poly-L-Lysine= 0.29 ± 0.06, on Collagen=1.53 ± 0.17, on Fibronectin=1.18 ± 0.14) (fig. 3.21C). In addition, western blot analysis revealed increased FAK phosphorylation levels for Fibronectin and Collagen as compared to PLL confirming integrin dependent activation of FAK signaling (fig. 3.21E).

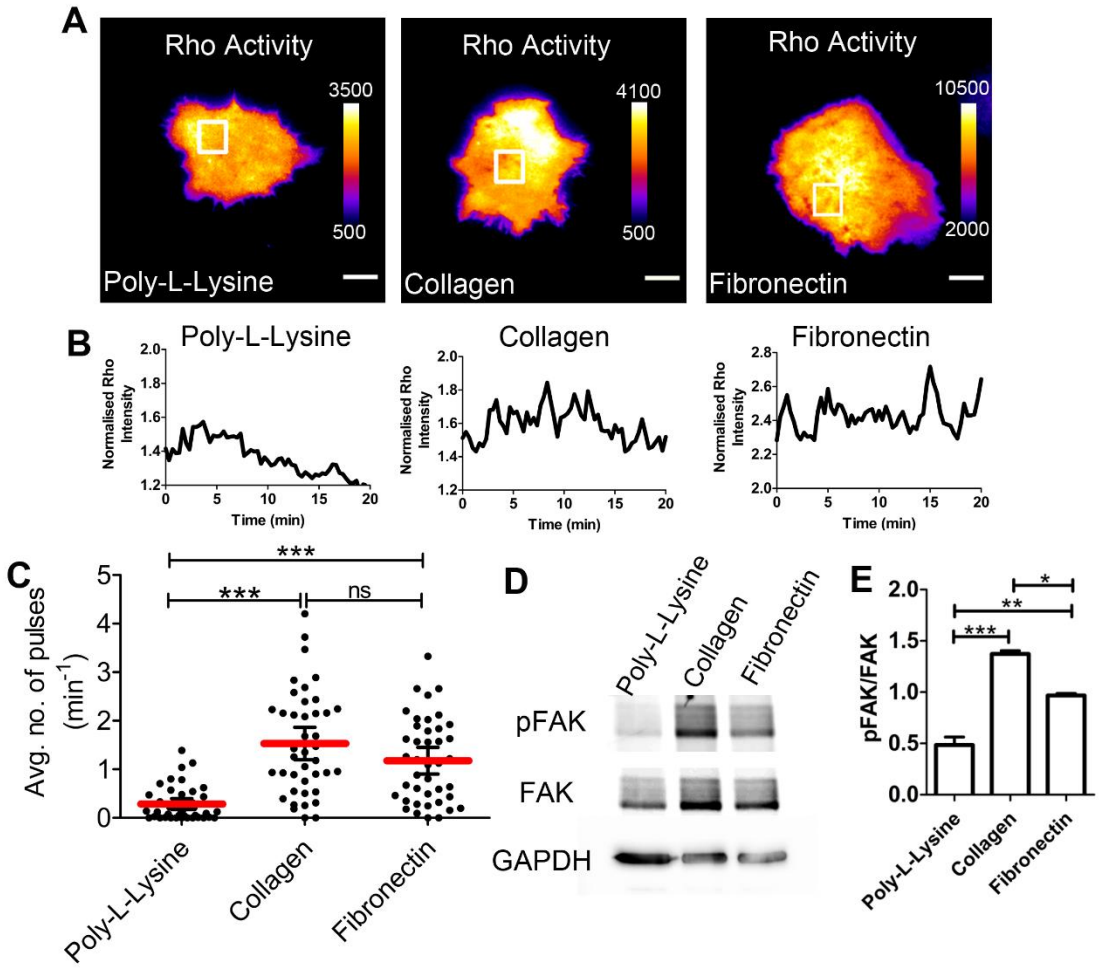

Figure 3.21: ECM components affect Rho activity pulses in U2OS cells. (A) Representative TIRF images of Rho activity sensor (delCMV-Rhotekin-RBD-mCherry) in cells seeded on different extracellular matrix proteins. Scale bar=10µm. (B) Rho activity signal intensity plots corresponding to region of interest shown in A normalized with averaged whole cell intensity at first frame. (C) Average number of Rho activity pulses (see methods) is elevated on Collagen and Fibronectin as compared to Poly-L-Lysine. N ≥41 cells per condition from 3 independent experiments. One-way Anova, Tukey's multiple comparison test with ns = not significant and ***, P=0.0001. (D) Representative western blot of FAK phosphorylation the individual substrates. (E) Measure of normalized pFAK/FAK based on western blot analysis (Data from 3 independent experiments, One-way Anova, Tukey's multiple comparison test, ***, P=0.0001, **, P=0.001, *, P=0.01).

3.3.2. ERM proteins Ezrin and Moesin are components of cortical Rho network

Ezrin/Radixin/Moesin (ERM) proteins link the plasma membrane to intracellular proteins and actin providing a hub for signaling and cortical protein dynamics (Tsukita and Yonemura 1999; Ivetic and Ridley 2004). As Rho activity pulses strongly correlate with cortical actin dynamics (Graessl et al. 2017), it was hypothesized that ERM proteins may also be components of the pulsatory Rho activity network regulating

subcellular contractions. Fluorescently tagged Ezrin (Ezrin-EGFP) and Moesin (Moesin-EGFP) were expressed in U2OS cells, respectively, and subcellular localization patterns were detected using TIRF microscopy. Distinct Ezrin and Moesin localization pulses were observed in U2OS cells (fig. 3.22 A-C) and pixel-based quantification of signal pulses of entire cells revealed significantly elevated pulse frequency, both for Ezrin and Moesin, as compared to the control pEGFP-N1 (fig. 3.22D).

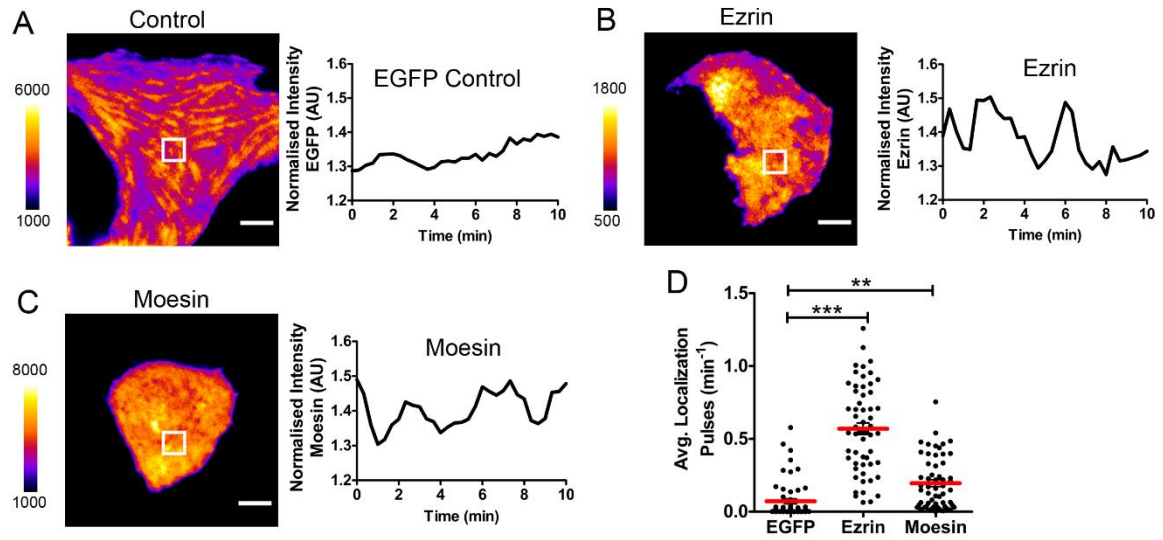

Figure 3.22: ERM proteins Ezrin and Moesin show cortical localization pulses in U2OS cells. (A)-(C) Left panels: Representative TIRF images of EGFP-N1 control, Ezrin-EGFP and Moesin-EGFP, respectively. Right panels: Normalised intensity of EGFP-localization over time in the white marked region in the corresponding cell image, normalised with whole cell intensity at first frame. (D) Quantification of average localization pulses per cell n≥55 cells per condition from 3 independent experiments. One-way Anova, Tukey's multiple comparison test with ***, P=0.001, **, P=0.01,)

Next, cross-correlation analysis with actin dynamics was performed. As local Ezrin pulses were more prominent as compared to Myosin signal dynamics, Ezrin localization was cross-correlated with cortical actin signals. As a result, Ezrin fluorescence signal dynamics was highly correlated with actin dynamics (Correlation co-efficient=0.44 ± 0.03) with a negligible average time delay of signal maxima (0.18 ± 0.2 sec) (fig. 3.23).

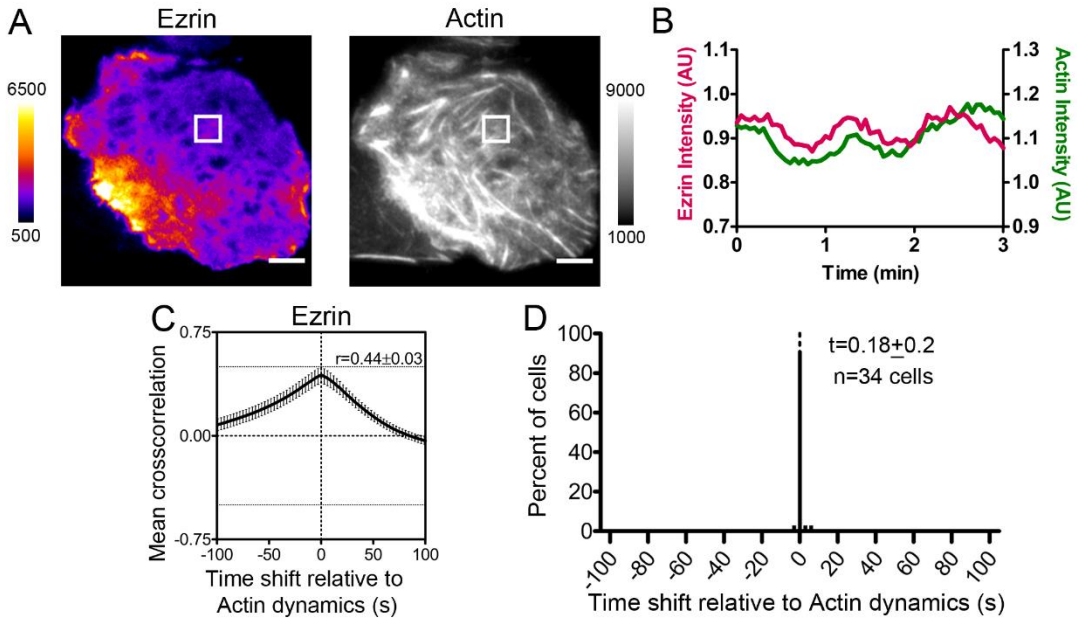

Figure 3.23: Ezrin localization dynamics correlates with actin dynamics. (A) Representative TIRF images of Ezrin-EGFP and actin-mCherry. Scale bar=10µm. (B) Normalised intensity of Actin and Ezrin over time corresponding to the marked region (white box) in A. (C) Pearson product moment correlation functions (see methods) to determine spatiotemporal correlation between Actin and Ezrin localization. (D) Histogram of time point of Ezrin signal maxima relative to occurrence of Rho activity signal maxima n≥ 34 cells from 3 independent experiments.

Activation of GEF-H1 by depolymerization of microtubules increases Rho activity pulses in U2OS cells (Graessl et al. 2017). Similarly, treatment of cells with nocodazole increased the pulsing of ERM proteins (data not shown) indicating that Ezrin acts downstream of Rho or might be a component of the pulsatory Rho network. Indeed cross-correlation analyses revealed that Ezrin localization highly correlated with Rho activity pulses with a significant time delay of 15.7 ± 2.2 sec (fig. 3.24).

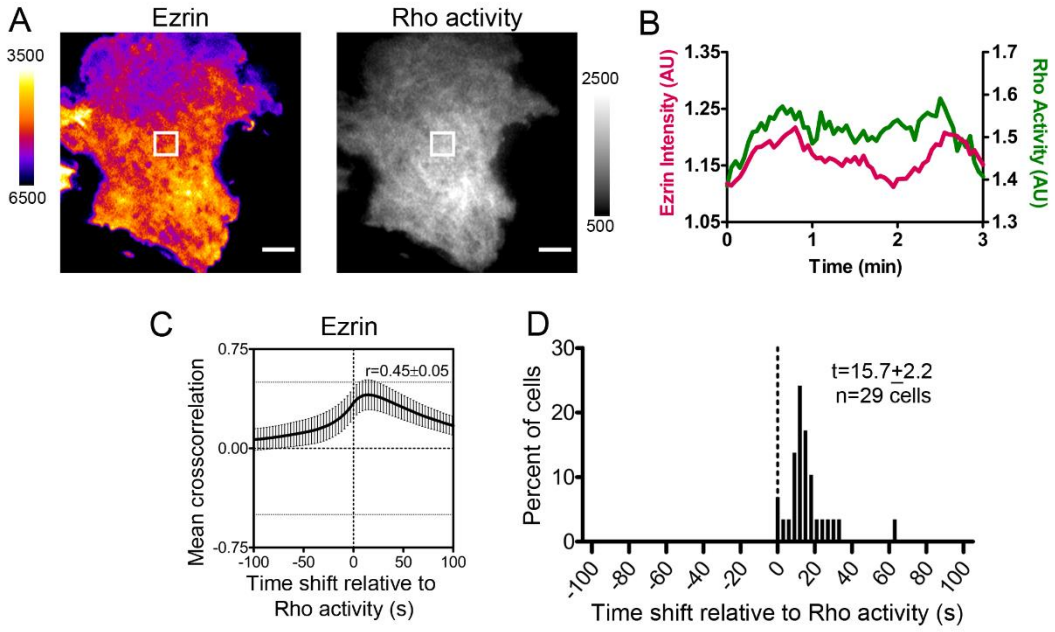

Figure 3.24: Ezrin localization correlates with Rho activity with a temporal delay. (A) Representative TIRF images of Ezrin-EGFP and Rho activity sensor (delCMV-Rhotekin-RBD-Cherry). Scale bar=10µm. (B) Normalized intensity plots of Ezrin localization and Rho activity signal for regions marked by white box indicated in A with average whole cell intensity at the first frame of respective channel. (C) Pearson product moment correlation functions (see methods) to determine spatiotemporal correlation between Rho activity and Ezrin localization. (D) Histogram of time point of Ezrin signal maxima relative to occurrence of Rho activity signal maxima n≥ 28 cells from 3 independent experiments.

Furthermore, earlier study reported phosphorylation and activation of ERM proteins by the Rho effector Rho effector kinase ROCK (Hébert et al. 2008). To assess, if Ezrin plasma membrane localization pulses might be downstream of the Rho network, pharmacological inhibition of ROCK was performed. Y compound treatment significantly dampened cortical Ezrin localization pulses as compared to water control (Average Rho activity pulses per min. on addition of Water control=0.40 ± 0.03 S.E.M. and on Y compound treatment =0.32 ± 0.2 S.E.M.) (fig. 3.25). However, not all Ezrin dynamics was lost upon Y compound treatment, indicating potential other network components co-ordinately regulating Ezrin plasma membrane dynamics.

Together, local pulses of ERM protein localization were found in U2OS cells that follow Rho activity pulses and that coincide with local actin dynamics. Perturbation of Rho signaling by ROCK inhibition lead to significant reduction of Ezrin pulses suggesting

Ezrin as a component of the pulsatory Rho signaling network in cells, likely to control linkage of Rho induced contractile actin nodes to the plasma membrane.

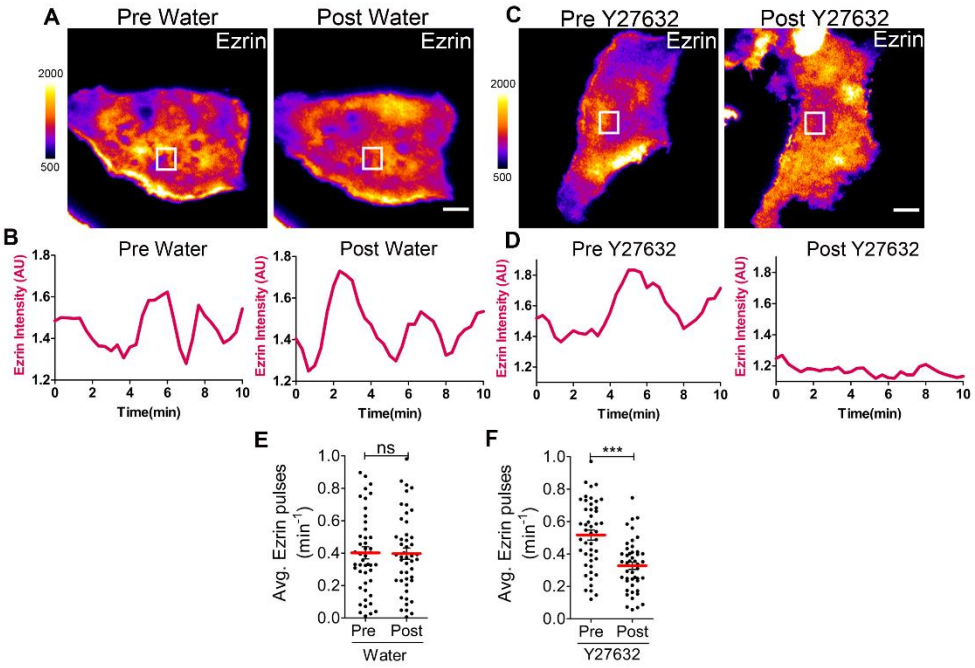

Figure 3.25: Ezrin is downstream of Rho-ROCK signaling. (A) Representative TIRF images of Ezrin-EGFP transfected cells before and after addition of water. Scale bar= 10µm. (B) Normalized intensity plots of Ezrin localization signal for regions marked by white box indicated in A with average whole cell intensity at the first frame. (C) Representative TIRF images of Ezrin-EGFP before and after Y compound (Y27632, 30µM) addition. Scale bar= 10µm. (D) Normalized intensity plots of Ezrin localization signal for regions marked by white box indicated in C with average whole cell intensity at the first frame. (E-F) Quantification of average Ezrin pulses upon treatment. n≥47 cells per condition from 3 independent experiments. Paired *t-test* with ***, P=0.0001.

4. Discussion and outlook

Migration is an important aspect not only in Keratinocyte homeostasis but also for wound healing. During wound healing, Keratinocytes respond to diverse range of cytokines and growth factors that stimulate proliferation and migration to allow closure of the wound bed (Schäfer and Werner 2008; Barrientos et al. 2008)). The growth factor EGF contributes to epidermal homeostasis, wound healing, chemotactic migration and stem cell maintenance (Barrientos et al. 2008). Temporal profiling of EGF stimulation showed activation migration related proteins at early time points followed by cell proliferation and differentiation (Blumenberg 2013). Thus, EGF is widely used to study induction of cell motility in Keratinocytes. Here, EGF treated motile Keratinocytes were used to understand the role of the Rho GTPase protein Cdc42 in the process of cell migration.

4.1. Cdc42 participates in Keratinocyte migration

Cdc42 is an evolutionary conserved Rho GTPase well-known for controlling actin dynamics (Hall 1998) by which it can regulate multiple cellular processes (Cotteret and Chernoff 2002) such as cell polarity, migration, protein trafficking, cytokinesis, gene transcription, apoptosis and cell proliferation (Hall 1998) (Cotteret and Chernoff 2002) (Hall 1998; Farhan and Hsu 2016; Lamarche et al. 1996; Lämmermann et al. 2009; Yasuda et al. 2004; Wedlich-Soldner et al. 2003; Baschieri et al. 2014). In mouse skin tissue, Cdc42 was shown to regulate progenitor cell differentiation to hair follicle lineage via stabilizing β-Catenin (Wu et al. 2006b) and also by basement membrane maintenance (Wu et al. 2006a). Furthermore, this GTPase controls melanoblast migration by promoting formin mediated actin polymerization, Myosin-II localization and integrin based adhesion (Woodham et al. 2017).

Here, the role of Cdc42 in human primary Keratinocytes was studied Cellular activity patterns of endogenous Cdc42 were studied using a previously described fluorescent protein tagged effector domain as activity sensor (Graessl et al. 2017) combined with TIRF microscopy. Our studies in Keratinocytes revealed two distinct Cdc42 activity localization patterns (figure 4.1). First, Cdc42 activity pulses were observed in cell centre and the lamellum region similar to Pulsatory Cdc42 activity

patterns previously observed in U2OS cells (Graessl et al. 2017). These were shown to temporally correlate with Rho activity pulses with a slight delay. Indicating the presence of a potential positive cross talk between the two GTPases. Excitable Cdc42 activity pulses and propagating waves were also observed by Yang and colleagues (Yang et al. 2016) on inhibition of actin polymerization. Cdc42 is among the major actin regulators and its main effects on actin polymerization is brought about by its downstream regulators such as Wiskott Aldrich Syndrome Protein (WASP), p21associated Kinases (PAKs), transducer of Cdc42 actin assembly (TOCA) and Lim Kinases (LIMK) (Watson et al. 2017). Further, Cdc42 also contributes to Myosin light chain activation by activating Myotonic dystrophy related Kinases (MRCKs) (Unbekandt and Olson 2014). In addition to its stimulatory role in actin polymerization, Cdc42 can thus also regulate actomyosin contractions in cells.

Surprisingly, we also observed a second type of Cdc42 activity pattern at the trailing edge of a migration Keratinocyte that was previously not shown. Cdc42 activity in this region was strongly elevated, however, more persistently as compared to activity pulses, and this activity pattern was observed exclusively in migrating cells. Upon depletion of Cdc42, this activity pattern was lost confirming that the strong sensor signal observed in the rear end was indeed due to elevated Cdc42 activity in this region. This is the first time, Cdc42 activity has been reported to be predominantly localized at the cell rear. Several groups have reported earlier Cdc42 activity at the cell front using varying live-cell approaches. Activity in protrusions was reported using organic, solvent-sensitive dye coupled effector domain sensors in mouse embryonic fibroblasts (Nalbant et al. 2004), fluorescent resonance energy transfer (FRET)-based probes (Hanna et al. 2014; Pertz 2010) rat embryonic fibroblasts (Martin et al. 2016), neutrophils (Yang et al. 2016) and optogenetics tools (effector N-WASP tagged to fluorescent protein for activity detection) in HeLa cells (Beco et al. 2018). Although, the sensors used in most of these methods were effector domain based, their detection was pursued using confocal or epifluorescence microscopy. Thus, TIRF microscopy in combination with an effector domain-based sensor of low expression levels due to a truncated promoter may have enabled us to detect endogenous Cdc42 activity in Keratinocytes more sensitively.

During migration, single Keratinocytes display a stable flat large lamellipodium protruding in direction of migration (Kirfel et al. 2004). Such protrusions are mainly formed by treadmilling of the actin network as previously shown in fish Keratocytes

(Keren et al. 2008) and are stabilised by ECM components and integrins (Frank and Carter 2004). At the cell rear, detachment depends on actin and actin-interacting proteins, adhesion molecules and enzymes as proteases, kinases and phosphatases (Kirfel et al. 2004; Frank and Carter 2004). Interestingly, during cell rear detachment, long tubular extensions called retraction fibres are formed leaving behind cellular material such as adhesion components (Kirfel et al. 2004) and ECM components (Frank and Carter 2004). The morphology of Keratinocytes is schematically depicted in figure 4.1.

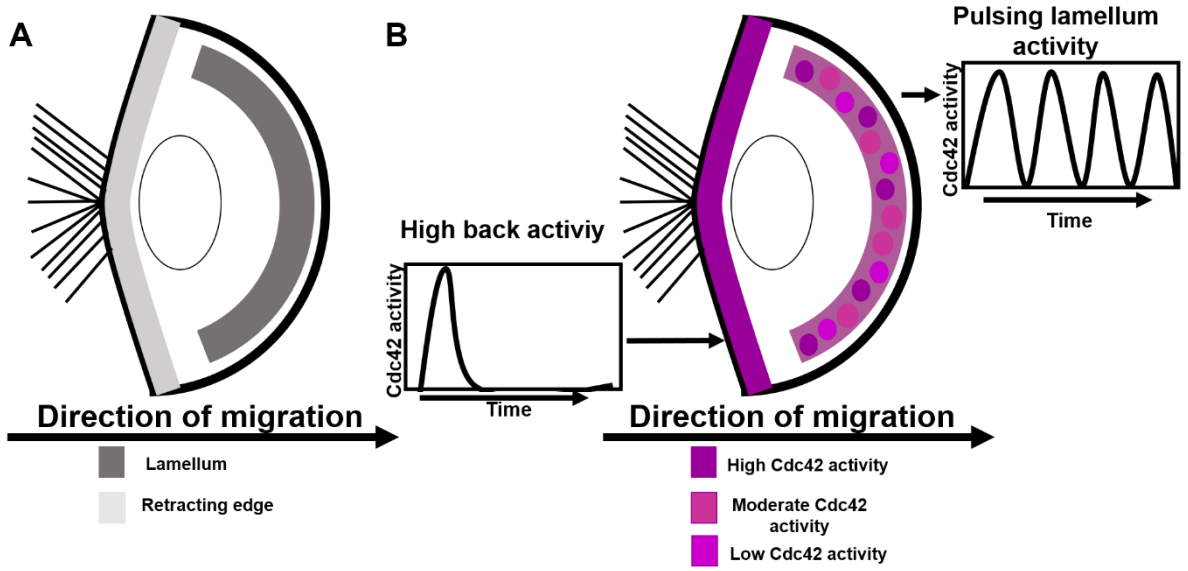

Figure 4.1: Schematic representation of Cdc42 activity pattern localization in migrating Keratinocyte. (A) Schematic representation of a migrating fan-shaped Keratinocyte with a flat lamellipodium in the front and the lamellum behind. The retracting or trailing edge of the cell shows extended retraction fibres. (Kirfel et al. 2004) (B) Intense levels of Cdc42 activity were observed at the trailing edge of migrating Keratinocytes. While pulsing Cdc42 activity persists in the lamellum region.

Cdc42 controls cell migration by regulating actin polymerization and dynamics at cell cortex (Hall 1998) but it can also control several other mechanisms to modulate cell migration. For example, in astrocytes, membrane trafficking dependent Cdc42 localization in the leading edge regulates cell migration during wound healing (Osmani et al. 2010). In neutrophils, Cdc42 maintains cell polarity and persistent migration by maintaining stable protrusions at the front and localizing Wiskott-Aldrich Syndrome Protein (WASP) to the uropod (a specialised cell region) and directs microtubule polarity (Kumar et al. 2012). The pronounced effect of Cdc42 on actin dynamics is brought about by its interaction with effectors such as WASP, which interacts with the

actin nucleators Arp2/3 complex (Symons et al. 1996). In the experiments here, in agreement with regulatory role of Cdc42 in actin dynamics, a temporal global correlation of Cdc42 activity dynamics with actin localization was observed and Distinct Cdc42 activity pulses in the lamellum correlated with actin localization. It could be thus speculated that the Cdc42 activity pulses in the relatively flat lamellum may be contributing to actin-based protrusions or actin treadmilling in this region.

At the trailing edge of Keratinocytes, along with strong actomyosin based contractions, dynamic reorganization of cell adhesions as hemidesmosomes or focal adhesions that facilitate cell to ECM contacts is also critical for control of migratory behaviour (Kirfel and Herzog 2004). Cdc42 is shown to be involved in desmosome turnover (Wu et al. 2006b). Thus, Cdc42 may control both actomyosin flow and adhesion turnover at the trailing edge. In agreement with this hypothesis, the data here displayed strong correlation of actin and Myosin-II retrograde flow with levels of Cdc42 activity at the trailing edge.

Cdc42 effectors not only regulate actin dynamics but also directly or indirectly affect Myosin activity and localization (Unbekandt and Olson 2014). In Keratinocytes, high Myosin flow corresponding to high Cdc42 activity at the trailing edge indicated that the GTPase might play a role in actomyosin flow in the trailing edge as well. Indeed, depletion of Cdc42 reduced the retrograde Myosin flow supporting this idea. Additional studies will thus help to determine if Cdc42 directly regulates Myosin dynamics or the effect on Myosin flow is indirectly due to altered actin polymerization.

Cdc42 depletion has varied effects on cell migration in different cell types. Cdc42 controls neutrophil polarity and chemotaxis via WASP (Kumar et al. 2012) and the phenotypic effects are mainly due to disrupted microtubule function. On the other hand, Cdc42 depletion in dendritic cells leads to reduction in cell motility and disruption in global actin dynamics (Lämmermann et al. 2009). Also, Cdc42 may be essential for binding and intercalation but not actual movement during trans-endothelial cell migration (Reymond et al. 2012). In Keratinocytes, depletion of Cdc42 reduced migration velocity and distance covered by individually moving cells as well as of those in colonies. Along with the decrease in migration velocity and distance, cells were unable to perform necessary contractions and hence stalled migration and displayed fewer contracting edges as compared to control cells. The cells also showed ectopic protrusions although not significantly high. Prior studies showed that mouse melanoblasts display migration defects on Cdc42 depletion due to deregulation of

contractility and actin dynamics (Woodham et al. 2017). Thus, delocalization of Myosin and impairment of actin dynamics may be also a core underlying reason for our finding that lack of Cdc42 leads defective migration in Keratinocytes. Overall, data gained in this study demonstrates that Cdc42 participates in efficient Keratinocyte migration and that localization activity patterns might be modulatory in this process.

4.1.1. Potential positive feedback mechanism controlling localized Cdc42 in the trailing edge of migrating Keratinocytes

In this study, high level of Cdc42 activity was persistently seen at the cells rear. To establish and maintain this elevated Cdc42 activity, a positive feedback mechanism involving self-amplification might be involved. Presence of a positive feedback can amplify a response, generate bistable switches or alter kinetics of the involved component (Brandman and Meyer 2008). For signal self-amplification, the core protein activity has to be positively coupled to upstream activating pathways and this might involve downstream effectors. Indeed, early studies suggest a positive feedback mechanism to amplify Cdc42 activity that involves the Cdc42 downstream effector PAK linked to the activating Cdc42 GEF βPix (Frank and Hansen 2008). PAKs are serine/threonine Kinases participating in cellular functions like cytoskeletal dynamics, cell motility, cell cycle, transcription and translation. In mammals, there are mainly six proteins in the PAK family (Molli et al. 2009). Of those, PAK1, PAK2 and as recently PAK4 have been extensively studied (Kichina et al. 2010). Downstream of Cdc42 and the related Rho protein Rac1, PAK1/2 (Manser et al. 1997) have been shown to activate Myosin dynamics via MLCK phosphorylation (Goeckeler et al. 2000), and inactivate cofilin via LIMK activity (Misra et al. 2005). Here, PAK phosphorylation was significantly decreased upon Cdc42 depletion suggesting similar role in Keratinocytes to potentially mediate Cdc42 functions. In agreement with a major role of PAK in our model system, inhibitor studies showed significant decrease in Keratinocyte migration. Interestingly, we also found that the trailing edge Cdc42 activity was significantly decreased upon PAK inhibition suggesting that the effector might be involved in the generation of this subcellular activity pattern of the GTPase as well. Depletion of PAK2 further supported this hypothesis (fig 3.8). PAK2 depletion also lead to significant decreased of the robust Cdc42 activity signal in the trailing edge indicative of a positive feedback mechanism. In addition, PAK2 depletion was also accompanied by

significant accumulation of Cdc42 activity at the cell front while transient Cdc42 activity pulses did not seem to be altered significantly (fig 3.8).

Prior studies showed that through the Pix binding motifs, group I PAKs directly interact with the SH3 domain of Pix family of proteins (Hofmann et al. 2004; Manser et al. 1997). This interaction brings together the Cdc42/ Rac1 downstream effector PAK and the upstream Pix proteins (Manser et al. 1997). The Pix proteins interact with GTPases via the DH domain while the CRIB domain on PAKs binds to the active GTPase (Koh et al. 2001; Frank and Hansen 2008) suggested to form a multi-protein complex. Further, PAK and Pix are involved in multiprotein signalling complexes at the adaptor protein GIT (Frank and Hansen 2008), and may be activating GTPase activity through such an adapter complex.

Rac/Cdc42-Pix-PAK was shown to control activity of the GTPase at focal adhesions and membrane ruffles (Koh et al. 2001). As this multi-protein complex co-localizes both, the downstream effector of Cdc42 and its activator, a positive feedback loop is enabled (fig 4.2) (Lawson and Ridley 2018; Manser et al. 1997). Thus, the role of βPix in control of Cdc42 activity patterns in Keratinocytes was studied. Knockdown of βPix in this study caused massive delocalisation of Cdc42 activity patterns. In particular, a high accumulation of Cdc42 activity was observed in the cell centre and front. In comparison to the high intensity in the centre, the trailing edge back activity was significantly diminished. This demonstrates that βPix is important for the persistent activation of Cdc42 at the trailing edge. While, the increase in pulsing Cdc42 activity in lamellum indicates the presence of another GEF that, in the absence of βPix, acts compensatory targeting the bulk Cdc42 to central and lamellar regions. In support of a compensatory mechanism, overall Cdc42 activity pulses increased on βPix knockdown also suggesting that this compensatory GEF might also be the regulatory GEF controlling Cdc42 activity pulses. Although this data clearly shows that βPix is crucial for targeting Cdc42 activity to the trailing edge, further data is needed to confirm that a potential positive feedback including PAK and βPix exists that facilitates self-amplification of Cdc42 activity at the trailing edge. One initial approach could be for example the overexpression of βPix and measurement of dynamic βPix localization patterns and Cdc42 activity within the same cell. This will reveal if the two signals substantially co-localize in distinct regions which is a prerequisite for a positive feedback. To link the three proteins to such molecular mechanism however, additional experiments need to be performed using RNAi depletion of βPix or PAK, respectively

and expression of siRNA resistant mutants that have been established to mediate the positive feedback.

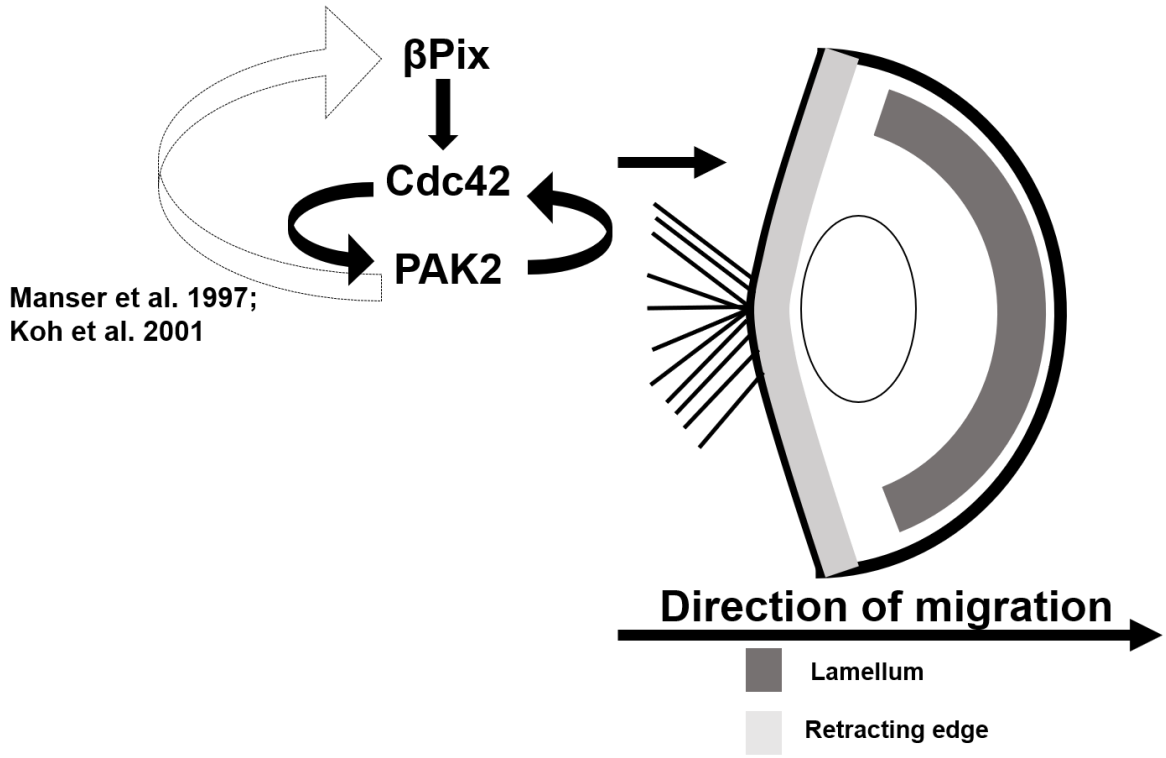

Figure 4.2: Schematic showing suggested components of a positive feedback mechanism to facilitate localization of Cdc42 activity at the trailing edge. Our data shows that localization of Cdc42 activity at the trailing edge depends both on PAK 2 and βPix (marked by bold black arrows). Further literature suggests interaction between PAK and βPix (outline arrow). Such a complex may be formed at the retracting edge of a migrating Keratinocyte which regulates actomyosin retrograde flow

The Pix-PAK complex is shown to form membrane ruffles and microvilli like structures in Hela and Cos 7 (Koh et al. 2001) cells but not in cell retraction or trailing edge. Cdc42 has been reported to regulate polarity, directionality and chemotaxis (Osmani et al. 2010). Here we can speculate that the trailing edge activity found in Keratinocytes might be important to maintain migration direction co-ordinating contractility within this region.

Our migration studies on βPix depletion showed no change in migration velocity or distance covered. βPix is a shared GEF for Cdc42 and Rac1 (Manser et al. 1997). Thus, it was conflicting to find out that depletion of βPix did not reduce Keratinocyte migration in this study. Earlier findings by Hiroyasu et al. showed that depletion of βPix

in HaCaT cells (immortalised Keratinocytes) enhanced individual cell migration on stiff substrates, whereas migration was not affected on soft substrates (Hiroyasu et al. 2017). Thus, future studies might require adjustment of experimental conditions to better understand relevance of βPix in Cdc42 mediated migration behaviour.

Data here reveals that Cdc42 is critical for the retrograde flow of actin and Myosin in the trailing edge of Keratinocytes. However, it is not clear how actomyosin dynamics is regulated downstream of Cdc42. The potential mechanism might involve activation of MLCK by the Cdc42 effector PAK. Another candidate effector that could also mediate the localization of Myosin downstream of Cdc42 is Myo18A. Myo18A is a class 18 Myosin, which forms heterodimers with Myosin-IIa (Billington et al. 2015). This Myosin was shown to bind to the Cdc42 GEF βPix (Hsu et al. 2014) in epithelial cells as well as to MRCK/LARP35a to form a tripartite complex in Hela cells (Tan et al. 2008). In Keratinocytes, it can be speculated that the tripartite complex localises Myosin-IIa-Myo18A heterodimers to the cell rear where they are further integrated to actin filament bundles (Tan et al. 2008) and mediating actomyosin contractility at the trailing edge. The data in this thesis already shows the dependence of Myosin-IIa retrograde flow on Cdc42 (fig.3.6). Further correlation, localization or biochemical studies of Myosin-IIa related Cdc42 effectors could provide more insight into cellular mechanisms relevant for the trailing edge flow in Keratinocytes.

Further studies could also aim at detection of other migration related GEFs such as TUBA, Intersectin, or Cdc42 specific DOCK proteins which may control Cdc42 activity in migrating Keratinocytes (Ridley 2001; Lawson and Ridley 2018), potentially via other mechanisms.

4.2. Control of spatio-temporal Rho activity signals during EGF stimulated migration

Wound healing is a highly complex process during which Keratinocytes flanking the wound respond to an array of external cues such as cytokines growth factors and changes in ECM (Evans et al. 2013). Epidermal growth factor receptor (EGFR) signaling is a major part of this processes and controls basal Keratinocyte proliferation, migration and delay of apoptosis (Schneider et al. 2008; Pastore et al. 2014; Shostak et al. 2014). Excessive uncontrolled EGFR signaling affects hair follicle development

(Fuchs 2007) and such aberrant signaling is also observed in many types of cancers (Vogelstein et al. 2013). In turn, when EGFR inhibitors are used during chemotherapy, they have several prominent side effects on skin (Pinto et al. 2011; Pastore et al. 2014).

Epidermal growth factor (EGF) has been long used in the field for studying Keratinocyte migration and is also shown to induce front rear polarity (Ho and Dagnino 2012). Transcriptome analyses upon EGF stimulation of Keratinocytes revealed upregulation of cytoskeletal genes at very early time points (30 min) followed by proliferation promoting and differentiation inducing genes at later time stages (Blumenberg 2013). Furthermore, upon EGF stimulation has been shown to lead to transient activation of RhoA, Rac and Cdc42 a number of cell types (El-Sibai et al. 2007; Kurokawa et al. 2004; Pertz 2010), albeit in none of these studies elevated activity was found at the trailing edge. Interestingly, we found that localized Cdc42 activity at the trailing edge of migrating Keratinocytes was not elevated upon EGF treatment suggesting that Cdc42 activity in this region might not be sensitive EGFR signaling.

RhoA is Cdc42 related Rho GTPase that has been shown to be activated upon EGF treatment (El-Sibai et al. 2007) in biochemical studies and plays a role in cell migration by controlling cell contractility (Ridley 2001; Pertz 2010; Worthylake et al. 2001). FRET based detection of spatio-temporal activity patterns of RhoA showed distinct activity at cell front and activity during cell retraction (Martin et al. 2016; Fritz and Pertz 2016; Pertz 2010). Our lab earlier showed excitable subcellular Rho activity pulses (Graessl et al. 2017) at the cell cortex in migratory U2OS cells which were linked with Myosin contractility. Since, Rho is known to be necessary for cell contraction and tail retraction (Worthylake et al. 2001), elevated Rho activity was expected at the trailing edge of migrating Keratinocytes. However, Rho activity was not localized in this region nor in the cell front during migration. However, in long-term (1 h) EGF stimulated migrating Keratinocytes, the subcellular Rho activity pulses were observed with a very low amplitude.

Earlier, another group found in mouse Keratinocytes defects in wound healing upon Rho depletion (Jackson et al. 2011) which may be due to lack of essential Rho activity responses at perhaps earlier stages of wound healing. RhoG has been shown to participate in Keratinocyte polarization (Ho and Dagnino 2012) and partly for directed cell migration (Jackson et al. 2011). Based on biochemical studies of Rho

GTPase activities, a transient increase of Rho activity at early time points after EGF stimulation is observed in other cell types. Thus, on-stage stimulation of Keratinocytes was performed to study Rho activity response to EGF at early time-points (from 0 to 11.66 minutes of EGF addition).

Similar as reported earlier in breast epithelial MCF10A cells, EGF treatment of Keratinocytes in this work lead to immediate protrusion formation approximately at 1 min which was followed by contraction of the entire periphery within minutes (Gagliardi et al. 2015). Based on Rho activity sensor fluorescence protrusions and retractions were also observed on EGF stimulation in TIRF measurements. There, we found that Rho activity steeply elevated at the peak of the protrusion phase and was followed by retraction of this region. This behavior was observed at the majority of the peripheral regions and thus could underly the global cell contraction upon EGF-stimulation.

The relevance of this EGF stimulated dynamic cell behavior at the cell periphery in Keratinocytes is not known. In Keratinocytes EGF stimulation negatively affects cell attachment to matrix due to disruption of hemidesmosome structures (Mainiero et al. 1996) and leads to increased migration towards the wound bed (Santoro and Gaudino 2005). The global formation of protrusions at the cell periphery is accompanied by enhanced turn-over of focal adhesions (Wozniak et al. 2004). Also, actin polymerization at the leading edge and coordinated actomyosin based contractility can give rise to alternating phases of protrusions and contractions (Burnette et al. 2011; Pertz 2010). It has been speculated that such protrusion-retraction cycles may be used by the cell for exploratory mechanisms during migration (Andrew and Insall 2007; Nalbant and Dehmelt 2018). Thus, transient formation of protrusion around the global cell periphery together with Rho induced global contraction might be prerequisite for priming the cells for such exploratory cell motility.

4.3. Lbc type Rho GEFs are potential regulators of Rho activity in Keratinocytes

Rapid local increase of signal pulses and propagating waves is a characteristic feature of excitable systems (Allard and Mogilner 2013). Such excitable networks usually have a positive feedback loop and a time delayed negative feedback loop. Graessl et al showed a Rho signalling network that generated pulses and propagating waves.

There, the Lbc type GEF GEF-H1 was shown to mediate positive feedback while actomyosin and associated GEFs relayed a negative feedback with temporal delay (Graessl et al. 2017). Upon EGF stimulation, peripheral Rho activity also rapidly increased before going back to initial levels and therefore this might be an outcome of excitable Rho activity in Keratinocytes. Similar to that in U2OS cells, GEF-H1 and/or other Lbc type GEFs may mediate Rho self-amplification on EGF stimulation.

GEF-H1 is activated downstream of mechanical responses to integrins (Guilluy et al. 2011b) and Junctional Adhesion molecule (JAM-A) (Scott et al. 2016). There, GEF-H1 was shown to be activated downstream of Erk signalling (Scott et al. 2016). Particularly, Erk1/2 might regulate GEF-H1 activity either positively by phosphorylation of GEF-H1 at T(678) (Fujishiro et al. 2008) or negatively by inactivating GEF-H1 by phosphorylation at S(959) (Thun et al. 2013). In our experiments, depletion of GEF-H1 did not block the occurrence of Rho activity peaks. Interestingly however, EGF induced Rho activity peaks in GEF-H1 depleted cells were detected slightly earlier as compared to control cells, implicating that GEF-H1 mediated Rho self-amplification mechanism does not underlie the Rho activity peak but might play a modulatory role.

GEF-H1 is a member of the Lbc type Rho GEF family with highly similar DH-PH domains that are critical for GEF activity and localization (Medina et al. 2013). Based on their structural similarity and previous studies, other Lbc type GEFs might mediate Rho activity dynamics upon EGF stimulation. In fact, AKAP13 along with a scaffolding protein Ksr-1, was shown to act downstream of EGF stimulation to contribute to Erk1/2 activation (Smith et al. 2010). Thus, a focused screen for induction of Rho activity pulses in Keratinocytes was performed to identify Lbc GEFs potentially contributing to EGF mediated Rho excitability in Keratinocytes.

In the majority of Dbl GEFs as in the Lbc type subgroup, the DH domain, which is the active GEF site for nucleotide exchange in Rho proteins, is followed by PH domain that can promote binding to phosphoinositide and localize the GEF to plasma membrane (Lemmon and Ferguson 2000). A study on all seven Lbc type GEFs including showed formation of a ternary complex of their respective DH-PH domains with both inactive and active Rho GTPase variants (Chen et al. 2010). These interactions were postulated to function in positive feedback loops facilitating self-amplification of Rho activity. The underlying mechanism was thought to include activation of Rho by the DH-domain of the GEF with subsequent interaction of the active Rho version with GEF-proteins allowing GEF-recruitment to close the positive

feedback loop (Medina et al. 2013). Recently, the presence of such a positive feedback loop involving Rho and GEF-H1 together with effector mediated delayed negative feedback was shown to underlie Rho activity pulses in U2OS cells (Graessl et al. 2017).

In this thesis here, overexpression of all seven Lbc type GEFs (all WT construct) gave rise to propagating Rho activity waves suggesting all tested GEFs are capable of facilitating Rho excitability in Keratinocytes. However, somewhat varying GEF-localization patterns were observed suggesting that the molecular mechanisms that underlie excitability might be distinct. For example, GEF-H1 localizes to microtubules and is there inactive (Krendel et al. 2002; Birkenfeld et al. 2008). In our experiments, this was mostly observed too, although a substantial portion of GEF-H1 was also found cytosolic. However, for all other six Lbc GEFs, bulk localization was observed in the cytoplasm. This was surprising as LARG, GEF-H1, p190 RhoGEF have been reported to localize to focal adhesions (Müller et al. 2018; Guilluy et al. 2011b). Thus, focal adhesion localization seems not to be relevant for Rho activity pulses and wave propagation in Keratinocytes. Instead, LARG and PDZ Rho GEF, were often seen to localize at the cell periphery, either in the cell front, the cell rear or both. Interestingly, in cells with such prominent GEF localization at the periphery no Rho activity waves were observed. Computational simulations to understand the Rho signal network dynamics revealed that global Rho activity levels have strong influence of subcellular Rho signal dynamics (Kamps et al, manuscript in preparation). Thus, further studies of GEF function in Keratinocytes, such as optogenetic titration of varying GEF-levels in individual cells may reveal the underlying relevance and mechanism of the interplay of Rho-GEF signaling complexes in Keratinocytes.

In this study human skin progenitor Keratinocytes were used with some heterogeneity with respect to their stem-cell properties. Some of these might be primed for renewal to stem cells (holoclones), some to progenitors (meroclones) and some simply transit amplifying cells (paraclones) (Fuchs 2007; Nanba et al. 2013). A small population of basal Keratinocytes residing in the epidermis have the ability to give rise to entire tissues during events such as wound healing providing the ultimate stem cell pool for the skin (holoclones) (Nanba et al. 2013). Expression levels of β1 integrins was shown to be one of the markers for stem cells, but conflicting data is available on this (Fuchs 2007). Absolute markers for skin stem cells are largely unknown making detection of stem cells very difficult. The Rho activity pulses and

propagating waves in Keratinocytes such as observed by EGF stimulation or by overexpression of Lbc GEFs were only observed in a subset of cells. This indeed may be due to heterogeneity of stemness within the population. Further studies with potential stem cell markers and Rho activity responses would help to provide a better understanding and differentiation of distinct stem cell pools in the epidermis.

4.4 Understanding excitable cortical Rho activity

Cells interact and respond to components in the extracellular matrix (ECM) and such interactions are crucial for cellular processes such as cell fate decisions (Engler et al. 2006; Engler et al. 2008), proliferation and migration (Provenzano et al. 2009; Geiger and Bershadsky 2002) and immune responses (Huveneers and Danen 2009). The integrin family of proteins are membrane receptors responding to ECM components (ref). Various combinations of integrin dimers respond to different ECM proteins such as collagen, laminin and fibronectin (Nardone et al. 2017; Huveneers and Danen 2009).

Here, the model system U2OS cells was used to study effect of ECM composition on Rho activity pulses. Distinct Rho activity response on individual ECM substrates (fig.) suggests that the excitable Rho network might be an integral part of cellular mechanisms of sensing the ECM composition. Earlier work from our group showed that subcellular Rho activity pulses give rise to cortical actin Myosin contractions which are affected by matrix stiffness (Graessl et al. 2017). In a separate work, Nardone and colleagues showed the response of the transcriptional co-activators YAP and TAZ (of the Hippo pathway) respond to ECM composition and stiffness via the Rho pathway (Nardone et al. 2017). Together, our data together with the above-mentioned studies underscore the sensitivity of the Rho activity response to ECM composition and stiffness and its potential relevance for cell migration, division or morphogenesis.

The cellular actin cortex is a thin meshwork of short cross-linked actomyosin filaments linked to the plasma membrane. Changes in organization or composition lead to changes in cortical tension which may result in local cellular contractions and deformations (Chugh and Paluch 2018). Cortical tension can contribute to cell polarization (Tsankova et al. 2017), cell division (Maddox and Burridge 2003), cell migration and tissue morphogenesis (Lecuit and Lenne 2007). Thus, understanding

molecular mechanisms that control cortical tension in space and time is elementary to appreciate these important processes.

In addition to the elementary modules of the pulsatory Rho activity network (involving GEF-H1 and Myosin) that control network dynamics, our early work also deciphered additional factors potentially involved in this mechanism. For example, cortical actin pulses correlated with Rho activity pulses and the formin FHOD1 showed cortical pulses with a temporal delay of approximately 6s (Graessl et al. 2017). There, ctin pulses were dampened on FHOD1 knockdown suggesting a modulatory role of the formin in cortical Rho activity and actin dynamics. ERM proteins link cortical actin filaments to the plasma membrane (Bretscher et al. 2002) and their activity is necessary for cell polarity and directed migration during development (Diz-Muñoz et al. 2010). Using EGFP-linked variants of the Ezrin and Moesin we showed in this work for the first time localized pulsatory dynamics of these two ERM proteins. Further analysis showed temporal delay of Ezrin localization dynamics (approximately 6s) with respect to Rho sensor signal maxima suggesting that the ERM protein might be downstream of Rho activity pulses. Indeed, use of ROCK inhibitor confirmed that Ezrin pulses are Rho-ROCK dependent. However, Ezrin pulses were not entirely abolished indicating that other proteins may also control Ezrin localization. The cytoskeletal changes brought about by Ezrin are not entirely understood. Ezrin has been shown to be necessary for membrane tension in fibroblast cells (Rouven Brückner et al. 2015), a process which was shown to be related to PIP2 signaling. Further, Ezrin can interact with a wide array of proteins, such as Erb2 (Asp et al. 2016) and formins (e.g. FHOD1) (Viswanatha et al. 2013). Interestingly, FHOD1 has been previously shown be fully activated by ROCK downstream of RhoA and is part of the pulsatory signal network associated with cortical actomyosin pulses (Schulze et al. 2014; Gasteier et al. 2003)(graessl). Thus, this formin might be involved in spatial and temporal control of Ezrin localization downstream of ROCK.

Combining the results from this work with prior knowledge from our group and others, we can formulate an advanced model that integrates Rho activity pulse generation with its downstream effectors at the cell cortex (fig 4.3. below). The pulsatory network that controls Rho activity is positively regulated by Lbc type GEFs such as GEF-H1 through the DH-PH domain and inhibited by time-delayed mechanisms via Myosin and activity of GAPs such as Myo9b (Graessl et al. 2017) (Müller et al. 1997). Furthermore, the Rho pulsing network can activate formins such as FHOD1 and ERM proteins (here:

Ezrin) to control actin polymerization and to link the actin meshwork to the plasma-membrane, respectively, and regulates actomyosin contractility at cell cortex via Myosin-IIa. In addition, dynamics of subcellular activity pulses are controlled by distinct ECM substrates suggesting that the system is capable of sensing the ECM composition. Overall, work presented here has advanced the knowledge of the composition of the pulsatory Rho activity network and its potential relevance for sensory processes in response to chemical and mechanical cues from the ECM.

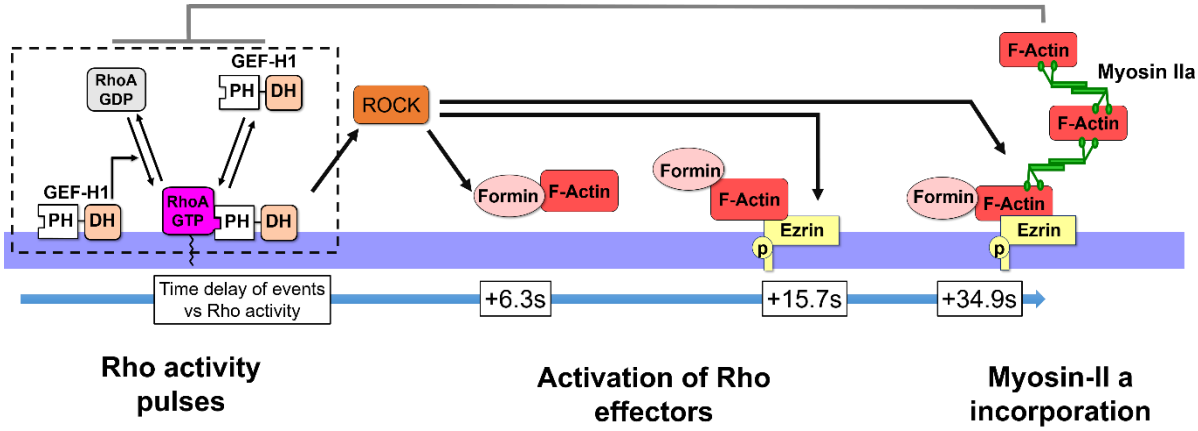

Figure 4.3: Time profile of Rho activity network mediated events at the cell cortex in epithelial U2OS cells: Rho is activated by regulator GEF-H1 via DH domain, which is in turn recruited by Rho to the plasma membrane via the PH domain, which recruits GEF-H1 to plasma membrane. This closes a positive feedback loop and allows self-amplification of Rho activity. Rho-ROCK effectors, the formin FHOD1, Myosin and Ezrin, are recruited/activated with a time delay with respect to Rho activity localization (black arrows). Actomyosin and associated GAPs such as Myo9b lead to time-delayed inhibition of Rho activity (grey arrows) and facilitate Rho activity signal dynamics. (Combined findings from Graessl et al., 2017 and this thesis)

References

Allard, Jun; Mogilner, Alex (2013): Traveling waves in actin dynamics and cell motility. In *Current opinion in cell biology* 25 (1), pp. 107–115. DOI: 10.1016/j.ceb.2012.08.012.

Amano, Mutsuki; Nakayama, Masanori; Kaibuchi, Kozo (2010): Rho-kinase/ROCK: A key regulator of the cytoskeleton and cell polarity. In *Cytoskeleton (Hoboken, N.J.)* 67 (9), pp. 545–554. DOI: 10.1002/cm.20472.

AMBROSE, E. J. (1956): A surface contact microscope for the study of cell movements. In *Nature* 178 (4543), p. 1194. DOI: 10.1038/1781194a0.

Ando, Y.; Jensen, P. J. (1993): Epidermal growth factor and insulin-like growth factor I enhance keratinocyte migration. In *The Journal of investigative dermatology* 100 (5), pp. 633–639. DOI: 10.1111/1523-1747.ep12472297.

Andrew, Natalie; Insall, Robert H. (2007): Chemotaxis in shallow gradients is mediated independently of PtdIns 3-kinase by biased choices between random protrusions. In *Nature cell biology* 9 (2), pp. 193–200. DOI: 10.1038/ncb1536.

Asp, Nagham; Kvalvaag, Audun; Sandvig, Kirsten; Pust, Sascha (2016): Regulation of ErbB2 localization and function in breast cancer cells by ERM proteins. In *Oncotarget* 7 (18), pp. 25443–25460. DOI: 10.18632/oncotarget.8327.

Axelrod, D.; Burghardt, T. P.; Thompson, N. L. (1984): Total internal reflection fluorescence. In *Annual review of biophysics and bioengineering* 13, pp. 247–268. DOI: 10.1146/annurev.bb.13.060184.001335.

Barrientos, Stephan; Stojadinovic, Olivera; Golinko, Michael S.; Brem, Harold; Tomic-Canic, Marjana (2008): Growth factors and cytokines in wound healing. In *Wound repair and regeneration : official publication of the Wound Healing Society [and] the European Tissue Repair Society* 16 (5), pp. 585–601. DOI: 10.1111/j.1524-475X.2008.00410.x.

Beco, S. de; Vaidžiulytė, K.; Manzi, J.; Dalier, F.; Di Federico, F.; Cornilleau, G. et al. (2018): Optogenetic dissection of Rac1 and Cdc42 gradient shaping. In *Nature communications* 9 (1), p. 4816. DOI: 10.1038/s41467-018-07286-8.

Bement, William M.; Leda, Marcin; Moe, Alison M.; Kita, Angela M.; Larson, Matthew E.; Golding, Adriana E. et al. (2015): Activator–inhibitor coupling between Rho signalling and actin assembly makes the cell cortex an excitable medium. In *Nature cell biology* 17 (11), p. 1471. DOI: 10.1038/ncb3251.

BERTANI, G. (1951): Studies on lysogenesis. I. The mode of phage liberation by lysogenic Escherichia coli. In *Journal of bacteriology* 62 (3), pp. 293–300.

Billington, Neil; Beach, Jordan R.; Heissler, Sarah M.; Remmert, Kirsten; Guzik-Lendrum, Stephanie; Nagy, Attila et al. (2015): Myosin 18A coassembles with nonmuscle myosin 2 to form mixed bipolar filaments. In *Current biology : CB* 25 (7), pp. 942–948. DOI: 10.1016/j.cub.2015.02.012.

Birkenfeld, Jörg; Nalbant, Perihan; Bohl, Benjamin P.; Pertz, Olivier; Hahn, Klaus M.; Bokoch, Gary M. (2007): GEF-H1 modulates localized RhoA activation during cytokinesis under the control of mitotic kinases. In *Developmental cell* 12 (5), pp. 699–712. DOI: 10.1016/j.devcel.2007.03.014.

Birkenfeld, Jörg; Nalbant, Perihan; Yoon, Soon-Hee; Bokoch, Gary M. (2008): Cellular functions of GEF-H1, a microtubule-regulated Rho-GEF: is altered GEF-H1 activity a crucial determinant of disease pathogenesis? In *Trends in cell biology* 18 (5), pp. 210–219. DOI: 10.1016/j.tcb.2008.02.006.

Blanchoin, Laurent; Boujemaa-Paterski, Rajaa; Sykes, Cécile; Plastino, Julie (2014): Actin dynamics, architecture, and mechanics in cell motility. In *Physiological reviews* 94 (1), pp. 235–263. DOI: 10.1152/physrev.00018.2013.

Blanpain, Cédric; Fuchs, Elaine (2006): Epidermal stem cells of the skin. In *Annual review of cell and developmental biology* 22, pp. 339–373. DOI: 10.1146/annurev.cellbio.22.010305.104357.

Blumenberg, Miroslav (2013): Profiling and metaanalysis of epidermal keratinocytes responses to epidermal growth factor. In *BMC genomics* 14, p. 85. DOI: 10.1186/1471-2164-14-85.

Bradford, M. M. (1976): A rapid and sensitive method for the quantitation of microgram quantities of protein utilizing the principle of protein-dye binding. In *Analytical biochemistry* 72, pp. 248–254. DOI: 10.1006/abio.1976.9999.

Brandman, Onn; Meyer, Tobias (2008): Feedback loops shape cellular signals in space and time. In *Science (New York, N.Y.)* 322 (5900), pp. 390–395. DOI: 10.1126/science.1160617.

Bravo-Cordero, Jose Javier; Hodgson, Louis; Condeelis, John (2012): Directed cell invasion and migration during metastasis. In *Current opinion in cell biology* 24 (2), pp. 277–283. DOI: 10.1016/j.ceb.2011.12.004.

Bretscher, Anthony; Edwards, Kevin; Fehon, Richard G. (2002): ERM proteins and merlin: integrators at the cell cortex. In *Nature reviews. Molecular cell biology* 3 (8), pp. 586–599. DOI: 10.1038/nrm882.

Burnette, Dylan T.; Manley, Suliana; Sengupta, Prabuddha; Sougrat, Rachid; Davidson, Michael W.; Kachar, Bechara; Lippincott-Schwartz, Jennifer (2011): A role for actin arcs in the leading-edge advance of migrating cells. In *Nature cell biology* 13 (4), pp. 371–381. DOI: 10.1038/ncb2205.

Burns, S.; Thrasher, A. J.; Blundell, M. P.; Machesky, L.; Jones, G. E. (2001): Configuration of human dendritic cell cytoskeleton by Rho GTPases, the WAS protein, and differentiation. In *Blood* 98 (4), pp. 1142–1149. DOI: 10.1182/blood.v98.4.1142.

Chen, Zhe; Medina, Frank; Liu, Mu-ya; Thomas, Celestine; Sprang, Stephen R.; Sternweis, Paul C. (2010): Activated RhoA binds to the pleckstrin homology (PH) domain of PDZ-RhoGEF, a potential site for autoregulation. In *The Journal of biological chemistry* 285 (27), pp. 21070–21081. DOI: 10.1074/jbc.M110.122549.

Chugh, Priyamvada; Paluch, Ewa K. (2018): The actin cortex at a glance. In *Journal of cell science* 131 (14). DOI: 10.1242/jcs.186254.

Chung, C. T.; Niemela, S. L.; Miller, R. H. (1989): One-step preparation of competent Escherichia coli: transformation and storage of bacterial cells in the same solution. In *Proceedings of the National Academy of Sciences of the United States of America* 86 (7), pp. 2172–2175. DOI: 10.1073/pnas.86.7.2172.

Cotteret, Sophie; Chernoff, Jonathan (2002): The evolutionary history of effectors downstream of Cdc42 and Rac. In *Genome biology* 3 (2), REVIEWS0002. DOI: 10.1186/gb-2002-3-2-reviews0002.

David, Muriel; Petit, Dominique; Bertoglio, Jacques (2012): Cell cycle regulation of Rho signaling pathways. In *Cell cycle (Georgetown, Tex.)* 11 (16), pp. 3003–3010. DOI: 10.4161/cc.21088.

Destaing, Olivier; Saltel, Frédéric; Gilquin, Benoit; Chabadel, Anne; Khochbin, Saadi; Ory, Stéphane; Jurdic, Pierre (2005): A novel Rho-mDia2-HDAC6 pathway controls podosome patterning through microtubule acetylation in osteoclasts. In *Journal of cell science* 118 (Pt 13), pp. 2901–2911. DOI: 10.1242/jcs.02425.

Devreotes, Peter; Horwitz, Alan Rick (2015): Signaling Networks that Regulate Cell Migration. In *Cold Spring Harbor perspectives in biology* 7 (8). DOI: 10.1101/cshperspect.a005959.

Diz-Muñoz, Alba; Krieg, Michael; Bergert, Martin; Ibarlucea-Benitez, Itziar; Muller, Daniel J.; Paluch, Ewa; Heisenberg, Carl-Philipp (2010): Control of directed cell migration in vivo by membrane-to-cortex attachment. In *PLoS biology* 8 (11), e1000544. DOI: 10.1371/journal.pbio.1000544.

Dulyaninova, Natalya G.; House, Reniqua P.; Betapudi, Venkaiah; Bresnick, Anne R. (2007): Myosin-IIA heavy-chain phosphorylation regulates the motility of MDA-MB-231 carcinoma cells. In *Molecular biology of the cell* 18 (8), pp. 3144–3155. DOI: 10.1091/mbc.e06-11-1056.

Duquette, Philippe M.; Lamarche-Vane, Nathalie (2014): Rho GTPases in embryonic development. In *Small GTPases* 5 (2), p. 8. DOI: 10.4161/sgtp.29716.

El-Sibai, Mirvat; Nalbant, Peri; Pang, Huan; Flinn, Rory J.; Sarmiento, Corina; Macaluso, Frank et al. (2007): Cdc42 is required for EGF-stimulated protrusion and motility in MTLn3 carcinoma cells. In *Journal of cell science* 120 (Pt 19), pp. 3465–3474. DOI: 10.1242/jcs.005942.

Engler, Adam J.; Carag-Krieger, Christine; Johnson, Colin P.; Raab, Matthew; Tang, Hsin-Yao; Speicher, David W. et al. (2008): Embryonic cardiomyocytes beat best on a matrix with heart-like elasticity: scar-like rigidity inhibits beating. In *Journal of cell science* 121 (Pt 22), pp. 3794–3802. DOI: 10.1242/jcs.029678.

Engler, Adam J.; Sen, Shamik; Sweeney, H. Lee; Discher, Dennis E. (2006): Matrix elasticity directs stem cell lineage specification. In *Cell* 126 (4), pp. 677–689. DOI: 10.1016/j.cell.2006.06.044.

Etienne-Manneville, Sandrine (2013): Microtubules in cell migration. In *Annual review of cell and developmental biology* 29, pp. 471–499. DOI: 10.1146/annurev-cellbio-101011-155711.

Evans, Nicholas D.; Oreffo, Richard O. C.; Healy, Eugene; Thurner, Philipp J.; Man, Yu Hin (2013): Epithelial mechanobiology, skin wound healing, and the stem cell niche. In *Journal of the mechanical behavior of biomedical materials* 28, pp. 397–409. DOI: 10.1016/j.jmbbm.2013.04.023.

Farhan, Hesso; Hsu, Victor W. (2016): Cdc42 and Cellular Polarity: Emerging Roles at the Golgi. In *Trends in cell biology* 26 (4), pp. 241–248. DOI: 10.1016/j.tcb.2015.11.003.

Fish, Kenneth N. (2009): Total internal reflection fluorescence (TIRF) microscopy. In *Current protocols in cytometry* Chapter 12, Unit12.18. DOI: 10.1002/0471142956.cy1218s50.

Frank, Diane E.; Carter, William G. (2004): Laminin 5 deposition regulates keratinocyte polarization and persistent migration. In *Journal of cell science* 117 (Pt 8), pp. 1351–1363. DOI: 10.1242/jcs.01003.

Frank, Scott R.; Hansen, Steen H. (2008): The PIX-GIT complex: a G protein signaling cassette in control of cell shape. In *Seminars in cell & developmental biology* 19 (3), pp. 234–244. DOI: 10.1016/j.semcdb.2008.01.002.

Friedl, Peter; Gilmour, Darren (2009): Collective cell migration in morphogenesis, regeneration and cancer. In *Nature reviews. Molecular cell biology* 10 (7), pp. 445–457. DOI: 10.1038/nrm2720.

Friedl, Peter; Mayor, Roberto (2017): Tuning Collective Cell Migration by Cell-Cell Junction Regulation. In *Cold Spring Harbor perspectives in biology* 9 (4). DOI: 10.1101/cshperspect.a029199.

Fritz, Rafael Dominik; Pertz, Olivier (2016): The dynamics of spatio-temporal Rho GTPase signaling: formation of signaling patterns. In *F1000Research* 5. DOI: 10.12688/f1000research.7370.1.

Fuchs, Elaine (2007): Scratching the surface of skin development. In *Nature* 445 (7130), pp. 834–842. DOI: 10.1038/nature05659.

Fujishiro, Shuh-Hei; Tanimura, Susumu; Mure, Shogo; Kashimoto, Yuji; Watanabe, Kazushi; Kohno, Michiaki (2008): ERK1/2 phosphorylate GEF-H1 to enhance its guanine nucleotide exchange activity toward RhoA. In *Biochemical and biophysical research communications* 368 (1), pp. 162–167. DOI: 10.1016/j.bbrc.2008.01.066.

Gagliardi, Paolo Armando; Puliafito, Alberto; Di Blasio, Laura; Chianale, Federica; Somale, Desiana; Seano, Giorgio et al. (2015): Real-time monitoring of cell protrusion dynamics by impedance responses. In *Scientific reports* 5, p. 10206. DOI: 10.1038/srep10206.

Gasteier, Judith E.; Madrid, Ricardo; Krautkrämer, Ellen; Schröder, Sebastian; Muranyi, Walter; Benichou, Serge; Fackler, Oliver T. (2003): Activation of the Rac-binding partner FHOD1 induces actin stress fibers via a ROCK-dependent mechanism. In *The Journal of biological chemistry* 278 (40), pp. 38902–38912. DOI: 10.1074/jbc.M306229200.

Geiger, Benjamin; Bershadsky, Alexander (2002): Exploring the Neighborhood. In *Cell* 110 (2), pp. 139–142. DOI: 10.1016/S0092-8674(02)00831-0.

Gerhardt, Matthias; Ecke, Mary; Walz, Michael; Stengl, Andreas; Beta, Carsten; Gerisch, Günther (2014): Actin and PIP3 waves in giant cells reveal the inherent length scale of an excited state. In *Journal of cell science* 127 (Pt 20), pp. 4507–4517. DOI: 10.1242/jcs.156000.

Giannone, Grégory; Dubin-Thaler, Benjamin J.; Rossier, Olivier; Cai, Yunfei; Chaga, Oleg; Jiang, Guoying et al. (2007): Lamellipodial actin mechanically links myosin activity with adhesion-site formation. In *Cell* 128 (3), pp. 561–575. DOI: 10.1016/j.cell.2006.12.039.

Glading, A.; Chang, P.; Lauffenburger, D. A.; Wells, A. (2000): Epidermal growth factor receptor activation of calpain is required for fibroblast motility and occurs via an ERK/MAP kinase signaling pathway. In *The Journal of biological chemistry* 275 (4), pp. 2390–2398. DOI: 10.1074/jbc.275.4.2390.

Goeckeler, Z. M.; Masaracchia, R. A.; Zeng, Q.; Chew, T. L.; Gallagher, P.; Wysolmerski, R. B. (2000): Phosphorylation of myosin light chain kinase by p21-activated kinase PAK2. In *The Journal of biological chemistry* 275 (24), pp. 18366–18374. DOI: 10.1074/jbc.M001339200.

Goicoechea, Silvia M.; Awadia, Sahezeel; Garcia-Mata, Rafael (2014): I'm coming to GEF you: Regulation of RhoGEFs during cell migration. In *Cell adhesion & migration* 8 (6), pp. 535–549. DOI: 10.4161/cam.28721.

Gorouhi, Farzam; Shah, Nihar M.; Krishna Raghunathan, Vijay; Mohabbati, Yasaman; Abbott, Nicholas L.; Isseroff, Roslyn R.; Murphy, Christopher J. (2014): Epidermal growth factor-functionalized polymeric multilayer films: interplay between spatial location and bioavailability of EGF. In *The Journal of investigative dermatology* 134 (6), pp. 1757–1760. DOI: 10.1038/jid.2014.7.

Grabocka, Elda; Wedegaertner, Philip B. (2007): Disruption of oligomerization induces nucleocytoplasmic shuttling of leukemia-associated rho Guanine-nucleotide exchange factor. In *Molecular pharmacology* 72 (4), pp. 993–1002. DOI: 10.1124/mol.107.035162.

Graessl, Melanie; Koch, Johannes; Calderon, Abram; Kamps, Dominic; Banerjee, Soumya; Mazel, Tomáš et al. (2017): An excitable Rho GTPase signaling network generates dynamic subcellular contraction patterns. In *The Journal of cell biology* 216 (12), pp. 4271–4285. DOI: 10.1083/jcb.201706052.

Grimsley, Cynthia M.; Kinchen, Jason M.; Tosello-Trampont, Annie-Carole; Brugnera, Enrico; Haney, Lisa B.; Lu, Mingjian et al. (2004): Dock180 and ELMO1 proteins cooperate to promote evolutionarily conserved Rac-dependent cell migration. In *The Journal of biological chemistry* 279 (7), pp. 6087–6097. DOI: 10.1074/jbc.M307087200.

Guilluy, Christophe; Garcia-Mata, Rafael; Burridge, Keith (2011a): Rho protein crosstalk: another social network? In *Trends in cell biology* 21 (12), pp. 718–726. DOI: 10.1016/j.tcb.2011.08.002.

Guilluy, Christophe; Swaminathan, Vinay; Garcia-Mata, Rafael; O'Brien, E. Timothy; Superfine, Richard; Burridge, Keith (2011b): The Rho GEFs LARG and GEF-H1 regulate the mechanical response to force on integrins. In *Nature cell biology* 13 (6), pp. 722–727. DOI: 10.1038/ncb2254.

Gupton, Stephanie L.; Anderson, Karen L.; Kole, Thomas P.; Fischer, Robert S.; Ponti, Aaron; Hitchcock-DeGregori, Sarah E. et al. (2005): Cell migration without a lamellipodium: translation of actin dynamics into cell movement mediated by tropomyosin. In *The Journal of cell biology* 168 (4), pp. 619–631. DOI: 10.1083/jcb.200406063.

Haase, Ingo; Evans, Richard; Pofahl, Ruth; Watt, Fiona M. (2003): Regulation of keratinocyte shape, migration and wound epithelialization by IGF-1- and EGF-dependent signalling pathways. In *Journal of cell science* 116 (Pt 15), pp. 3227–3238. DOI: 10.1242/jcs.00610.

Haataja, L.; Groffen, J.; Heisterkamp, N. (1997): Characterization of RAC3, a novel member of the Rho family. In *The Journal of biological chemistry* 272 (33), pp. 20384–20388. DOI: 10.1074/jbc.272.33.20384.

Hall, Alan (1998): Rho GTPases and the Actin Cytoskeleton. In *Science* 279 (5350), pp. 509–514. DOI: 10.1126/science.279.5350.509.

Hanna, Samer; Miskolci, Veronika; Cox, Dianne; Hodgson, Louis (2014): A New Genetically Encoded Single-Chain Biosensor for Cdc42 Based on FRET, Useful for Live-Cell Imaging. In *PloS one* 9 (5), e96469. DOI: 10.1371/journal.pone.0096469.

Hébert, Marylise; Potin, Sophie; Sebbagh, Michaël; Bertoglio, Jacques; Bréard, Jacqueline; Hamelin, Jocelyne (2008): Rho-ROCK-dependent ezrin-radixin-moesin phosphorylation regulates Fas-mediated apoptosis in Jurkat cells. In *Journal of immunology (Baltimore, Md. : 1950)* 181 (9), pp. 5963–5973. DOI: 10.4049/jimmunol.181.9.5963.

Hernández-Negrete, Ivette; Carretero-Ortega, Jorge; Rosenfeldt, Hans; Hernández-García, Ricardo; Calderón-Salinas, J. Victor; Reyes-Cruz, Guadalupe et al. (2007): P-Rex1 links mammalian target of rapamycin signaling to Rac activation and cell migration. In *The Journal of biological chemistry* 282 (32), pp. 23708–23715. DOI: 10.1074/jbc.M703771200.

Hiroyasu, Sho; Stimac, Gregory P.; Hopkinson, Susan B.; Jones, Jonathan C. R. (2017): Loss of β-PIX inhibits focal adhesion disassembly and promotes keratinocyte motility via myosin light chain activation. In *Journal of cell science* 130 (14), pp. 2329–2343. DOI: 10.1242/jcs.196147.

Ho, Ernest; Dagnino, Lina (2012): Epidermal growth factor induction of front-rear polarity and migration in keratinocytes is mediated by integrin-linked kinase and ELMO2. In *Molecular biology of the cell* 23 (3), pp. 492–502. DOI: 10.1091/mbc.E11-07-0596.

Hodge, Richard G.; Ridley, Anne J. (2016): Regulating Rho GTPases and their regulators. In *Nature reviews. Molecular cell biology* 17 (8), pp. 496–510. DOI: 10.1038/nrm.2016.67.

Hofmann, Clemens; Shepelev, Mikhail; Chernoff, Jonathan (2004): The genetics of Pak. In *Journal of cell science* 117 (Pt 19), pp. 4343–4354. DOI: 10.1242/jcs.01392.

Hsu, Rae-Mann; Hsieh, Ya-Ju; Yang, Tsung-Han; Chiang, Yi-Chien; Kan, Chih-Yen; Lin, Yu-Tsuen et al. (2014): Binding of the extreme carboxyl-terminus of PAK-interacting exchange factor β (βPIX) to myosin 18A (MYO18A) is required for epithelial cell migration. In *Biochimica et biophysica acta* 1843 (11), pp. 2513–2527. DOI: 10.1016/j.bbamcr.2014.06.023.

Huveneers, Stephan; Danen, Erik H. J. (2009): Adhesion signaling - crosstalk between integrins, Src and Rho. In *Journal of cell science* 122 (Pt 8), pp. 1059–1069. DOI: 10.1242/jcs.039446.

Iglesias, Pablo A.; Devreotes, Peter N. (2012): Biased excitable networks: how cells direct motion in response to gradients. In *Current opinion in cell biology* 24 (2), pp. 245–253. DOI: 10.1016/j.ceb.2011.11.009.

Itakura, Asako; Aslan, Joseph E.; Kusanto, Branden T.; Phillips, Kevin G.; Porter, Juliana E.; Newton, Paul K. et al. (2013): p21-Activated kinase (PAK) regulates cytoskeletal reorganization and directional migration in human neutrophils. In *PloS one* 8 (9), e73063. DOI: 10.1371/journal.pone.0073063.

Ivetic, Aleksandar; Ridley, Anne J. (2004): Ezrin/radixin/moesin proteins and Rho GTPase signalling in leucocytes. In *Immunology* 112 (2), pp. 165–176. DOI: 10.1111/j.1365-2567.2004.01882.x.

Jackson, Ben; Peyrollier, Karine; Pedersen, Esben; Basse, Astrid; Karlsson, Richard; Wang, Zhipeng et al. (2011): RhoA is dispensable for skin development, but crucial for contraction and directed migration of keratinocytes. In *Molecular biology of the cell* 22 (5), pp. 593–605. DOI: 10.1091/mbc.E09-10-0859.

Keren, Kinneret; Pincus, Zachary; Allen, Greg M.; Barnhart, Erin L.; Marriott, Gerard; Mogilner, Alex; Theriot, Julie A. (2008): Mechanism of shape determination in motile cells. In *Nature* 453 (7194), pp. 475–480. DOI: 10.1038/nature06952.

Khamviwath, Varunyu; Hu, Jifeng; Othmer, Hans G. (2013): A continuum model of actin waves in Dictyostelium discoideum. In *PloS one* 8 (5), e64272. DOI: 10.1371/journal.pone.0064272.

Kichina, Julia V.; Goc, Anna; Al-Husein, Belal; Somanath, Payaningal R.; Kandel, Eugene S. (2010): PAK1 as a therapeutic target. In *Expert opinion on therapeutic targets* 14 (7), pp. 703–725. DOI: 10.1517/14728222.2010.492779.

Kirfel, G.; Herzog, V. (2004): Migration of epidermal keratinocytes: mechanisms, regulation, and biological significance. In *Protoplasma* 223 (2-4), pp. 67–78. DOI: 10.1007/s00709-003-0031-5.

Kirfel, Gregor; Rigort, Alexander; Borm, Bodo; Herzog, Volker (2004): Cell migration: mechanisms of rear detachment and the formation of migration tracks. In *European journal of cell biology* 83 (11-12), pp. 717–724. DOI: 10.1078/0171-9335-00421.

Kiyokawa, E.; Hashimoto, Y.; Kurata, T.; Sugimura, H.; Matsuda, M. (1998): Evidence that DOCK180 up-regulates signals from the CrkII-p130(Cas) complex. In *The Journal of biological chemistry* 273 (38), pp. 24479–24484. DOI: 10.1074/jbc.273.38.24479.

Koh, C. G.; Manser, E.; Zhao, Z. S.; Ng, C. P.; Lim, L. (2001): Beta1PIX, the PAK-interacting exchange factor, requires localization via a coiled-coil region to promote microvillus-like structures and membrane ruffles. In *Journal of cell science* 114 (Pt 23), pp. 4239–4251.

Koubek, Emily J.; Santy, Lorraine C. (2018): ARF1 and ARF6 regulate recycling of GRASP/Tamalin and the Rac1-GEF Dock180 during HGF-induced Rac1 activation. In *Small GTPases* 9 (3), pp. 242–259. DOI: 10.1080/21541248.2016.1219186.

Kovacs, Eva M.; Makar, Robert S.; Gertler, Frank B. (2006): Tuba stimulates intracellular N-WASP-dependent actin assembly. In *Journal of cell science* 119 (Pt 13), pp. 2715–2726. DOI: 10.1242/jcs.03005.

Kraynov, V. S.; Chamberlain, C.; Bokoch, G. M.; Schwartz, M. A.; Slabaugh, S.; Hahn, K. M. (2000): Localized Rac activation dynamics visualized in living cells. In *Science (New York, N.Y.)* 290 (5490), pp. 333–337. DOI: 10.1126/science.290.5490.333.

Krendel, Mira; Zenke, Frank T.; Bokoch, Gary M. (2002): Nucleotide exchange factor GEF-H1 mediates cross-talk between microtubules and the actin cytoskeleton. In *Nat Cell Biol* 4 (4), pp. 294–301. DOI: 10.1038/ncb773.

Kumar, Sachin; Xu, Juying; Perkins, Charles; Guo, Fukun; Snapper, Scott; Finkelman, Fred D. et al. (2012): Cdc42 regulates neutrophil migration via crosstalk between WASp, CD11b, and microtubules. In *Blood* 120 (17), pp. 3563–3574. DOI: 10.1182/blood-2012-04-426981.

Kurokawa, Kazuo; Itoh, Reina E.; Yoshizaki, Hisayoshi; Nakamura, Yusuke Ohba Takeshi; Matsuda, Michiyuki (2004): Coactivation of Rac1 and Cdc42 at lamellipodia and membrane ruffles induced by epidermal growth factor. In *Molecular biology of the cell* 15 (3), pp. 1003–1010. DOI: 10.1091/mbc.e03-08-0609.

Laemmli, U. K. (1970): Cleavage of structural proteins during the assembly of the head of bacteriophage T4. In *Nature* 227 (5259), pp. 680–685. DOI: 10.1038/227680a0.

Lämmermann, Tim; Renkawitz, Jörg; Wu, Xunwei; Hirsch, Karin; Brakebusch, Cord; Sixt, Michael (2009): Cdc42-dependent leading edge coordination is essential for interstitial dendritic cell migration. In *Blood* 113 (23), pp. 5703–5710. DOI: 10.1182/blood-2008-11-191882.

Lawson, Campbell D.; Ridley, Anne J. (2018): Rho GTPase signaling complexes in cell migration and invasion. In *The Journal of cell biology* 217 (2), pp. 447–457. DOI: 10.1083/jcb.201612069.

Lecuit, Thomas; Lenne, Pierre-François (2007): Cell surface mechanics and the control of cell shape, tissue patterns and morphogenesis. In *Nature reviews. Molecular cell biology* 8 (8), pp. 633–644. DOI: 10.1038/nrm2222.

Lemmon, M. A.; Ferguson, K. M. (2000): Signal-dependent membrane targeting by pleckstrin homology (PH) domains. In *Biochemical Journal* 350 (Pt 1), pp. 1–18.

Li, Zhong; Hannigan, Michael; Mo, Zhicheng; Liu, Bo; Lu, Wei; Wu, Yue et al. (2003): Directional Sensing Requires Gβγ-Mediated PAK1 and PIXα-Dependent Activation of Cdc42. In *Cell* 114 (2), pp. 215–227. DOI: 10.1016/S0092-8674(03)00559-2.

Linder, Stefan; Kopp, Petra (2005): Podosomes at a glance. In *Journal of cell science* 118 (Pt 10), pp. 2079–2082. DOI: 10.1242/jcs.02390.

Lindsay, Colin R.; Lawn, Samuel; Campbell, Andrew D.; Faller, William J.; Rambow, Florian; Mort, Richard L. et al. (2011): P-Rex1 is required for efficient melanoblast migration and melanoma metastasis. In *Nature communications* 2, p. 555. DOI: 10.1038/ncomms1560.

Machacek, Matthias; Hodgson, Louis; Welch, Christopher; Elliott, Hunter; Pertz, Olivier; Nalbant, Perihan et al. (2009): Coordination of Rho GTPase activities during cell protrusion. In *Nature* 461 (7260), pp. 99–103. DOI: 10.1038/nature08242.

Maddox, Amy Shaub; Burridge, Keith (2003): RhoA is required for cortical retraction and rigidity during mitotic cell rounding. In *The Journal of cell biology* 160 (2), pp. 255–265. DOI: 10.1083/jcb.200207130.

Mainiero, F.; Pepe, A.; Yeon, M.; Ren, Y.; Giancotti, F. G. (1996): The intracellular functions of alpha6beta4 integrin are regulated by EGF. In *The Journal of cell biology* 134 (1), pp. 241–253. DOI: 10.1083/jcb.134.1.241.

Malosio, M. L.; Gilardelli, D.; Paris, S.; Albertinazzi, C.; Curtis, I. de (1997): Differential expression of distinct members of Rho family GTP-binding proteins during neuronal development: identification of Rac1B, a new neural-specific member of the family. In *The Journal of neuroscience : the official journal of the Society for Neuroscience* 17 (17), pp. 6717–6728.

Manser, E.; Huang, H. Y.; Loo, T. H.; Chen, X. Q.; Dong, J. M.; Leung, T.; Lim, L. (1997): Expression of constitutively active alpha-PAK reveals effects of the kinase on actin and focal complexes. In *Molecular and cellular biology* 17 (3), pp. 1129–1143. DOI: 10.1128/mcb.17.3.1129.

Manser, E.; Leung, T.; Salihuddin, H.; Zhao, Z. S.; Lim, L. (1994): A brain serine/threonine protein kinase activated by Cdc42 and Rac1. In *Nature* 367 (6458), pp. 40–46. DOI: 10.1038/367040a0.

Marei, Hadir; Carpy, Alejandro; Woroniuk, Anna; Vennin, Claire; White, Gavin; Timpson, Paul et al. (2016): Differential Rac1 signalling by guanine nucleotide exchange factors implicates FLII in regulating Rac1-driven cell migration. In *Nature communications* 7, p. 10664. DOI: 10.1038/ncomms10664.

Martin, Katrin; Reimann, Andreas; Fritz, Rafael D.; Ryu, Hyunryul; Jeon, Noo Li; Pertz, Olivier (2016): Spatio-temporal co-ordination of RhoA, Rac1 and Cdc42 activation during prototypical edge protrusion and retraction dynamics. In *Scientific reports* 6, p. 21901. DOI: 10.1038/srep21901.

Martin, P.; Nunan, R. (2015): Cellular and molecular mechanisms of repair in acute and chronic wound healing. In *The British journal of dermatology* 173 (2), pp. 370–378. DOI: 10.1111/bjd.13954.

Medina, Frank; Carter, Angela M.; Dada, Olugbenga; Gutowski, Stephen; Hadas, Jana; Chen, Zhe; Sternweis, Paul C. (2013): Activated RhoA is a positive feedback regulator of the Lbc family of Rho guanine nucleotide exchange factor proteins. In *The Journal of biological chemistry* 288 (16), pp. 11325–11333. DOI: 10.1074/jbc.M113.450056.

Meller, Nahum; Merlot, Sylvain; Guda, Chittibabu (2005): CZH proteins: a new family of Rho-GEFs. In *Journal of cell science* 118 (Pt 21), pp. 4937–4946. DOI: 10.1242/jcs.02671.

Mertens, Alexander E. E.; Rygiel, Tomasz P.; Olivo, Cristina; van der Kammen, Rob; Collard, John G. (2005): The Rac activator Tiam1 controls tight junction biogenesis in keratinocytes through binding to and activation of the Par polarity complex. In *The Journal of cell biology* 170 (7), pp. 1029–1037. DOI: 10.1083/jcb.200502129.

Mikelis, Constantinos M.; Palmby, Todd R.; Simaan, May; Li, Wenling; Szabo, Roman; Lyons, Ruth et al. (2013): PDZ-RhoGEF and LARG are essential for embryonic development and provide a link between thrombin and LPA receptors and Rho activation. In *The Journal of biological chemistry* 288 (17), pp. 12232–12243. DOI: 10.1074/jbc.M112.428599.

Miller, N. L. G.; Kleinschmidt, E. G.; Schlaepfer, D. D. (2014): RhoGEFs in cell motility: novel links between Rgnef and focal adhesion kinase. In *Current molecular medicine* 14 (2), pp. 221–234.

Molli, P. R.; Li, D. Q.; Murray, B. W.; Rayala, S. K.; Kumar, R. (2009): PAK signaling in oncogenesis. In *Oncogene* 28 (28), pp. 2545–2555. DOI: 10.1038/onc.2009.119.

Montoya, María C.; Sancho, David; Vicente-Manzanares, Miguel; Sánchez-Madrid, Francisco (2002): Cell adhesion and polarity during immune interactions. In *Immunological reviews* 186, pp. 68–82.

Moreau, Violaine; Tatin, Florence; Varon, Christine; Génot, Elisabeth (2003): Actin can reorganize into podosomes in aortic endothelial cells, a process controlled by Cdc42 and RhoA. In *Molecular and cellular biology* 23 (19), pp. 6809–6822. DOI: 10.1128/mcb.23.19.6809-6822.2003.

Müller, Paul M.; Rademacher, Juliane; Bagshaw, Richard D.; Alp, Keziban M.; Giudice, Girolamo; Heinrich, Louise E. et al. (2018): Spatial Organization of Rho GTPase signaling by RhoGEF/RhoGAP proteins (13).

Müller, R. T.; Honnert, U.; Reinhard, J.; Bähler, M. (1997): The rat myosin myr 5 is a GTPase-activating protein for Rho in vivo: essential role of arginine 1695. In *Molecular biology of the cell* 8 (10), pp. 2039–2053. DOI: 10.1091/mbc.8.10.2039.

Nalbant, Perihan; Chang, Yuan-Chen; Birkenfeld, Jörg; Chang, Zee-Fen; Bokoch, Gary M. (2009): Guanine nucleotide exchange factor-H1 regulates cell migration via localized activation of RhoA at the leading edge. In *Molecular biology of the cell* 20 (18), pp. 4070–4082. DOI: 10.1091/mbc.E09-01-0041.

Nalbant, Perihan; Dehmelt, Leif (2018): Exploratory cell dynamics: a sense of touch for cells? In *Biological chemistry* 399 (8), pp. 809–819. DOI: 10.1515/hsz-2017-0341.

Nalbant, Perihan; Hodgson, Louis; Kraynov, Vadim; Toutchkine, Alexei; Hahn, Klaus M. (2004): Activation of endogenous Cdc42 visualized in living cells. In *Science (New York, N.Y.)* 305 (5690), pp. 1615–1619. DOI: 10.1126/science.1100367.

Nanba, Daisuke; Toki, Fujio; Matsushita, Natsuki; Matsushita, Sachi; Higashiyama, Shigeki; Barrandon, Yann (2013): Actin filament dynamics impacts keratinocyte stem cell maintenance. In *EMBO molecular medicine* 5 (4), pp. 640–653. DOI: 10.1002/emmm.201201839.

Nardone, Giorgia; La Oliver-De Cruz, Jorge; Vrbsky, Jan; Martini, Cecilia; Pribyl, Jan; Skládal, Petr et al. (2017): YAP regulates cell mechanics by controlling focal adhesion assembly. In *Nature communications* 8, p. 15321. DOI: 10.1038/ncomms15321.

Nobes, Catherine D.; Hall, Alan (1995): Rho, Rac, and Cdc42 GTPases regulate the assembly of multimolecular focal complexes associated with actin stress fibers, lamellipodia, and filopodia. In *Cell* 81 (1), pp. 53–62. DOI: 10.1016/0092-8674(95)90370-4.

Novák, Béla; Tyson, John J. (2008): Design principles of biochemical oscillators. In *Nature reviews. Molecular cell biology* 9 (12), pp. 981–991. DOI: 10.1038/nrm2530.

Omary, M. Bishr; Coulombe, Pierre A.; McLean, W. H. Irwin (2004): Intermediate filament proteins and their associated diseases. In *The New England journal of medicine* 351 (20), pp. 2087–2100. DOI: 10.1056/NEJMra040319.

Osmani, Naël; Peglion, Florent; Chavrier, Philippe; Etienne-Manneville, Sandrine (2010): Cdc42 localization and cell polarity depend on membrane traffic. In *The Journal of cell biology* 191 (7), pp. 1261–1269. DOI: 10.1083/jcb.201003091.

Osmani, Naël; Vitale, Nicolas; Borg, Jean-Paul; Etienne-Manneville, Sandrine (2006): Scrib controls Cdc42 localization and activity to promote cell polarization during astrocyte migration. In *Current biology : CB* 16 (24), pp. 2395–2405. DOI: 10.1016/j.cub.2006.10.026.

Parsons, J. Thomas; Horwitz, Alan Rick; Schwartz, Martin A. (2010): Cell adhesion: integrating cytoskeletal dynamics and cellular tension. In *Nature reviews. Molecular cell biology* 11 (9), pp. 633–643. DOI: 10.1038/nrm2957.

Pastore, Saveria; Lulli, Daniela; Girolomoni, Giampiero (2014): Epidermal growth factor receptor signalling in keratinocyte biology: implications for skin toxicity of tyrosine kinase inhibitors. In *Archives of toxicology* 88 (6), pp. 1189–1203. DOI: 10.1007/s00204-014-1244-4.

Perrot, Valerie; Vazquez-Prado, Jose; Gutkind, J. Silvio (2002): Plexin B regulates Rho through the guanine nucleotide exchange factors leukemia-associated Rho GEF (LARG) and PDZ-RhoGEF. In *The Journal of biological chemistry* 277 (45), pp. 43115–43120. DOI: 10.1074/jbc.M206005200.

Pertz, Olivier (2010): Spatio-temporal Rho GTPase signaling - where are we now? In *Journal of cell science* 123 (Pt 11), pp. 1841–1850. DOI: 10.1242/jcs.064345.

Petrie, Ryan J.; Gavara, Núria; Chadwick, Richard S.; Yamada, Kenneth M. (2012): Nonpolarized signaling reveals two distinct modes of 3D cell migration. In *The Journal of cell biology* 197 (3), pp. 439–455. DOI: 10.1083/jcb.201201124.

Petrie, Ryan J.; Yamada, Kenneth M. (2012): At the leading edge of three-dimensional cell migration. In *Journal of cell science* 125 (Pt 24), pp. 5917–5926. DOI: 10.1242/jcs.093732.

Pinto, Carmine; Barone, Carlo Antonio; Girolomoni, Giampiero; Russi, Elvio Grazioso; Merlano, Marco Carlo; Ferrari, Daris; Maiello, Evaristo (2011): Management of Skin Toxicity Associated with Cetuximab Treatment in Combination with Chemotherapy or Radiotherapy. In *The Oncologist* 16 (2), pp. 228–238. DOI: 10.1634/theoncologist.2010-0298.

Plutoni, Cédric; Bazellieres, Elsa; Le Borgne-Rochet, Maïlys; Comunale, Franck; Brugues, Agusti; Séveno, Martial et al. (2016): P-cadherin promotes collective cell migration via a Cdc42-mediated increase in mechanical forces. In *The Journal of cell biology* 212 (2), pp. 199–217. DOI: 10.1083/jcb.201505105.

Pollard, Thomas D.; Borisy, Gary G. (2003): Cellular Motility Driven by Assembly and Disassembly of Actin Filaments. In *Cell* 112 (4), pp. 453–465. DOI: 10.1016/S0092-8674(03)00120-X.

Pothula, Swetha; Bazan, Haydee E. P.; Chandrasekher, Gudiseva (2013): Regulation of Cdc42 expression and signaling is critical for promoting corneal epithelial wound healing. In *Investigative ophthalmology & visual science* 54 (8), pp. 5343–5352. DOI: 10.1167/iovs.13-11955.

Provenzano, P. P.; Inman, D. R.; Eliceiri, K. W.; Keely, P. J. (2009): Matrix density-induced mechanoregulation of breast cell phenotype, signaling and gene expression through a FAK-ERK linkage. In *Oncogene* 28 (49), pp. 4326–4343. DOI: 10.1038/onc.2009.299.

Qin, J.; Xie, Y.; Wang, B.; Hoshino, M.; Wolff, D. W.; Zhao, J. et al. (2009): Upregulation of PIP3-dependent Rac exchanger 1 (P-Rex1) promotes prostate cancer metastasis. In *Oncogene* 28 (16), pp. 1853–1863. DOI: 10.1038/onc.2009.30.

Razidlo, Gina L.; Schroeder, Barbara; Chen, Jing; Billadeau, Daniel D.; McNiven, Mark A. (2014): Vav1 as a central regulator of invadopodia assembly. In *Current biology : CB* 24 (1), pp. 86–93. DOI: 10.1016/j.cub.2013.11.013.

Reymann, Anne-Cécile; Boujemaa-Paterski, Rajaa; Martiel, Jean-Louis; Guérin, Christophe; Cao, Wenxiang; Chin, Harvey F. et al. (2012): Actin network architecture can determine myosin motor activity. In *Science (New York, N.Y.)* 336 (6086), pp. 1310–1314. DOI: 10.1126/science.1221708.

Reymond, Nicolas; Im, Jae Hong; Garg, Ritu; Vega, Francisco M.; Borda d'Agua, Barbara; Riou, Philippe et al. (2012): Cdc42 promotes transendothelial migration of cancer cells through β1 integrin. In *The Journal of cell biology* 199 (4), pp. 653–668. DOI: 10.1083/jcb.201205169.

Ridley, A. J. (2001): Rho GTPases and cell migration. In *Journal of cell science* 114 (Pt 15), pp. 2713–2722.

Rossman, Kent L.; Der, Channing J.; Sondek, John (2005): GEF means go: turning on RHO GTPases with guanine nucleotide-exchange factors. In *Nature reviews. Molecular cell biology* 6 (2), pp. 167–180. DOI: 10.1038/nrm1587.

Rouven Brückner, Bastian; Pietuch, Anna; Nehls, Stefan; Rother, Jan; Janshoff, Andreas (2015): Ezrin is a Major Regulator of Membrane Tension in Epithelial Cells. In *Scientific reports* 5, p. 14700. DOI: 10.1038/srep14700.

Ryan, Gillian L.; Petroccia, Heather M.; Watanabe, Naoki; Vavylonis, Dimitrios (2012): Excitable actin dynamics in lamellipodial protrusion and retraction. In *Biophysical journal* 102 (7), pp. 1493–1502. DOI: 10.1016/j.bpj.2012.03.005.

Safferling, Kai; Sütterlin, Thomas; Westphal, Kathi; Ernst, Claudia; Breuhahn, Kai; James, Merlin et al. (2013): Wound healing revised: A novel reepithelialization mechanism revealed by in vitro and in silico models. In *The Journal of cell biology* 203 (4), pp. 691–709. DOI: 10.1083/jcb.201212020.

Sailem, Heba; Bousgouni, Vicky; Cooper, Sam; Bakal, Chris (2014): Cross-talk between Rho and Rac GTPases drives deterministic exploration of cellular shape space and morphological heterogeneity. In *Open Biol.* 4 (1), p. 130132. DOI: 10.1098/rsob.130132.

Santoro, Massimo M.; Gaudino, Giovanni (2005): Cellular and molecular facets of keratinocyte reepithelization during wound healing. In *Experimental cell research* 304 (1), pp. 274–286. DOI: 10.1016/j.yexcr.2004.10.033.

Scarpa, Elena; Mayor, Roberto (2016): Collective cell migration in development. In *The Journal of cell biology* 212 (2), pp. 143–155. DOI: 10.1083/jcb.201508047.

Schäfer, Matthias; Werner, Sabine (2008): Cancer as an overhealing wound: an old hypothesis revisited. In *Nature reviews. Molecular cell biology* 9 (8), pp. 628–638. DOI: 10.1038/nrm2455.

Schneider, Marlon R.; Werner, Sabine; Paus, Ralf; Wolf, Eckhard (2008): Beyond wavy hairs: the epidermal growth factor receptor and its ligands in skin biology and pathology. In *The American journal of pathology* 173 (1), pp. 14–24. DOI: 10.2353/ajpath.2008.070942.

Schulze, Nina; Graessl, Melanie; Blancke Soares, Alexandra; Geyer, Matthias; Dehmelt, Leif; Nalbant, Perihan (2014): FHOD1 regulates stress fiber organization by controlling the dynamics of transverse arcs and dorsal fibers. In *Journal of cell science* 127 (Pt 7), pp. 1379–1393. DOI: 10.1242/jcs.134627.

Scott, David W.; Tolbert, Caitlin E.; Burridge, Keith (2016): Tension on JAM-A activates RhoA via GEF-H1 and p115 RhoGEF. In *Molecular biology of the cell* 27 (9), pp. 1420–1430. DOI: 10.1091/mbc.E15-12-0833.

Seeger, Mark A.; Paller, Amy S. (2015): The Roles of Growth Factors in Keratinocyte Migration. In *Advances in wound care* 4 (4), pp. 213–224. DOI: 10.1089/wound.2014.0540.

Seth, Divya; Cheldize, Khatiya; Brown, Danielle; Freeman, Esther F. (2017): Global Burden of Skin Disease: Inequities and Innovations. In *Current dermatology reports* 6 (3), pp. 204–210. DOI: 10.1007/s13671-017-0192-7.

Shostak, Kateryna; Zhang, Xin; Hubert, Pascale; Göktuna, Serkan Ismail; Jiang, Zheshen; Klevernic, Iva et al. (2014): NF-κB-induced KIAA1199 promotes survival through EGFR signalling. In *Nature communications* 5, p. 5232. DOI: 10.1038/ncomms6232.

Smith, F. Donelson; Langeberg, Lorene K.; Cellurale, Cristina; Pawson, Tony; Morrison, Deborah K.; Davis, Roger J.; Scott, John D. (2010): AKAP-Lbc enhances cyclic AMP control of the ERK1/2 cascade. In *Nature cell biology* 12 (12), pp. 1242–1249. DOI: 10.1038/ncb2130.

Sugihara, K.; Nakatsuji, N.; Nakamura, K.; Nakao, K.; Hashimoto, R.; Otani, H. et al. (1998): Rac1 is required for the formation of three germ layers during gastrulation. In *Oncogene* 17 (26), pp. 3427–3433. DOI: 10.1038/sj.onc.1202595.

Svitkina, Tatyana (2018): The Actin Cytoskeleton and Actin-Based Motility. In *Cold Spring Harbor perspectives in biology* 10 (1). DOI: 10.1101/cshperspect.a018267.

Symons, Marc; Derry, Jonathan M.J; Karlak, Brian; Jiang, Sharon; Lemahieu, Vanessa; McCormick, Frank et al. (1996): Wiskott–Aldrich Syndrome Protein, a Novel Effector for the GTPase CDC42Hs, Is Implicated in Actin Polymerization. In *Cell* 84 (5), pp. 723–734. DOI: 10.1016/S0092-8674(00)81050-8.

Tan, Ivan; Yong, Jeffery; Dong, Jing Ming; Lim, Louis; Leung, Thomas (2008): A Tripartite Complex Containing MRCK Modulates Lamellar Actomyosin Retrograde Flow. In *Cell* 135 (1), pp. 123–136. DOI: 10.1016/j.cell.2008.09.018.

Thun, Anne von; Preisinger, Christian; Rath, Oliver; Schwarz, Juliane P.; Ward, Chris; Monsefi, Naser et al. (2013): Extracellular signal-regulated kinase regulates RhoA activation and tumor cell plasticity by inhibiting guanine exchange factor H1 activity. In *Molecular and cellular biology* 33 (22), pp. 4526–4537. DOI: 10.1128/MCB.00585-13.

Tsankova, Anna; Pham, Tri Thanh; Garcia, David Salvador; Otte, Fabian; Cabernard, Clemens (2017): Cell Polarity Regulates Biased Myosin Activity and Dynamics during Asymmetric Cell Division via Drosophila Rho Kinase and Protein Kinase N. In *Developmental cell* 42 (2), 143-155.e5. DOI: 10.1016/j.devcel.2017.06.012.

Tsukita, S.; Yonemura, S. (1999): Cortical actin organization: lessons from ERM (ezrin/radixin/moesin) proteins. In *The Journal of biological chemistry* 274 (49), pp. 34507–34510. DOI: 10.1074/jbc.274.49.34507.

Tyson, John J.; Chen, Katherine C.; Novak, Bela (2003): Sniffers, buzzers, toggles and blinkers: dynamics of regulatory and signaling pathways in the cell. In *Current opinion in cell biology* 15 (2), pp. 221–231. DOI: 10.1016/S0955-0674(03)00017-6.

Unbekandt, Mathieu; Olson, Michael F. (2014): The actin-myosin regulatory MRCK kinases: regulation, biological functions and associations with human cancer. In *Journal of molecular medicine (Berlin, Germany)* 92 (3), pp. 217–225. DOI: 10.1007/s00109-014-1133-6.

Valdes, Julie L.; Tang, Jingrong; McDermott, Mark I.; Kuo, Jean-Cheng; Zimmerman, Seth P.; Wincovitch, Stephen M. et al. (2011): Sorting nexin 27 protein regulates trafficking of a p21-activated kinase (PAK) interacting exchange factor (β-Pix)-G protein-coupled receptor kinase interacting protein (GIT) complex via a PDZ domain interaction. In *The Journal of biological chemistry* 286 (45), pp. 39403–39416. DOI: 10.1074/jbc.M111.260802.

Vicente-Manzanares, Miguel; Newell-Litwa, Karen; Bachir, Alexia I.; Whitmore, Leanna A.; Horwitz, Alan Rick (2011): Myosin IIA/IIB restrict adhesive and protrusive signaling to generate front-back

polarity in migrating cells. In *The Journal of cell biology* 193 (2), pp. 381–396. DOI: 10.1083/jcb.201012159.

Vicente-Manzanares, Miguel; Webb, Donna J.; Horwitz, A. Rick (2005): Cell migration at a glance. In *Journal of cell science* 118 (Pt 21), pp. 4917–4919. DOI: 10.1242/jcs.02662.

Viswanatha, Raghuvir; Wayt, Jessica; Ohouo, Patrice Y.; Smolka, Marcus B.; Bretscher, Anthony (2013): Interactome analysis reveals ezrin can adopt multiple conformational states. In *The Journal of biological chemistry* 288 (49), pp. 35437–35451. DOI: 10.1074/jbc.M113.505669.

Vogelstein, Bert; Papadopoulos, Nickolas; Velculescu, Victor E.; Zhou, Shibin; Diaz, Luis A.; Kinzler, Kenneth W. (2013): Cancer genome landscapes. In *Science (New York, N.Y.)* 339 (6127), pp. 1546–1558. DOI: 10.1126/science.1235122.

Wang, Shujie; Watanabe, Takashi; Matsuzawa, Kenji; Katsumi, Akira; Kakeno, Mai; Matsui, Toshinori et al. (2012): Tiam1 interaction with the PAR complex promotes talin-mediated Rac1 activation during polarized cell migration. In *The Journal of cell biology* 199 (2), pp. 331–345. DOI: 10.1083/jcb.201202041.

Watanabe, N.; Kato, T.; Fujita, A.; Ishizaki, T.; Narumiya, S. (1999): Cooperation between mDia1 and ROCK in Rho-induced actin reorganization. In *Nature cell biology* 1 (3), pp. 136–143. DOI: 10.1038/11056.

Watanabe, Naoki; Mitchison, Timothy J. (2002): Single-molecule speckle analysis of actin filament turnover in lamellipodia. In *Science (New York, N.Y.)* 295 (5557), pp. 1083–1086. DOI: 10.1126/science.1067470.

Watanabe, Tomonobu M.; Tokuo, Hiroshi; Gonda, Kohsuke; Higuchi, Hideo; Ikebe, Mitsuo (2010): Myosin-X induces filopodia by multiple elongation mechanism. In *The Journal of biological chemistry* 285 (25), pp. 19605–19614. DOI: 10.1074/jbc.M109.093864.

Watson, Joanna R.; Owen, Darerca; Mott, Helen R. (2017): Cdc42 in actin dynamics: An ordered pathway governed by complex equilibria and directional effector handover. In *Small GTPases* 8 (4), pp. 237–244. DOI: 10.1080/21541248.2016.1215657.

Wei, Q.; Adelstein, R. S. (2000): Conditional expression of a truncated fragment of nonmuscle myosin II-A alters cell shape but not cytokinesis in HeLa cells. In *Molecular biology of the cell* 11 (10), pp. 3617–3627. DOI: 10.1091/mbc.11.10.3617.

Weiner, Orion D.; Marganski, William A.; Wu, Lani F.; Altschuler, Steven J.; Kirschner, Marc W. (2007): An actin-based wave generator organizes cell motility. In *PLoS biology* 5 (9), e221. DOI: 10.1371/journal.pbio.0050221.

Woodham, Emma F.; Paul, Nikki R.; Tyrrell, Benjamin; Spence, Heather J.; Swaminathan, Karthic; Scribner, Michelle R. et al. (2017): Coordination by Cdc42 of Actin, Contractility, and Adhesion for Melanoblast Movement in Mouse Skin. In *Current biology : CB* 27 (5), pp. 624–637. DOI: 10.1016/j.cub.2017.01.033.

Worthylake, R. A.; Lemoine, S.; Watson, J. M.; Burridge, K. (2001): RhoA is required for monocyte tail retraction during transendothelial migration. In *The Journal of cell biology* 154 (1), pp. 147–160. DOI: 10.1083/jcb.200103048.

Wozniak, Michele A.; Modzelewska, Katarzyna; Kwong, Lina; Keely, Patricia J. (2004): Focal adhesion regulation of cell behavior. In *Biochimica et biophysica acta* 1692 (2-3), pp. 103–119. DOI: 10.1016/j.bbamcr.2004.04.007.

Wu, Min; Wu, Xudong; Camilli, Pietro de (2013): Calcium oscillations-coupled conversion of actin travelling waves to standing oscillations. In *Proceedings of the National Academy of Sciences of the United States of America* 110 (4), pp. 1339–1344. DOI: 10.1073/pnas.1221538110.

Wu, Xunwei; Quondamatteo, Fabio; Brakebusch, Cord (2006a): Cdc42 expression in keratinocytes is required for the maintenance of the basement membrane in skin. In *Matrix biology : journal of the International Society for Matrix Biology* 25 (8), pp. 466–474. DOI: 10.1016/j.matbio.2006.09.001.

Wu, Xunwei; Quondamatteo, Fabio; Lefever, Tine; Czuchra, Aleksandra; Meyer, Hannelore; Chrostek, Anna et al. (2006b): Cdc42 controls progenitor cell differentiation and beta-catenin turnover in skin. In *Genes & development* 20 (5), pp. 571–585. DOI: 10.1101/gad.361406.

Yamaguchi, Hideki; Condeelis, John (2007): Regulation of the actin cytoskeleton in cancer cell migration and invasion. In *Biochimica et biophysica acta* 1773 (5), pp. 642–652. DOI: 10.1016/j.bbamcr.2006.07.001.

Yan, Jie; Yao, Mingxi; Goult, Benjamin T.; Sheetz, Michael P. (2015): Talin Dependent Mechanosensitivity of Cell Focal Adhesions. In *Cellular and molecular bioengineering* 8 (1), pp. 151–159. DOI: 10.1007/s12195-014-0364-5.

Yang, Hee Won; Collins, Sean R.; Meyer, Tobias (2016): Locally excitable Cdc42 signals steer cells during chemotaxis. In *Nature cell biology* 18 (2), pp. 191–201. DOI: 10.1038/ncb3292.

Yi, Kexi; Unruh, Jay R.; Deng, Manqi; Slaughter, Brian D.; Rubinstein, Boris; Li, Rong (2011): Dynamic maintenance of asymmetric meiotic spindle position through Arp2/3 complex-driven cytoplasmic streaming in mouse oocytes. In *Nature cell biology* 13 (10), pp. 1252–1258. DOI: 10.1038/ncb2320.

Zhou, Wu; Li, Xiaobo; Premont, Richard T. (2016): Expanding functions of GIT Arf GTPase-activating proteins, PIX Rho guanine nucleotide exchange factors and GIT-PIX complexes. In *Journal of cell science* 129 (10), pp. 1963–1974. DOI: 10.1242/jcs.179465.

Acknowledgements

I would now like to express my gratitude for completion of this work.

I would start by thanking, Prof. Dr. Perihan Nalbant for being my mentor and giving me the opportunity be a part of her group. The love and support you provide to your group, is simply overwhelming. You have aptly provided the motivation and guidance which has helped me develop scientifically. I have immensely learnt not just science, but also leadership, flexibility and interpersonal skills from you. I consider myself fortunate to have a mentor like you.

I would then like to thank Dr. Leif Dehmelt for the numerous discussions and scientific advice for this work. It was amazing how you patiently explained the mathematical and data analysis part of the work time and again. It was easy to approach you with all questions ranging from microscopy to data analysis, and you always had a solution. Your enthusiasm for science is very inspiring. It was also a nice opportunity to work in your lab for my secondment.

I would like to thank all the former and current members of Nalbant group, for being a friendly, acceptable easy-going team. A special thanks to Dr. Melanie Gräßl and Dr. Johannes Koch for teaching me most of the experimental work I have done in this group. I thank Dr. Manuela Kowalczyk for the numerous discussions, cell culture handling and for guiding me throughout for western blotting procedures. I thank Jana Quentin, for the administrative things she helped me with during the beginning and the good scientific and non-scientific discussions during the day. I also thank, Dr. Nina Schulze for patiently teaching me microscopy and for the discussion throughout. I thank, Hildegard Eling, for taking care of the unseen but essential lab stuff, numerous mini-preps and of course, for practising German with me. I thank Jana, Johannes and Melanie for accompanying me as during my visa appointments. A special thanks to Manuela and Jana for translation of the summary. Finally, thanks to Jessica Wagner, Kristina Murg and Imke Ramminger for all the help in the lab and fun in our office. I also thank Claudia Wilmes, for all the official help she has provided throughout. I also thank members of Dehmelt lab in Dortmund, specially Dominic Kamps for the co-ordination between two labs. I had the opportunity to work with Jonas, and Tina as my students. It was a pleasure working with you both. I thank Tina for her work on migration on PAK inhibition.

I would like to thank Dr. Bernd Hoffmann for the elastomeric surfaces he provided and for allowing me to visit the lab for my secondment.

I thank the ZMB groups of Ehrmann's, Meyer's, Knauer's, Vortkamp's and the remaining for sharing materials and reagents in time of need. I thank Prof. Stefan Westermann for reviewing the thesis.

I thank, Prof. Rudolf Leube, the co-ordinator of InCeM allowing me to be a part of InCeM. I also thank all the InCeM members for the scientific and non-scientific discussions, breaks and the fun during meetings. It was a pleasure to be a part of InCeM. I thank all the university staff and ZMB members who have helped me in one or many procedures during my stay here. I would like to thank InCeM and University of Duisbur-Essen for my funding.

Finally, I thank my friends and family. I am grateful to my parents for their strength and support and Abhishek for his love.

Curriculum vitae

Der Lebenslauf ist in der Online-Version aus Gründen des Datenschutzes nicht enthalten.

Erklärung:

Hiermit erkläre ich, gem. § 7 Abs. (2) d) + f) der Promotionsordnung der Fakultät für Biologie zur Erlangung des Dr. rer. nat., dass ich die vorliegende Dissertation selbständig verfasst und mich keiner anderen als der angegebenen Hilfsmittel bedient, bei der Abfassung der Dissertation nur die angegeben Hilfsmittel benutzt und alle wörtlich oder inhaltlich übernommenen Stellen als solche gekennzeichnet habe.

Essen, den _____ _____

Rutuja Patwardhan

Erklärung:

Hiermit erkläre ich, gem. § 7 Abs. (2) e) + g) der Promotionsordnung der Fakultät für Biologie zur Erlangung des Dr. rer. nat., dass ich keine anderen Promotionen bzw. Promotionsversuche in der Vergangenheit durchgeführt habe und dass diese Arbeit von keiner anderen Fakultät/Fachbereich abgelehnt worden ist.

Essen, den _____ _____

Rutuja Patwardhan

Erklärung:

Hiermit erkläre ich, gem. § 6 Abs. (2) g) der Promotionsordnung der Fakultät für Biologie zur Erlangung der Dr. rer. nat., dass ich das Arbeitsgebiet, dem das Thema „Role of Rho GTPase networks in Keratinocyte migration“ zuzuordnen ist, in Forschung und Lehre vertrete und den Antrag von *(Rutuja Patwardhan)* befürworte und die Betreuung auch im Falle eines Weggangs, wenn nicht wichtige Gründe dem entgegenstehen, weiterführen werde.

Essen, den _____ _____

Prof. Dr. Perihan Nalbant

DOI: 10.17185/duepublico/71244
URN: urn:nbn:de:hbz:465-20240325-082113-5